UNIVERSIDADE FEDERAL DE MINAS GERAIS
FACULDADE DE ENGENHARIA
PROGRAMA DE PÓS-GRADUAÇÃO EM ENGENHARIA DE ESTRUTURAS

Marco Túlio dos Santos

Hierarchical Models for Aircraft Joints Analyses

Belo Horizonte

2022

UNIVERSIDADE FEDERAL DE MINAS GERAIS
FACULDADE DE ENGENHARIA
PROGRAMA DE PÓS-GRADUAÇÃO EM ENGENHARIA DE ESTRUTURAS

Marco Túlio dos Santos

Hierarchical Models for Aircraft Joints Analyses

Dissertação de Mestrado apresentada ao Programa de Pós-Graduação em Engenharia de Estruturas da Escola de Engenharia, Universidade Federal de Minas Gerais como requisito parcial ao título de mestre .

Área de concentração: Engenharia de Estruturas
Linha de Pesquisa: Mecânica das Estruturas e dos Materiais
Orientador: Marcelo Greco

Belo Horizonte

2022

Santos, Marco Túlio dos.
S237h Hierarchical models for aircraft joints analyses [recurso eletrônico] / Marco Túlio dos Santos. - 2022.
1 recurso online (129 f. : il., color.) : pdf.

Orientador: Marcelo Greco.

Dissertação (mestrado) - Universidade Federal de Minas Gerais, Escola de Engenharia.

Apêndices: f. 125-129.

Bibliografia: f. 119-122.
Exigências do sistema: Adobe Acrobat Reader.

1. Engenharia de estruturas - Teses. 2. Aeronaves - Teses. 3. Método dos elementos finitos - Teses. I. Greco, Marcelo. II. Universidade Federal de Minas Gerais. Escola de Engenharia. III Título.

CDU: 624(043)

Ficha catalográfica elaborada pela Bibliotecária Roseli Alves de Oliveira CRB/6 2121
Biblioteca Prof. Mário Werneck, Escola de Engenharia da UFMG

UNIVERSIDADE FEDERAL DE MINAS GERAIS

PROGRAMA DE PÓS-GRADUAÇÃO EM ENGENHARIA DE ESTRUTURAS

PROPEEs UFMG

ATA DA DEFESA DE DISSERTAÇÃO DE MESTRADO EM ENGENHARIA DE ESTRUTURAS Nº: 385 DO ALUNO MARCO TÚLIO DOS SANTOS

Às **14:00** horas do dia **29** do mês de **abril** de **2022**, reuniu-se, totalmente por videoconferência para atender aos novos protocolos de distanciamento social adotados pelo Governo Federal e pela Prefeitura de Belo Horizonte, que integram medidas para combater o avanço da pandemia de Covid-19, provocada pelo novo coronavírus, a Comissão Examinadora indicada pelo Colegiado do Programa em 11 de abril de 2022, para julgar a defesa da Dissertação de Mestrado intitulada **"Hierarchical Models for Aircraft Joints Analyses"**, cuja aprovação é um dos requisitos para a obtenção do Grau de MESTRE EM ENGENHARIA DE ESTRUTURAS na área de Estruturas.

Abrindo a sessão, o Presidente da Comissão, **Prof. Dr. Marcelo Greco**, após dar a conhecer aos presentes o teor das Normas Regulamentares passou a palavra ao candidato para apresentação de seu trabalho. Seguiu-se a arguição pelos examinadores, com a respectiva defesa do candidato. Logo após, a Comissão se reuniu, sem a presença do candidato e do público, para julgamento e expedição do resultado final. Foram atribuídas as seguintes indicações:

Prof. Dr. Marcelo Greco - DEES - UFMG (Orientador)
Prof. Dr. Eduardo Bauzer Medeiros - DEMEC-UFMG
Prof. Dr. Daniel Nelson Maciel - UFRN
Profa. Dra. Cristina Ferreira de Paula - EMBRAER

Pelas indicações acima, o candidato foi considerado APROVADO, conforme pareceres em anexo.

O resultado final foi comunicado publicamente ao candidato pelo Presidente da Comissão. Nada mais havendo a tratar, o Presidente encerrou a reunião e lavrou a presente ATA, que será assinada por todos os membros participantes da Comissão Examinadora.

Belo Horizonte, 29 de abril de 2022.

Observações:

1. A aprovação do candidato na defesa da Dissertação de Mestrado não significa que o mesmo tenha cumprido todos os requisitos necessários para obtenção do Grau de Mestre em Engenharia de Estruturas;
2. Este documento não terá validade sem a assinatura do Coordenador do Programa de Pós-Graduação.

Documento assinado eletronicamente por **Marcelo Greco**, **Professor do Magistério Superior**, em 29/04/2022, às 15:59, conforme horário oficial de Brasília, com fundamento no art. 5º do Decreto nº 10.543, de 13 de novembro de 2020.

Documento assinado eletronicamente por **Eduardo Bauzer Medeiros**, **Membro de comissão**, em 02/05/2022, às 10:57, conforme horário oficial de Brasília, com fundamento no art. 5º do Decreto nº 10.543, de 13 de novembro de 2020.

Documento assinado eletronicamente por **Daniel Nelson Maciel**, **Usuário Externo**, em 04/05/2022, às 14:42, conforme horário oficial de Brasília, com fundamento no art. 5º do Decreto nº 10.543, de 13 de novembro de 2020.

Documento assinado eletronicamente por **Cristina Ferreira de Paula**, **Usuária Externa**, em 04/05/2022, às 20:09, conforme horário oficial de Brasília, com fundamento no art. 5º do Decreto nº 10.543, de 13 de novembro de 2020.

Documento assinado eletronicamente por **Felicio Bruzzi Barros**, **Subcoordenador(a)**, em 16/05/2022, às 11:23, conforme horário oficial de Brasília, com fundamento no art. 5º do Decreto nº 10.543, de 13 de novembro de 2020.

A autenticidade deste documento pode ser conferida no site https://sei.ufmg.br/sei/controlador_externo.php?acao=documento_conferir&id_orgao_acesso_externo=0, informando o código verificador **1380619** e o código CRC **41737C49**.

Referência: Processo nº 23072.221061/2022-84 SEI nº 1380619

UNIVERSIDADE FEDERAL DE MINAS GERAIS
ESCOLA DE ENGENHARIA
PROGRAMA DE PÓS-GRADUAÇÃO EM ENGENHARIA DE ESTRUTURAS

"HIERARCHICAL MODELS FOR AIRCRAFT JOINTS ANALYS"

Marco Túlio dos Santos

Dissertação apresentada ao Programa de Pós-Graduação em Engenharia de Estruturas da Escola de Engenharia da Universidade Federal de Minas Gerais, como parte dos requisitos necessários à obtenção do título de "Mestre em Engenharia de Estruturas".

Comissão Examinadora:

Prof. Dr. Marcelo Greco - DEES - UFMG (Orientador)

Prof. Dr. Eduardo Bauzer Medeiros - DEMEC - UFMG

Prof. Dr. Daniel Nelson Maciel - UFRN

Profa. Dra. Cristina Ferreira de Paula - EMBRAER

Belo Horizonte, 29 de abril de 2022

Documento assinado eletronicamente por **Marcelo Greco**, **Professor do Magistério Superior**, em 02/05/2022, às 07:34, conforme horário oficial de Brasília, com fundamento no art. 5º do Decreto nº 10.543, de 13 de novembro de 2020.

Documento assinado eletronicamente por **Eduardo Bauzer Medeiros**, **Membro de comissão**, em 02/05/2022, às 10:48, conforme horário oficial de Brasília, com fundamento no art. 5º do Decreto nº 10.543, de 13 de novembro de 2020.

Documento assinado eletronicamente por **Daniel Nelson Maciel**, **Usuário Externo**, em 04/05/2022, às 14:42, conforme horário oficial de Brasília, com fundamento no art. 5º do Decreto nº 10.543, de 13 de novembro de 2020.

Documento assinado eletronicamente por **Cristina Ferreira de Paula**, **Usuária Externa**, em 05/05/2022, às 20:06, conforme horário oficial de Brasília, com fundamento no art. 5º do Decreto nº 10.543, de 13 de novembro de 2020.

A autenticidade deste documento pode ser conferida no site https://sei.ufmg.br/sei/controlador_externo.php?acao=documento_conferir&id_orgao_acesso_externo=0, informando o código verificador **1380968** e o código CRC **6392E381**.

Referência: Processo nº 23072.221061/2022-84 SEI nº 1380968

Dedico esse trabalho à toda a minha família e aos meus amigos mais próximos que sempre me apoiaram, em especial minha esposa e filho que estão sempre comigo nos momentos difíceis. Não poderia deixar de citar especificamente meu pai, que infelizmente nos deixou enquanto eu desenvolvia esse estudo, e que sempre foi um pilar na minha vida.

Agradecimentos

Primeiramente eu gostaria de agradecer toda a minha familia, que sempre esteve comigo nos momentos difíceis que permearam o periodo que desenvolvi esse trabalho, em especial a minha esposa Camila que sempre me apoiou nos momentos difíceis e ao meu filho Lucca que me inspirou em sempre continuar.

Agradeço também ao departamento de Pós Graduação em Engenharia de Estruturas da UFMG que me forneceu todo o suporte necessário para desenvolver o meu trabalho e me muniu com o conhecimento necessário para tal. Em especial gostaria de agradecer ao professor Marcelo Greco, que sempre transmitiu uma tranquilidade que todo aluno de pós graduação precisa, sendo solícito e disponível para ajudar e tirar dúvida sempre que preciso.

Gostaria de agradecer a Embraer que me forneceu toda a infraestrutura para o desenvolvimento do trabalho, além de subsidiar o tempo necessário para o desenvolvimento desse estudo. Para que isso fosse possível, contei com a colaboração irrestrita dos meus lideres imediatos.

Por fim gostaria de agradecer ao meu falecido pai, que nos deixou enquanto eu desenvolvi esse trabalho e que sempre foi um pilar na minha vida. Sua partida me inspirou para poder continuar e concluir o trabalho da melhor forma que pude, que acredito que consegui apesar da pandemia que assolou e ainda assola a humanidade nesse período.

"All models are wrong, but some are useful."
(George A. P. Box)

Resumo

O processo para se projetar peças estruturais de uma aeronave é amplamente conhecido e discutido na academia e na indústria e vem sendo aprimorado ao longo dos tempos. Trata-se de um processo minucioso de estudos de cargas aerodinâmicos acoplados ou não às especificações exigidas pelos órgãos reguladores. Além disso, várias interações são necessárias para se definir o crítico estado de tensão da estrutura submetida aquela condição de carga, pois trata-se de uma estrutura complexa que precisa ser atualizada com frequência (considerando os requisitos que exigem um processo de montagem e desmontagem mais simples). Vários componentes de uma aeronave estão ligados uns aos outros por meio de fixadores que podem ser rebites, parafusos com porcas com diferentes tipos de materiais (alumínio, aço, titânio dentre outros). De fato, não é fácil obter o estado de tensão da estrutura aeronáutica para as condições reais de carregamento e também é difícil calcular a carga atuante em cada uma das juntas. Vários estudos já foram realizados a fim de obter o correto entendimento de como as cargas estão distribuídas nos prendedores de uma determinada junta. O presente trabalho tem como objetivo calcular a carga atuante nas juntas da aeronave (com foco nas regiões de longarina e intra e extra dorso), considerando três tipos de abordagem de modelagem, sendo cada uma com tal nível de detalhamento e então entender as diferenças na resposta estrutural. Além disso, também serão analisados três tipos de configuração de juntas, nas quais serão considerados os fixadores distribuídos em uma e duas fileiras e será utilizada a configuração escalonada considerando a mesma distância entre os fixadores para todos os modelos. Modelos de Elementos Finitos foram construídos nos softwares Hyperworks e Femap e serão resolvidos usando o solver Nastran. O estudo proposto mostrou uma boa correlação entre os modelos com níveis de detalhamento baixo e intermediário, além do modelo com baixo nível de detalhamento ter apresentado uma abordagem conservadora para calcular as juntas das aeronaves durante o processo de desenvolvimento do produto.

Palavras-chave: Modelos Hierarquicos. Juntas estrutural de aeronaves. Método dos Elementos Finitos. Prendedores aeronáuticos.

Abstract

The procedure of structural design for aircraft parts is widely known and discussed in the academy and in the industry, although it has been improved along the time. It is based on a detailed process of aerodynamics loads study coupled or not with specifications required by regulatory agencies. Further, several interactions of analysis are done to define the critical stress state of the structure submitted to load conditions, because it is a complex structure that needs to be often improved and updated (considering the requirement of assembly/disassembly simplicity). There are several components in an aircraft attached to each other by the use of fasteners, rivets or nuts made of different materials (aluminum, steel, titanium among others). In fact, it is not to easy to obtain stress state of the aeronautical structure for the actual loading conditions and also it is also difficult to calculate the load acting on each one of the joints. Several studies were already performed in order to obtain the correct understanding of how actual loads is distributed through the joints. The present work aims to calculate the load acting in aircraft joints (focusing in spar and skin regions), considering three types of modeling approach, being each one with a such level of detail and then understand the differences in the structural response. Furthermore three types of joint configuration will also be analyzed, in which it will be considered the fasteners distributed in a single and double row and also is used staggered configuration considering the same distance between the fasteners for all models. Finite Element models made using Hyperworks and Femap software were performed and they are going to be solved using Nastran solver. The study proposed has shown a good correlation between the models with low and intermediate level of detail, besides the model with low level of detail has shown a conservative approach to calculate aircraft joints during the product development process.

Keywords: Hierarchical models; Aircraft joints, Finite Element Methods, Aircraft Fasteners.

List of Figures

List of Tables

Contents

1 INTRODUCTION

The procedure to built a new aircraft lies in a long-term product development cycle which have a great amount of the resource and time consumed during the execution process. Thus it is time do define the load distribution thought the parts, the dimension of the components and all the needed specifications to comply with the regulators agency requirements.

Basically, a commercial aircraft is lifted by its wing, while the fuselage is responsible to carry the payload and the empenage is responsible to stabilize the load distribution during the flight . Hence, the main load of an aircraft flows from the wings to the fuselage and the components used to build these parts and to connect them must be able to withstand those flow of load.

Besides, an aircraft is composed of hundreds of parts and thousands of fasteners are used to connect them. The aircraft load distribution must necessarily flow from one part to another through the fasteners and those connections must to withstand those loads.

The step to structural sizing an aircraft components is also withing the execution process, in which it is required from the team a high efficiency, quality, and assertiveness in the response. Several parts of the aircraft must be sizing by means of a high interaction of different technology and they have to specify the dimensions, material, heat treatment, fasteners and several characteristics that will define the capability of the component to withstand to all flight conditions envelope and its applicable safety factor which was already defined by the requirements.

Withing this environment of a race against the time during the product development process, there is the structural engineering department which is responsible to define the better strategy to be used to mathematically represent a structure and then obtain the better condition of its internal strains which will precisely reproduce the actual structure and its stress field. Thus, several mathematical tools can be used to support the engineering in such a task, as the Finite element Method for instance. But only the choose of the method is not enough to correctly obtain the strain field of a component. It is also needed to define the correct level of detail to be used to obtain satisfactory results.

Several authors have already studied the better way to obtain the load distribution in aircraft joints, being them homogeneous or hybrid (when used composite parts connect to metallic). Rutman, Viisoreanu e Parad (2000) has proposed complete way to define the joint connections and its translational or rotational stiffness. Additionally (MARTINS; ERNANI; SANTOS, 2018) has studied the impact and differences in using different method to calculate joint stiffness and the effect of the secondary bending in those joints.

In contrast of detailed model which demand a high computational cost and a great amount of time needed to built the models, there are models with low level of detail to represent joint but with a good accuracy and confident in the result.

The present work will focus on a structural analysis, common in aeronautical industry, for the determination of the flow of load between two parts connected by fasteners. The work will concentrate the effort in understand the impact in change the level of detail of a mathematical model used to simulate a region of an aircraft wing under a hypothetical flight load. Besides it is going to be simulated the three types of fastener configuration , being them single, staggered and double.

In this way, it is going to be simulated joints attached by fastener by considering some typical connections type used in aeronautical industry and with three level of detail in order to compare the results. The model that consider a high level of detail is going to be used as the reference to obtain joint stiffness and to compare the results.

A total of seven mathematical model will be built to perform the analysis being them:

- One mathematical model to represent model with low level of detail
- Three mathematical models to represent intermediate level of detail (one for single, one for staggered and one for double configuration)
- Three mathematical models model to represent model with high level of detail (one for single, one for staggered and one for double configuration)

Note that for model with low level of detail, only one model is needed to perform the analysis and a post processor package is going to be built, by using Rossum e Jr (1995), in order to extract the results and extrapolate for the three types of configuration (single, staggered and double).

The software MSC Nastran (2021) is going to be used to solver the finite element models which are going to be built by using Altair Hyperworks (2014) and a post processor built by using Rossum e Jr (1995) to collect the results in a fast way. Besides the Altair Hyperworks (2014) and Simcenter FEMAP (2019) softwares are going to be used in order to post processor the results when a more refined analysis are demanded.

This work will start presenting a bibliographic review of aircraft structural analysis by focusing in the joints and the modeling techniques coupled with analytical procedure to represent the attachment region. It is going to be presented the references to calculate the load distribution along the wing span wise and then it is going to be presented how the (ROSSUM; JR, 1995) works with the oriented object paradigm. Then, the work will present the methodology used to perform the analysis, detailing the procedure to built

each model and how the results are going to be collected and processed. Finally it is going to be presented all the results obtained for all the models analyzed. The Figure 1 presents a workflow of this work to facilitate the reader understanding.

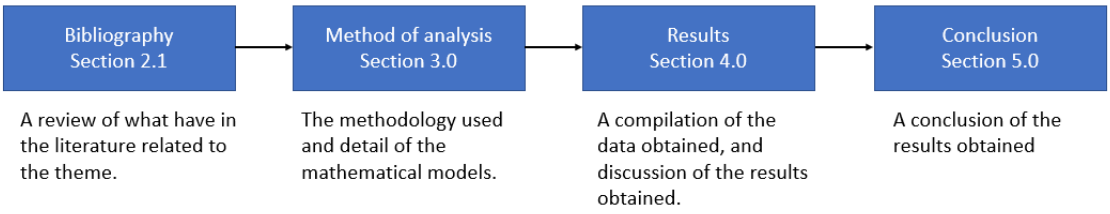

Figure 1 – Text structure

2 Development

2.1 BIBLIOGRAPHY

2.1.1 Aircraft Joints

Differently from the vehicle and naval industry, where the components are largely assembled by welding, in the aircraft industry the components are attached each other by rivets, screws and nuts, which become easier the process of maintenance. Several parts of an aircraft must be able to be disassembled and assembled depend on the necessity (e.g there is a process of maintenance in which some parts of the aircraft must be inspected in a period of time and then the operator looks for cracks, that can appear and propagate during the flight operation). Once finding some crack, the part with the damage must be replaced or repaired according to aircraft manual.

Some classical authors are largely used to perform aircraft structural analysis and also specific for joint regions. Niu (1997) is a complete bibliography regarding to aircraft structure where he discuss about all themes related to the structure of an aircraft. Also Bruhn (1954) is a complete book in which it is possible to understand better the structures and how it is sizing in the aeronautical industry.

Chaves e Fernandez (2016) has discussed regarding the aircraft joints and there, it is presented several of the mainly types of aircraft joints, its capabilities, its particularities and also how the load are distributed and transferred throughout the parts connected. Figure 2 presents the type of joints discussed by Chaves e Fernandez (2016), in which figs (a), (b) and (c) present the shear joints and fig (d) and (e) present tension joints. It is very important to understand the actual function of a joint in order to optimize the procedure of choose the best fastener to be used, the thickness and the material of the plates connected.

During the process of sizing the aircraft joints, some failure modes has to be considered. As it was discussed by Chaves e Fernandez (2016), the failure modes related to a shear joint is presented in Figure 3.

Chaves e Fernandez (2016) has discussed regarding the way to obtain the allowable for this joints, where "... fastener shear-out and the plate failure modes may be predicted by easy calculation based on the material strength allowable (i.e yielding rupture), holes bearing is a somehow more complex failure mode, and allowable for hole bearing are usually obtained by experiments..." Chaves e Fernandez (2016).

Niu (1997) has proposed some analytical procedure to obtain the bearing allowable

stress by means of material properties which can be obtained in Rice et al. (2003).

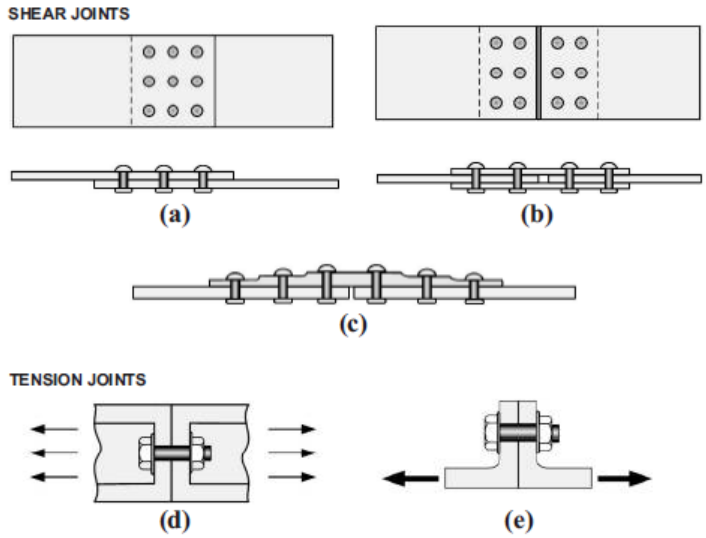

Notes: (a) Lap joint, single shear; (b) Butt joint, double shear; (c) Butt joint – stepped; (d) Axial (No bending); (e) Tension and bending

Figure 2 – Type of joints (Adaptation of Figure 1 of Chaves e Fernandez (2016))

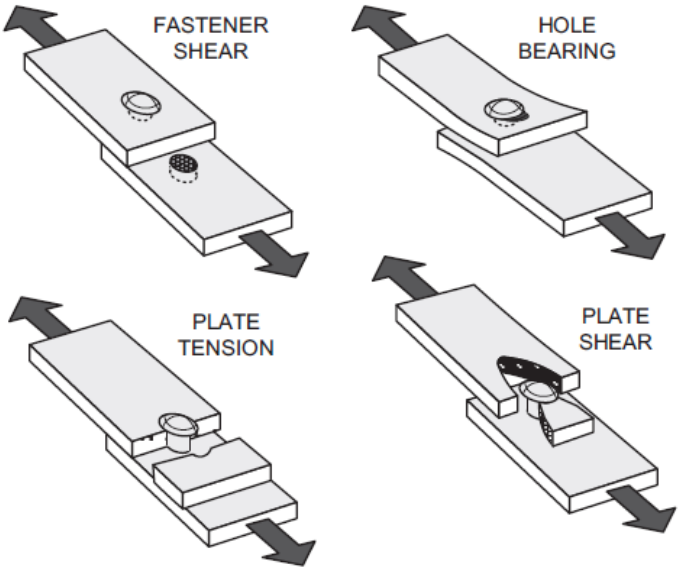

Figure 3 – Static failure modes in joints (Adaptation of Figure 3 of Chaves e Fernandez (2016))

Another important consideration which do not have to be forgotten is the load transferred and by pass load. In a joint with several rows, the load transferred for each fastener is known as bearing load, and the load that remains in the plate is called by pass load, as it is presented in Figure. 4. Some authors as Swift (1971) or Niu (1997) were already proposed a way to provide the load distribution by means of determination of the joint flexibility.

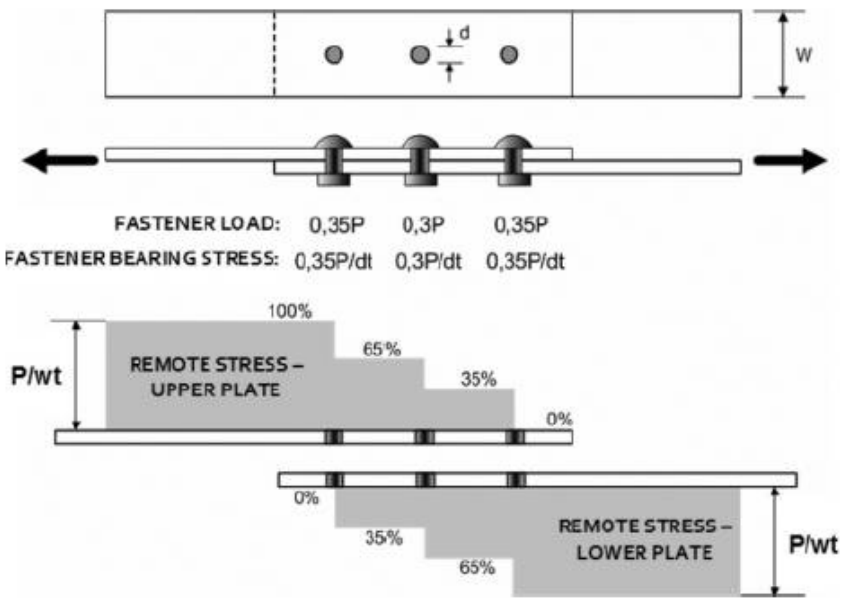

Figure 4 – Representation of load transfer through a fastened lap joint with three rows of rivets (Adaptation of Figure 4 of Chaves e Fernandez (2016))

Rivet joint procedure are very complex and depend on the integrated effect of a large number of variable related to joint design, production and applied load condition, already discussed by Skorupa e Korbel (2008)

The most of aircraft joints are assembled with rivets, which is easier to assemble and disassemble. Furthermore, some specifics methods of connection can be considered, like the insertion of adhesive in riveting joint, already discussed by Sadowski et al. (2013) or Sadowski, Golewski e Zarzeka-Raczkowska (2011).

In such studies it relates the comparison of three types of configuration, being spot welding plus adhesive, rivet bonded and clinch bonded joint. It is also possible to see the positive effect of apply adhesive which makes the joint more strength and with better fatigue properties, better corrosion resistance and also the possibility to remove the sealing in operation process. Figure 5 shows the comparison and the advantages of using the adhesive in joint, but it is also important to highlight the disadvantage during the process of assemble and disassemble.

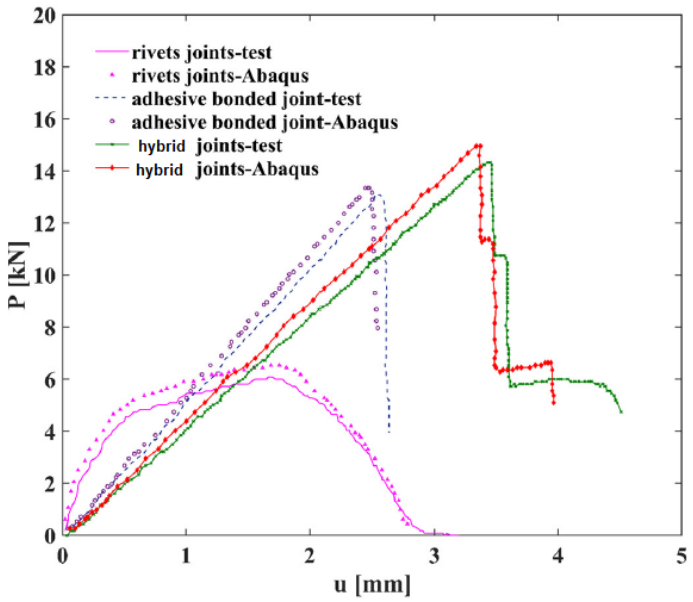

Figure 5 – Comparisons of force on the joint between conventional rivet and adhesive joints and hybrid joint (Adaptation of Figure 12b of Zhao et al. (2020))

Huan e Liu (2017) has discussed regarding the squeeze force and presented in Figure 6, which is the force to conform the rivet and press one plate to another. Those study have compared the effect of increasing this force in static behavior of rivet lap joint. Several other studies have shown that from 50 percent to 90 percent of the fatigue crack originates near fasteners hole, in aircraft industry.

The study presented by Huan e Liu (2017) simulates three levels of force in order to evaluate the influence of this force in static behavior. Finally the study conclude that the squeeze force does not have influence in joint stiffness, but results in a slight decrease in joint strength and also that the great squeeze force "will increase the uniformity of the joint and reduce the possibility to the damage to the side of the rivet head." (Huan e Liu (2017)), increasing the fatigue property.

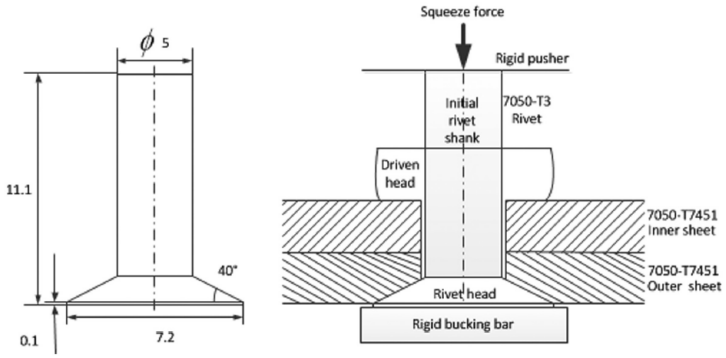

Figure 6 – Effect of squeeze force (Adaptation of Figure 1 of Huan e Liu (2017))

It is also depicted by Skorupa et al. (2010) the relevance of the secondary bending in rivet lap joint, specially related to fatigue life. This effect occur due to an eccentricity at the joint and can be assumed as the responsible for the crack nucleation at the rivet hole region, causing a crack propagation will cause a catastrophic failure if don't identified in time.

As it was discussed by Skorupa et al. (2010), the effect of secondary bending can be accounted by using differential equation, although this simplification is not able to predict this stress for thinner sheet and as a conclusion it is shown the nonlinear behaviour of secondary bending, in which it can be decreased by increasing the pitch of fasteners or decreasing the thickness of the plate. The secondary bending effect can be seen on Figure. 7

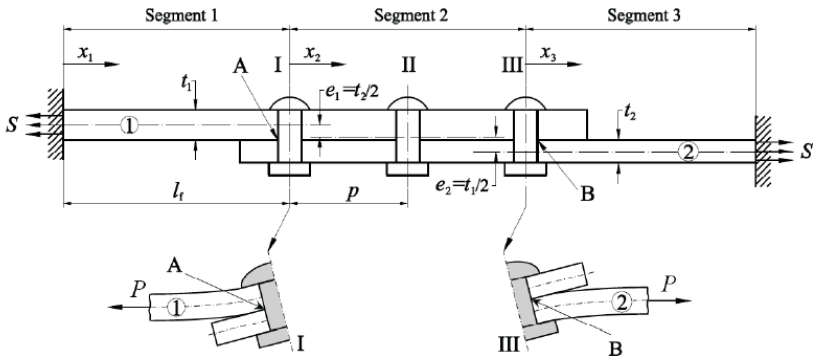

Figure 7 – Secondary Bending Effect (Adaptation of Figure 1 of Skorupa e Korbel (2008))

2.1.2 Hierarchical Model

Hierarchical model for engineering design was fully discussed by Bucalem e Bathe (2011), in which it is presented how important is to understand the level of detail a given model must have depending on what type of response is desired.

The Figure. 8 presents the flow of the hierarchical process for a structural analysis in which a physical problem must be idealized by means of abstraction or laws previous studied that will represent this problem through a mathematical model. This process to transform a physical problem into a mathematical model can have a sub process in which it must be chosen what type of idealization or abstraction will approximate more of the real problem.

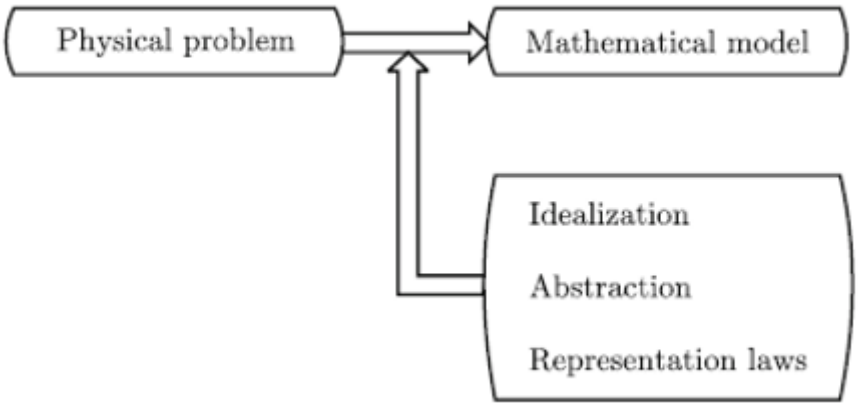

Figure 8 – Concepts involved in the construction of a mathematical model(Adaptation of Figure 1.1 of Bucalem e Bathe (2011))

Figure. 9 can be considered as an expansion of Figure. 8 in which it is possible to see that a given problem could be divided into several mathematical models with different types of detail or representativeness that can be used in order to obtain a result good enough for the problem struggled in a process of engineering design. In those process it is very important to do a better interpretation of the result and to decide if the solution met the expectations or if it is needed to refine the analysis in order to give a more precise result.

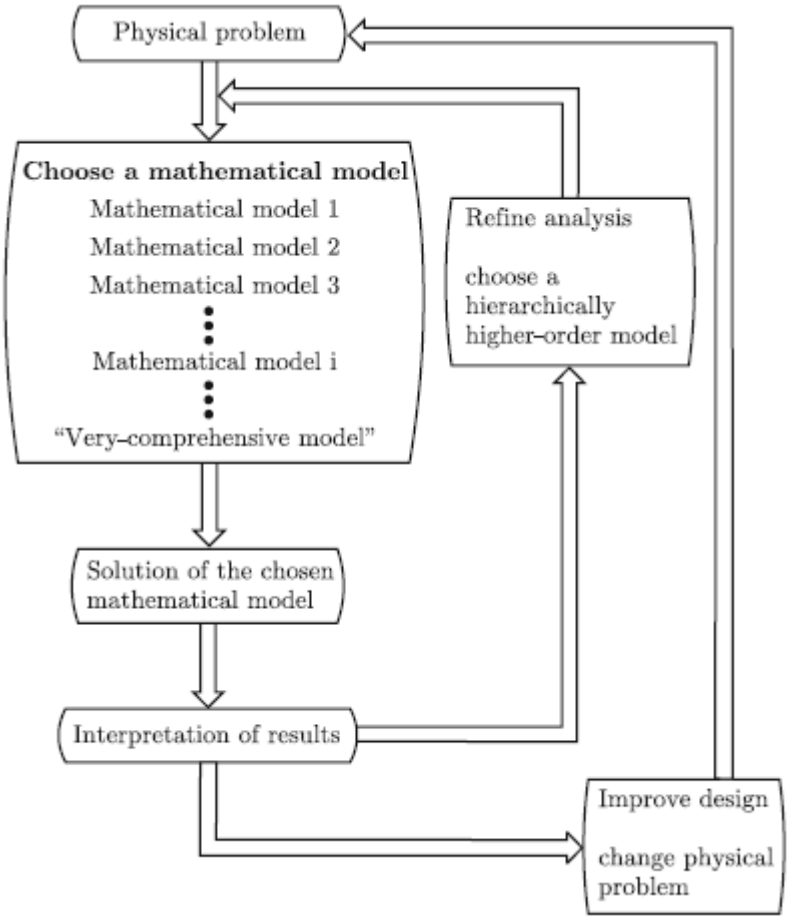

Figure 9 – Process of engineering design(Adaptation of Figure 1.13 of Bucalem e Bathe (2011))

The improvement of techniques to work with different mathematical model walks together with the improvement of the computers and the finite element method approach. With the effect of development in computational engineering it is possible to solve many problems that couldn't do some decades ago, where the analytical process was restricted to the capacity of process of human brain which is slower than computer process capacity nowadays.

A very complex component can be draw considering its spatial coordinate and it can be divided into several number of solid elements, furthermore with a specific engineering software it can be analyzed considering its boundary conditions. But the question is, how detailed must be such model? The origin of this question comes from two other question that must be answered: "1) the structure is safe? 2) Will the structure work in operational conditions required?" Bucalem e Bathe (2011)

Nowadays, due to advance of computer engineering, it is possible to simulate a complex structure without having the actual structure to be tested and with a good

accuracy. It was different in the past, where the design process has depended of a trial error procedure and the previously experience gathered. Although depending on the level of detail the model is built, the time spent become critical. For example, a model with high level of detail which is built considering solid elements, nonlinearities of material and geometry and modeling techniques advanced demands much more time of analysis than a model analyzed considering plate or bar elements and performing only linear solution without needed to iterate into convergence process.

In Bucalem e Bathe (2011) it can be seen some examples of hierarchical model techniques as the typical problem of a built-in cantilever subjected to a tip load where the results of three types of modeling approach where compared:

- Model 1: Bernoulli-Euler beam model
- Model 2: Timoshenko beam model
- Model 3: Plane stress model (only performed considering finite element approach)

As the conclusion the example shows the differences in normal stress behavior throughout the span of the cantilever from model one thru three, this difference is also few for the displacement at the tip of the cantilever. But there is a significant difference in shear stress distribution through the section. This is easy to understand since the finite element model is more precise in predict the behavior of shear stress throughout the section if it is compared with Bernoulli-Euler or Timoshenko beam model, which is a simplification and only consider the inertia of the section.

Thus, based on the results obtained, if a cantilever beam will be simulated only to represent a load path in a given structure where other component will be analyzed with more detail, a simple bar element with Bernoulli-Euler equation is more than enough. Otherwise if the cantilever is the focus of the analysis and the stress distribution throughout the section is needed in order to have more precise conclusion, this component must be simulated with more detail and maybe a finite element model with all nonlinearities is required.

2.1.3 Finite Element Model

Finite element method is an old methodology which is being improved along the years. The procedure consists in divide a continuo geometry into a several small parts with no infinitesimal size, connected each other by nodes and governed by physical theories lied in Boresi, Chong e Lee (2010) or Mal e Singh (1991), as it can be seen on Figure. 10. Moreover, approximate functions are used to describe relevant fields, such as displacements, stresses strain, etc.

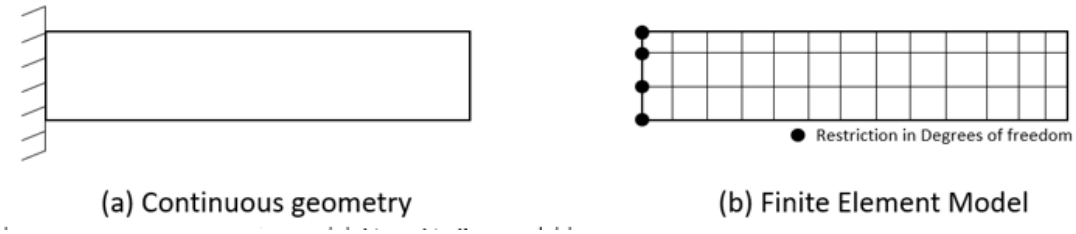

Figure 10 – Continuous vs Finite element model

In a point of view of structural analysis, several elements were already developed considering different function of shape and several software has a vast library of this elements and they can be used depends on the problem faced. Some examples are presented on Figure 11.

In the figure there are the simpler element used for structural analysis:

- Truss element: element where only axial behavior is considered. This element cannot be used to simulate columns, booms, bars, etc.
- Beam element: a little more complex element where the stiffness for bending and torsion is considered.
- Quadrilateral shear elements: It is composed with four nodes with 8 degrees of freedom, although it can have more nodes depending on the order used in the function of shape.
- Triangular shear elements: three nodes elements with 6 degrees of freedom, but as same as quadrilateral elements, the triangular can have more nodes depending on the order.
- Plate element: it can be quadrilateral or triangular elements that may be subjected to bending and its function of shape is governed by the theory of flexure in plates according to Weaver (2007)

- Shell elements: Some theories consider shell elements as an specialized solid element which are thin in one direction. Basically, it "... is a combination of generic and nodal displacements for the membrane (plane-stress) and flexural (plate-bending) components" Weaver (2007).

- Solid elements: It is a more complex element where the volume is fully represent, in contrast it has a high computational costs because of the number of nodes. This type of element is recommended when the geometry can not be represented by the other simplifications such as beam, plate or shell elements. The Figure 11 shows only CHEXA element, but there is other formulations for solid elements, e.g Tetrahedron, CPENTA, etc.

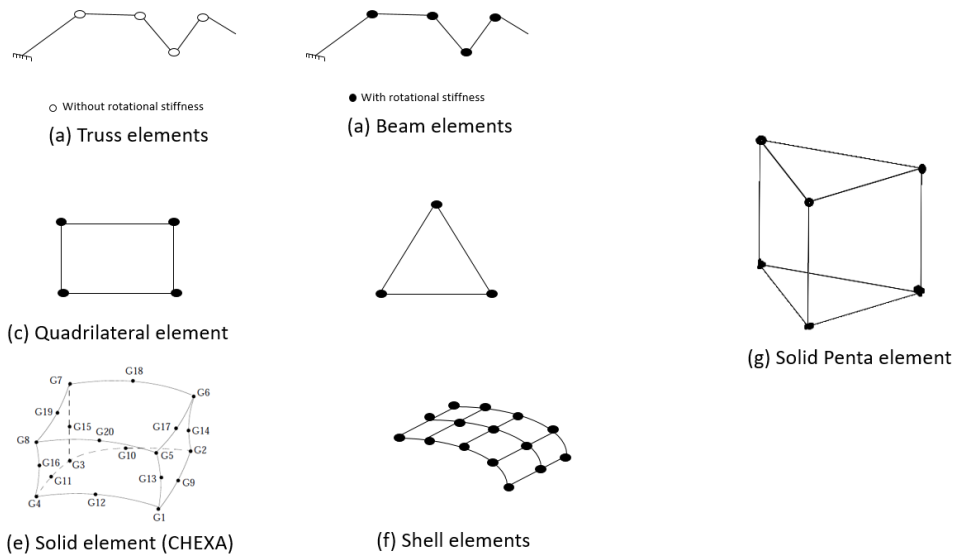

Figure 11 – Type of Elements

Another's simpler elements were developed in order to facilitate some type of analysis. They can be a simple 1d element without considering any function of shape or dimension and they are used only to connect two nodes by means of an infinite stiffness or a stiffness knew beforehand. Those elements are widely used when a complex structure is going to be analyzed, they are presented in Figure. 12.

Figure 12 – 1D Elements

More and more sophisticated elements are being created and the examples cited above are only the beginning of a study which do not stopped from many years and it is still in course. In the structure field, people are developing elements capable to simulate a tip of crack which will propagate during a cycle of load, elements able to simulate the interaction between the plies in a composite structure or even the rupture of this plies due to a fail in the bond region. Several and more complex elements are being studied in fluid dynamics, nuclear, biologic and bio-mechanics field, and this method, when well used can help to predict the behavior of a given component without the needed of built and test. It is not purpose of this work to go inside the details of the mathematical procedure for finite element analysis, since other authors have done this more precise and clearer, as it can be seen on Mirzazadeh e Green (2017), Zienckiewics e Morgan (2006), Zienckiewic, Taylor e Zhu (2013), Hughes (2012), Kj (1982), Jacob e Ted (2007), Weaver (2007) and several others.

This section has proposed an overview of the potential of finite element analysis. Furthermore this section also intends to bring to light the care that must be done while working with this method and the need to know well its capabilities, restrictions and also known beforehand the consequences of the indiscriminate use of elements which its behavior is not knew.

2.1.4 Mathematical models proposed to simulate joints

This section aims to show the principals studies already proposed to simulate joints, its applicability, the advantages and its limitations.

The load distribution in a joint can be influenced by several factors like materials properties, squeeze force, thickness of the plates attached, among others. The best way to simulate the load transferred in a joint using finite element approach is by using a higher order solid element, considering the nonlinearities of material, geometry, the contact between the parts and the squeeze force at the joint.

In hierarchical model's point of view, the abstraction of using a high complex nonlinear model refers to a more representative model, with high level of detail but difficult to execute in practice. In a full model of a wing, with thousands of rivets used to attach spars with skins and rib with skins, it is not feasible in practice, not only due to hardware limitation, but also due to the product cycle deadline.

Because of such complexity, some intermediates models are proposed in order to accelerate the process of sizing a complex component with several attachment regions, but even so using an assertive approach.

In 2015 Askri et al. (2015) has proposed a reduced model by using multi-connected Rigid surface, as it is presented in Figure 13, to predict the stress field at local region of the fastener and also do predict the load distribution in fasteners. In this model, also called MCRS, the authors has included the effect of pre-load and friction coefficient and it is concluded a "very satisfactory results, not only for global stiffness and the distribution of load between fasteners, but also for local response assessed from contact pressure field and stress field.

In 2016, by using the same approach (MCRS), Askri, Bois e Wargnier (2016) has proposed a study to investigate the effect of hole location error on the strength of fastened multi-material joint, and the study was performed considering statistical approaches. In this work it is shown the link between the transmitter load with the bolt-hole clearance.

Askri, Bois e Danoun (2021), by exploring the same methodology of MCRS, has proposed another study to investigate the effect of shape defect in multi-fastened joint during the assembly process. The numerical model previously proposed has shown the ability to simulate different clamp sequences and to capture the interaction between shape effects, bolt-hole clearance and target axial pre-load. Although the success in the results for the model proposed is limited to its specific applicability and for each specific situation new models must be considered.

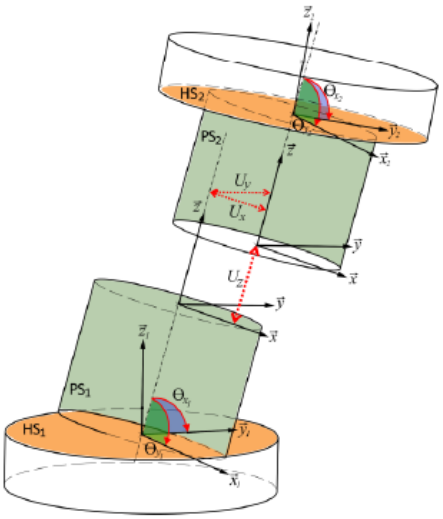

Figure 13 – Adaptation of Figure 3 of Askri, Bois e Wargnier (2016) - Kinematic behaviour of reduced bold model (MCRS

In 2011, Gray e McCarthy (2011) has proposed a combination of analytical and numerical approach to simulate a bolted composite joint. Besides it is used a semi-empirical approach for model failure initiation and energy absorption. It is proposed an element in which it is able to represent the nonlinearities, load-displacement behaviour of composite joint ranging from bolt-hole clearance and friction effect to eventual joint failure. The author has concluded that the model proposed is robust and has presented a good correlation with the actual model, besides the model has shown the capability to capture complex load distribution for more then twenty bolts.

In 2015, by testing a series of single bolt joints with various bolt-holes clearance and bolt tightening torques in an attempt to confirm the influence coefficient of the joint stiffness model, Liu et al. (2015) has presented a good correlation with the experimental testes, furthermore the study has proposed a joint stiffness model. Another interesting point observed by Liu et al. (2015) is the influence of the friction in load transference and it is proved that when it is applied a great torque, the bolt starts to transfer the load only after the frictional load be overcomed. It is also showed that for fasteners finger-tight there is almost zero frictional load and the load is transferred only by the fasteners. Figure 14 shows a qualitative graph which represent the load transmitional between fasteners with high torque and with finger-tight.

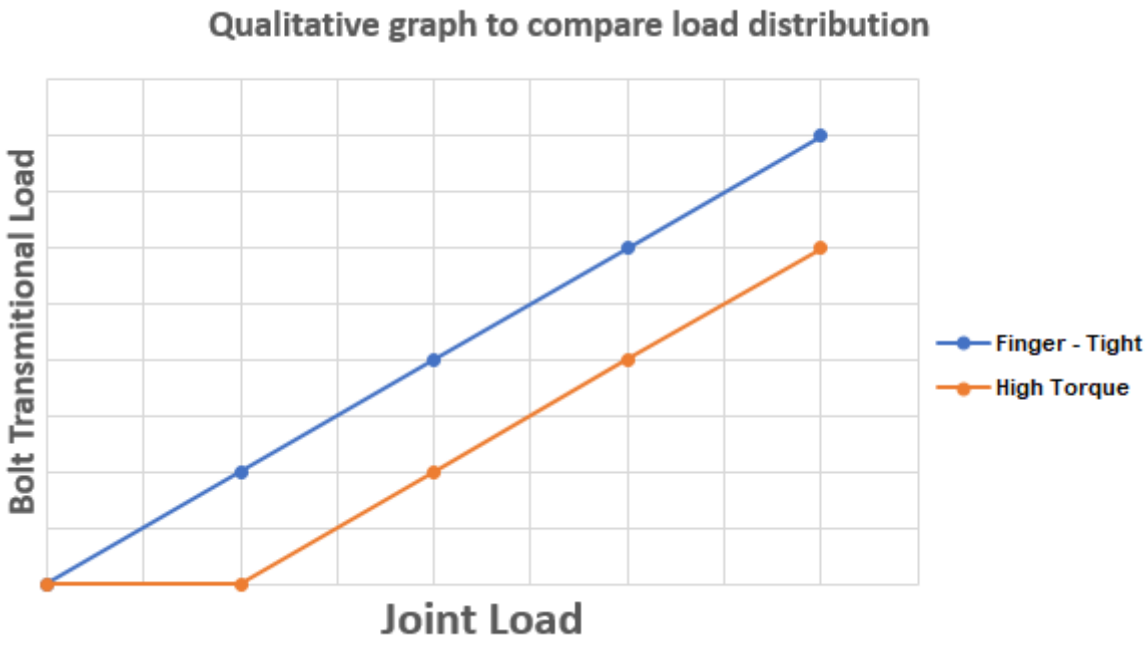

Figure 14 – Qualitative graph to represent high torque and finger-tight

Liu et al. (2020) has continued its study and has proposed an improved 2d finite element model for bolt load distribution analysis of composite multi-bolt single-lap joints. The author uses 2d finite element to simulate a single lap joint and uses a 3d model to validate the results.

Liu et al. (2020) has simulate HST10-10 bolt and uses ABAQUS techniques to calculate the bolts by an improvement of the technique proposed by Gray e McCarthy (2011). Besides it is replacing the load displacement curve with the bolt stiffness model already proposed by Liu et al. (2015). Furthermore it is added bolt holes in the model, taking the area of bolt head as the size of influence region of coupling constraints. The author has concluded there is no significant influence in change simulation approaches of the bolt-stiffness from load-displacement, besides the bolt holes influences the accuracy of the calculation, but the area of influence region has no effect on the load distribution, although it influences in predict the secondary bending effect.

Another interesting study proposed by HUSKAMURI e LAGDIVE (2017), which aims to sumulate the load transferred between the fasteners by using a 3D ANSYS model. In this study the numerical results has shown not conservative and more accurate study must be performed to achieve better results.

Verwaerde, Guidault e Boucard (2021) uses a non-linear connector to simulate the behaviour of bolt assembly to simulation bolt pre-load, friction and plastic material parameters. The connection is implemented using ABAQUS through user-element subroutine

and the result is compared with large scale 3D calculation, which has presented a very good correlation, but the reduced model has cpu time reducing compared with 3D model.

According it was discussed in section 2.1.3 a great amount of elements with different functionalities were developed and are able to be used in several commercial and free software. So, combining more than one element and by considering its behavior could help to simulate some connections which is difficult to simulate using standards procedure.

Martins, Ernani e Santos (2018) has presented in its study the variability of the load distribution in joints by considering different type of approaches. In the study it has compared results for experimental tests and numerical simulation for joints modeled with different techniques in which it raging from the simplest to the most complex (as presented in section 2.1.5. Furthermore, the work shows more joints configuration comparison).

As it was aforesaid, several authors have tried to simplifies the modeling approaches of connections without loss of accuracity, sometimes by using analytical approaches, sometimes by using 2d/1d FEM models or even a compound of both. Martins, Ernani e Santos (2018) have compile several of those methodologies and concluded Rutman approach can be used as a simplification for a complex joint.

It is important to point out although the hierarchical mind set is used implicitly in several works, the applicability of this approach is not explored enough by the authors, which studies rivet or bolt connections. This approach must be studied more and improved in order to enhanced the process of aircraft certification.

The next section will explore with more detail the Rutman approach which will be used in this work as a step of joint modeling approach.

2.1.5 Rutman Approach

One of the joint studied by Martins, Ernani e Santos (2018) was firstly presented by Rutman, Viisoreanu e Parad (2000), where it has presented a joint connection with high level of detail. Rutman uses bar elements using Euler's formulation (Falsone e Settineri (2011)) connected to the plates by means of a bush element, as it can be seen on Figure 15.

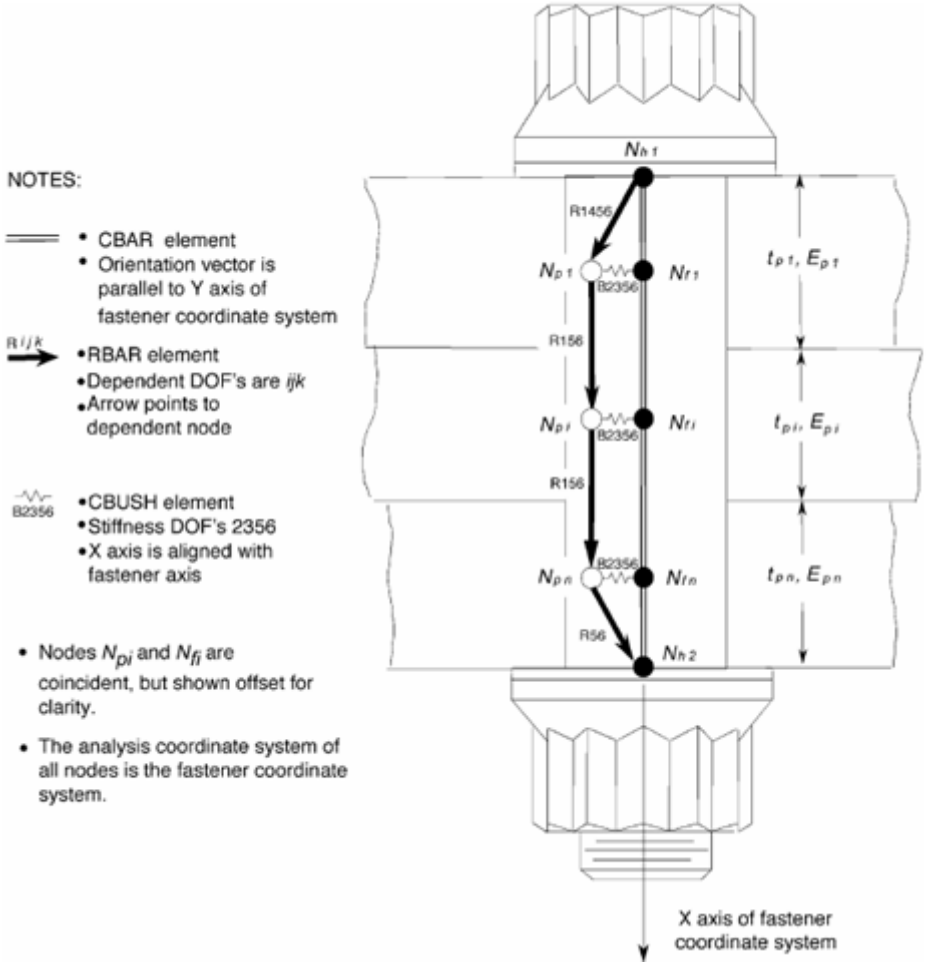

Figure 15 – Fastener Joint modeling (Adaptation of Figure 3 of Rutman, Viisoreanu e Parad (2000))

The model proposed by Rutman, Viisoreanu e Parad (2000) has some characteristics which is listed below:

- Translational plate bearing stiffness.
- Translational fastener bearing stiffness.
- Rotational plate bearing stiffness.

- Rotational fastener bearing stiffness.
- Fastener shear stiffness.
- Fastener bending stiffness.

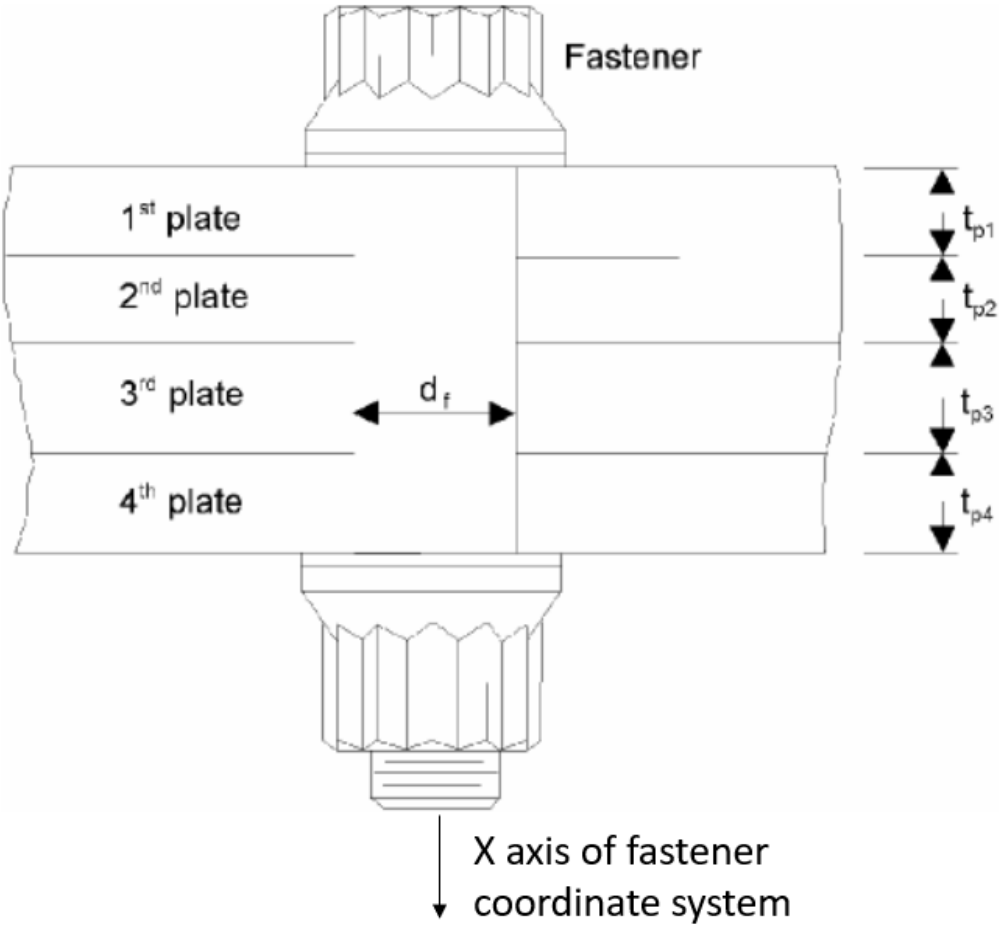

Figure 16 – Fastener joint (Adaptation of Figure 1 of Rutman, Viisoreanu e Parad (2000))

The flexibility calculation proposed by Rutman could be done as follow (the thickness of the plate ti is from Figure 16):

"Under load, the plates slide relative to each other. This causes the translational bearing deformation of joined plates and a fastener."

The translational bearing flexibility of plate I is:

$$C_{btp_i} = \frac{1}{E_{cp_i}.t_{p_i}} \tag{2.1}$$

Where:

E_{cp_i} - Compression modulus of plate I material;

t_{p_i} - thickness of plate i

The fastener translational bearing flexibility at plate i

$$C_{btf_i} = \frac{1}{E_{cf}.t_{p_i}} \tag{2.2}$$

Where:

E_{cf} - Compression modulus of fastener material;

Combined fastener and plate translational bearing flexibility at plate i:

$$C_{bt_i} = C_{btp_i} + C_{btf_i} \tag{2.3}$$

Combined translational bearing stiffness at plate i

$$S_{bt_i} = \frac{1}{C_{bt_i}} \tag{2.4}$$

The relative rotation of the plate and fastener creates a moment in the plate-fastener interaction. The bearing deformation caused by this relative rotation are assumed distributed linearly along the plate thickness.

$$\delta = x\varphi \tag{2.5}$$

Where:

x - coordinate along the plate thickness;

φ - angle of relative rotation of the plate and fastener stiffness of a dx thickness slice of plate i is:

$$dS_{btp_i} = E_{cp_i}dx \tag{2.6}$$

Load on dx thickness slice of plate I caused by the plate bearing deformation

$$dF = \delta dS_{btp_i} = x\varphi E_{cp_i}dx \tag{2.7}$$

Moment of df force about the plate I center line

$$dM = xdF = E_{cp_i}\varphi x^2 dx \tag{2.8}$$

Moment in the plate-fastener contact caused by the plate deformation

$$M = \int_{\frac{-t_{p_i}}{2}}^{\frac{t_{p_i}}{2}} x^2\, dx \;= Ecp_i\varphi\frac{t_{p_i}^3}{12} \tag{2.9}$$

The rotational bearing flexibility of plate i

$$C_{brp_i} = \frac{\varphi}{M} = \frac{12}{E_{cp_i}t_{p_i}^3} \tag{2.10}$$

The fastener rotational bearing flexibility at plate i

$$C_{brp_i} = \frac{12}{E_{cf}t_{p_i}^3} \tag{2.11}$$

Combined fastener and plate rotational bearing flexibility at plate i

$$C_{br_i} = C_{brp_i} + C_{brf_i} \tag{2.12}$$

Combined rotational bearing stiffness at plate i

$$S_{br_i} = \frac{1}{C_{br_i}} \tag{2.13}$$

The bearing stiffness is modeled by elastic elements. The shear and bending stiffness of a fastener are represented by a beam element." Rutman, Viisoreanu e Parad (2000)

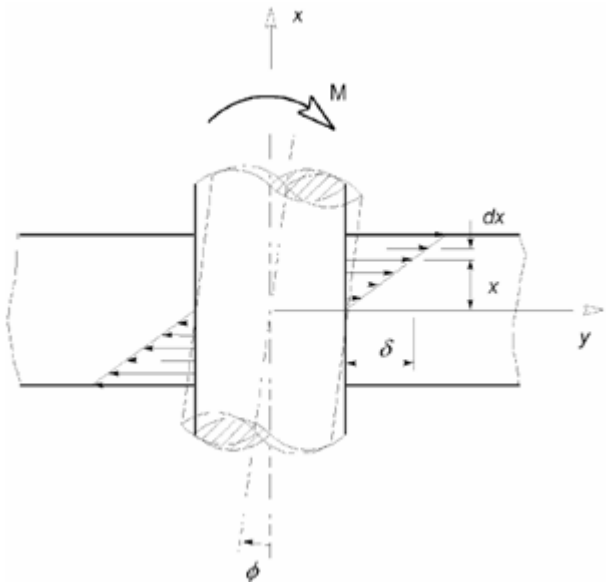

Figure 17 – Rotational bearing stiffness definition (Adaptation of Figure 2 of Rutman, Viisoreanu e Parad (2000))

There is already an automated process previous created to build each element depending only of the thickness and material properties of the plates connected, and this approach is also presented in Rutman, Viisoreanu e Parad (2000) and expanded in Rutman et al. (2007) and Rutman et al. (2009).

The present work aims to use the Rutman approach in order to simulate the connection between skin and spar for model intermediate (see sec 3.0.3). Thus, it is expected that this model provides more detailed results (when compared with the coarse model) and confer some flexibility to the model since it is considering several stiffness which was not considered in model 1, or considered in a simplest way. The comparison of these models is presented in section 4.

2.1.6 Load Distribution through the wing spanwise

Before starts to talk about the load distribution through the wing spanwise, it is good to understand a little the process of sizing an aircraft inside a aeronautical company. As it is described by ISCOLD (2002) the load calculation lies on the beginning of the process, which is already in the conceptual formulation of the project. In this way the responsible sector have to interact with several parts inside the company in order to receive and provide the data related to the aircraft, such as the weight and aerodynamics information according it can be seen on Figure 18. The Figure 18 is also exposing that the process must to be iterated until converge to an aircraft which is secure enough according to the requirements provided from ANAC (Agencia Nacional de Aviação civil), FAA (Federal Aviation Administration), EASA (European Union Aviation Safety Agency) and others regulatory agencies around the world where the company is intending to have its aircraft flying in such sky.

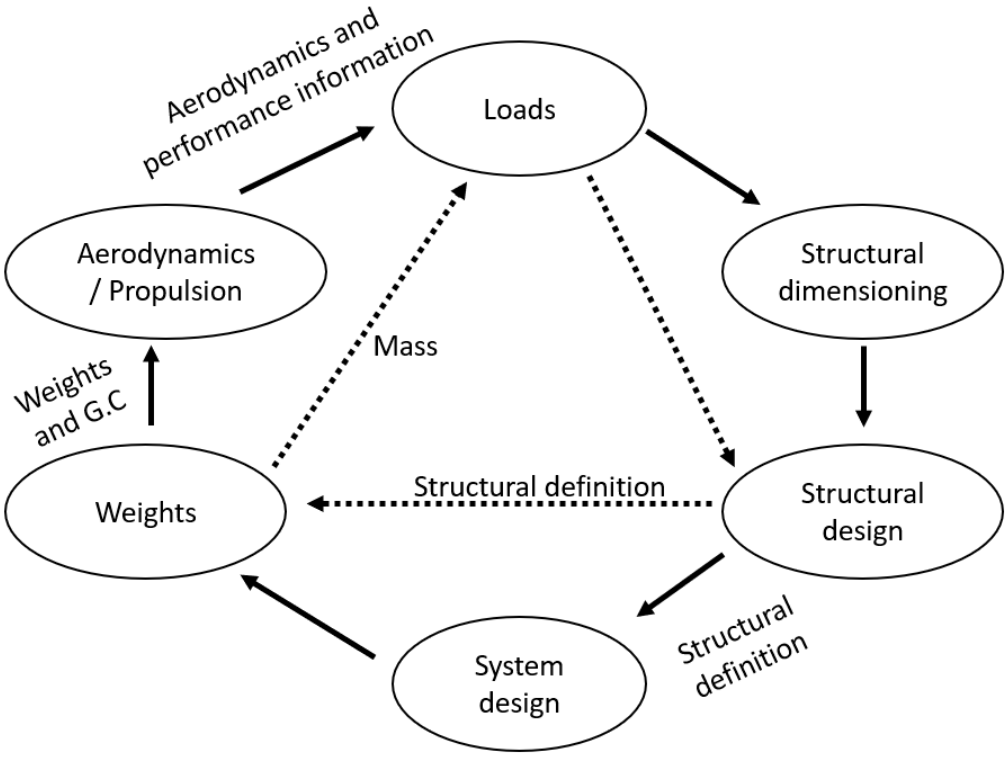

Figure 18 – The relationship between the sectors of an aeronautical company during the the project (Adaptation of Figure 1 ISCOLD (2002))

According to presented by ISCOLD (2002) it is important for the sector responsible to accomplish the load calculation to have some understanding beforehand. Those understands involves concepts of the type of load, if it is going to be static or dynamic, concepts of the nomenclature of weights and the velocities, have to understand the factors needed

to be applied and it is also in its responsibility to taking into account the requirements engaged in the process of loads definition.

The work proposed here do not intend to go deep in the process of load definition, but it will use the correct concepts for the loads in which a wing is submitted. For this purpose the stender method discussed by ISCOLD (2002) will be used in order to define the load distribution in a finite wing.

For the static load ISCOLD (2002) shows that the stender method is "based on the hypothesis in which the wing spanwise load distribution is proportional the area of a imaginary wing in which its chords are the geometric average of the actual chords and of a eliptic wing with the same wingspan" ISCOLD (2002), as it is presented in Figure. 19

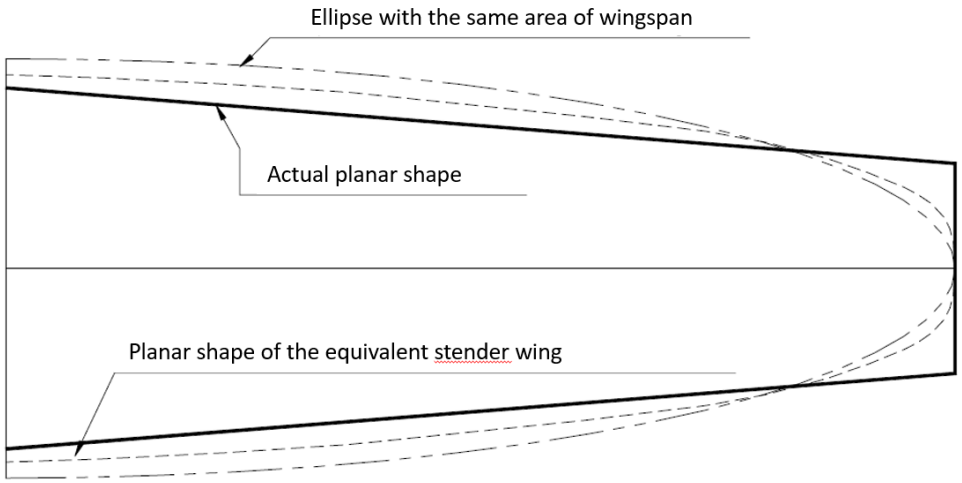

Figure 19 – The relationship between the actual, elliptical and stender wings (Adaptation of Figure 1, page 121 of ISCOLD (2002))

So, the stender chords are:

$$C_s = \sqrt{C_g.C_e} \tag{2.14}$$

Where:

Cs - stender chord

Cg - Actual wing chord

Ce - eliptical wing chord

The Figure 20 presents an example showed in ISCOLD (2002) of how the chord is distributed throughout the wing spanwise. Considering that the lift is proportional to the

chord, it is possible to see that the root of the wing is the region more loaded while the tip is the less one.

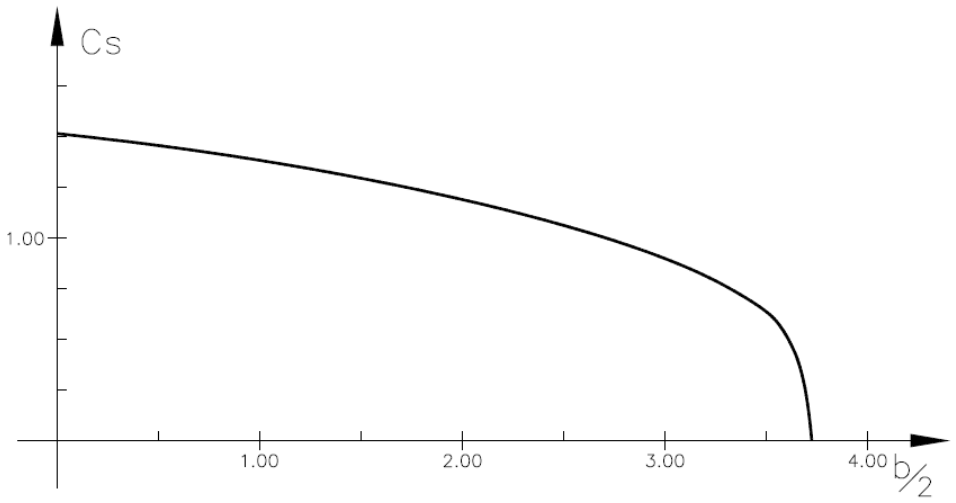

Figure 20 – Chord distribution for the Stender wing (Adaptation of Figure 4 page 124 of ISCOLD (2002))

The stender method alone will not be able to represent all the behaviour of the wing that is desired by this study, since the method calculate the load distribution along the wingspan but do not depict the torsion in which an actual wing is submitted.

In order to refine more the load distribution throughout the chordwise, the theory of the wing section proposed by Abbott e Doenhoff (2012) was took account and the load acting in each section of the wing obtained by the stender method will produce a portion of lift and a portion of pitching moment. This moment occurs because of the differences in position of center of pressure and the geometric center of the wing section in which it will depend on a wing profile, already discussed by Abbott e Doenhoff (2012).

For further details of how the load and the moment are applied through the wingspan and the profile chosen, see section 3.0.5.2). At this moment it is important to realize that the load applied will be a combination of the load provided by stender method and the load distribution throughout the chordwise and discussed by Abbott e Doenhoff (2012).

2.1.7 Python in Oriented object approach

Kristem Nygaard and Ole-Johan Dahal were the pioneers in oriented object programing and because of this they have received the ACM turing Award “for ideas fundamental to the emergence of object-oriented programming in 2001” (Black (2013)). Thanks to them, and because of its insight, there are many softwares that uses this approach and in

which it was possible to improve the capacity of this programming to abstract problems into classes and objects that can be instantiated and reused as much as needed.

This paradigm is based on the concept of object in which it can contains data, methods and other objects. Those objects are an instance of one class that can be a subclass of others. Many existents languages nowadays are able to work with oriented object abstraction and several libraries previous developed can be reused and save during the implementation process.

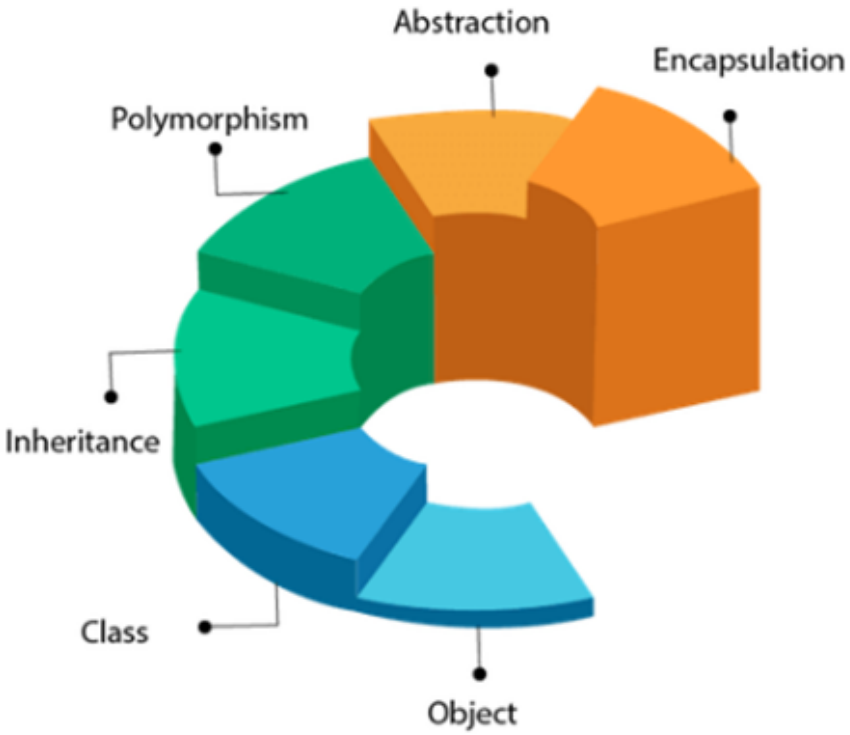

Figure 21 – Oriented Object philosophy

Python is an open source software, free available in the web (Ref python (1000)) with a big community behind it, and also support oriented object paradigm which is ease to be implemented. There are several libraries available to be used with python for a great amount of scientific areas and the most popular are:

- Tensor flow: Library for high performance numerical computation (Google (2021)
- Keras: High-level neural networks API (Chollet (2020)).
- Scipy: Software for mathematics, science, and engineering (Develpoers (2021)).
- Theano: Allows you to define, optimize, and efficiently evaluate mathematical expressions involving multi-dimensional arrays (Laboratory (2020)).

- Panda: Machine learning library that provide data structures of high-level and a wide variety of tools for analysis (PandaStream (2015)).
- EletricPy: "Python Libraries with functions and constants related to electrical engineering." (Stanley (2021)).
- Physics: Educational libraries that can be used for school projects (pyTeens (2018)).
- Engineering Tool: The tool is a physic formula for Engineering or Science (Thotaboot (2018)).

As it can be noted, several of depicted libraries work similar but depending on the application one can be most useful then other and they also can interact each other. There are also others libraries which are not so popular as the machine learning, e.g PyNastran (Doyle (2020)), see Figure 22 as an example.

Figure 22 – Python most popular libraries

The work proposed here are going to use the oriented-object paradigm through the python with some implemented libraries (such as: Panda, Pynastran, Scipy, NumPy) in order to compile the data from the models. The abstraction adopted to perform the analysis and the detail of the package created for the compilation can be seen on section 3.0.6.

3 Method of analysis

3.0.1 Strategy of the Study

An aircraft is composed basically from 3 main components: Wing, fuselage and empennage; and they are sub-divided in several others components. Those components are responsible to distribute the load throughout the aircraft and keep it in equilibrium during the flight.

The main role of the fuselage is to "provide space for cargo controls, accessories, passenger and other equipment" (FAA (2018)). The wing "are airfoils that, when moved rapidly through the air create lift" (FAA (2018)). The empennage has as main functionality to stabilize the aircraft during the flight, since the center of gravity is not coincident with the center of lift.

The present work are going to focus on the wing, the component responsible to keep the lift of the aircraft while it is flying. It is going to be studied the load distribution along the wing spanwise and how this load flow through one component to another such as spar to skin and skin to rib. The methodology used to calculate load distribution along the wing spanwise was discussed in 2.1.6.

There are several configurations of a wing and also great amount of ways in which the wing can be attached to the fuselage. According it was described in (FAA (2018)) "The internal structures of most wings are made up of spars and stringers running spanwise and ribs and formers on bulkheads running chordwise (leading edge to trailing edge)". In the Figure 23 it is possible to see the principal components that comprises an aircraft wing, in which the manufacturing process of those components can vary according to the aircraft and also the way in which the components are attached each other is not a pattern.

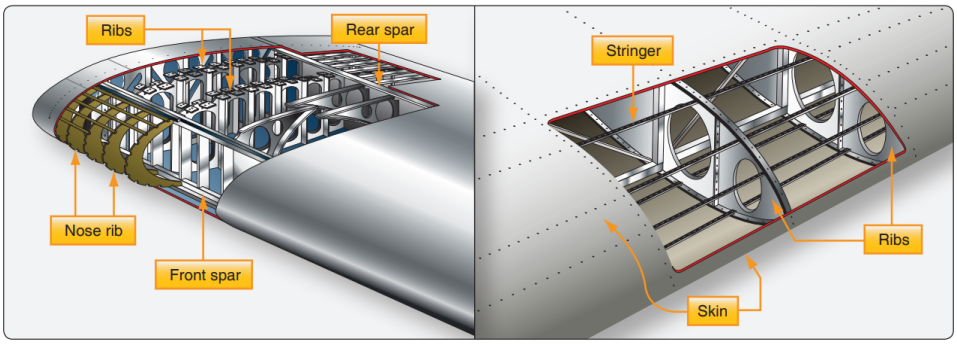

Figure 23 – Wing structure nomenclature (Adaptation of Figure 1-23 of FAA (2018))

In order to simplify the analysis and make possible to focus in what really matter for the study proposed, a didactic wing box with two spars attached to the skin and some ribs distributed along the spanwise are going to be simulated. Since the work is going to address the wing structure and specially the attachment between skin and spa, the wing trailing and leading edges were not considered in the model.

The wing, ribs and spars are supposed to be built by 7475-T761 aluminum, and its properties are provided from Niu (1997), the thickness of the components are presented in table 1 and the overview of the wing studied is presented in Figure. 24.

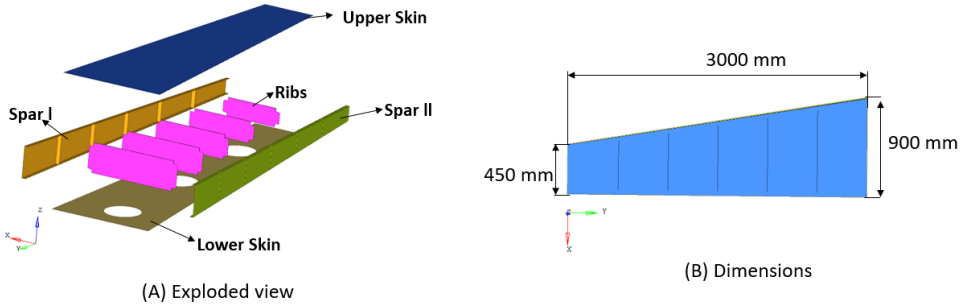

Figure 24 – Wing overview and dimensions

Table 1 – Components and thickness of the wing analyzed

Component	Thickness [mm]	Material
Skin	3.00	
skin Reinforcement	3.75	7475- T761
Ribs	3.00	
Spars	4.50	

The fastener used to accomplish the attachment is going to be HST-10, made of titanium in which its properties is shown on Table 2 and are provided from tek.com/ (2018). In Figure. 25 it is also possible to see the detail of the fastener used in this study.

Table 2 – Fasteners used

Fastener	Diameter [mm]	Material
HST10-5	3.97	Titanium

The attachment between the ribs and spars and between the ribs and skins are going to be a shear joint (see section 2.1.1) with a single row and with at least 3 times the diameter of the fasteners for the distance between the fasteners and 2 times the diameter

for the distance between the center of the hole and the edge, as it can be seen on Figure 25.

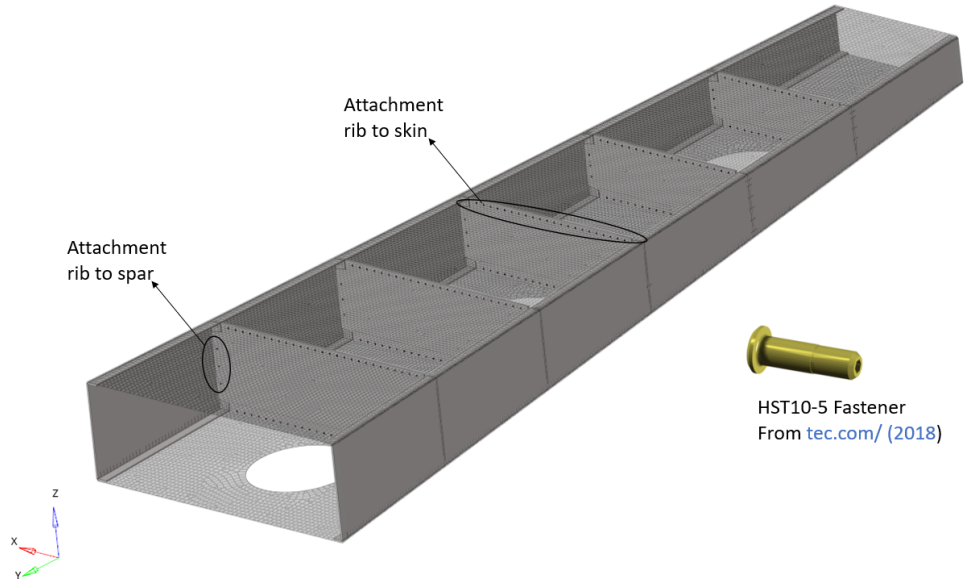

Figure 25 – Ribs attachment region

In this way, by considering different level of modelling approach, the propose is to investigate the behaviour of the load distribution throughout the attachment region between the spar and skin in an aircraft wing under flight loads. Furthermore, as an additional, the configuration of the joint will also be investigated. In this way three types of attachment between the skin and spar are going to be analyzed, being them: single, staggered and double, as it can be seen on Figure 26.

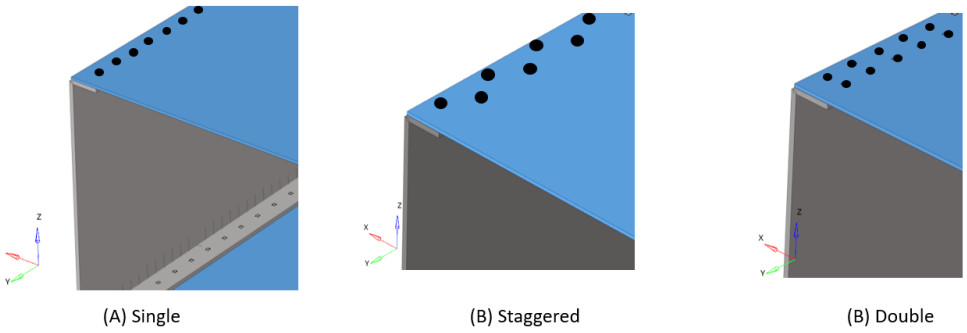

Figure 26 – Types of attachment analyzed in spar region

No differences between the single and staggered attachment is expected if the wing was submitted only for bending load. So, according to section 18 the load distribution

throughout wing spanwise will comprises bending and torsion. The torsion load will drive the load throughout the X direction and because of this the difference between single and staggered can be investigated.

The models described above are going to be the focus of this study and it will be built in three different levels of details in order to compare the results. The models from 1 thru 3 are going to follow the hierarchical tree according to section 8 and Figure 27, in which the model 1 is going to be the less representative, while the model 3 will be the one with more detail to represent the actual structure and it will be used as the reference to compare the results.

The results are going to be compared considering four corners being the corners 1 and 4 located at the upper skin and corners 2 and 3 at the lower skin

The following sections will detail each one of the models, going deep in the modeling approach, the type of element used and the way the load will be extracted from the models.

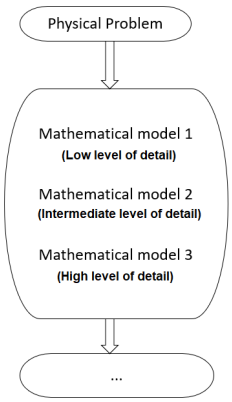

Figure 27 – Hierarchical scheme for the study proposed

3.0.2 Model with low level of detail)

The model with low level of detail comprises the most simple model capable to represent the geometry without loss of the actual representation of the structure, using the most simple elements able to represent thickness, curvature and flexibility. In this model the stiffness of the joint, in which are comprises the hole, the body of the fastener, the clamp between the plates and other joints characteristics are going to be omitted and the connection between the skin and spars, and even the connections between the skin and ribs are going to be simulated by means of coincident nodes.

Due to the simplification, this model will not represent the types of attachment proposed in section 2.1.5 and also some loss of flexibility is expected. In this way the load distribution in the fasteners along the wing spanwise for those different type of fasteners are going to be followed the methodology described in 3.0.6.

Two nodes bar elements with Bernoulli-Euler's formulation are going to be used to simulated reinforcement and caps of spar and skin, as it can be seen on Figure 28

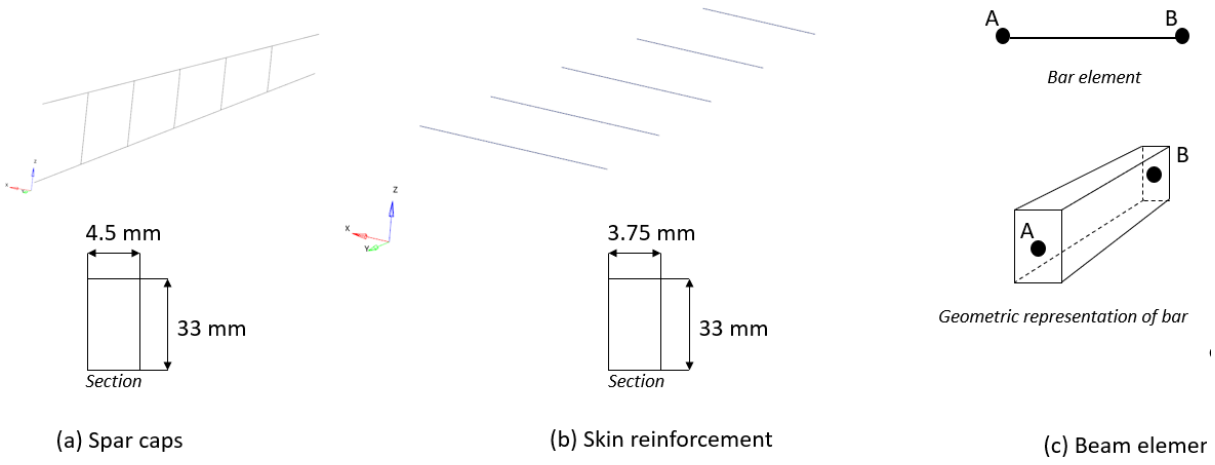

Figure 28 – Bar element representation

The Table 3 presents the properties of the bar elements used in each region and it was performed in order to keep inertia of the regions.

The bar elements has a characteristic in its properties which it is possible to confer displacements in x, y and z direction as it can be seen on Figure 29.

Table 3 – Elemen bar properties

Region	Area [mm^2]	Displacement	Inertia Ix [mm^4]	Inertia Iy [mm^4]
Spar cap (Left)	148.5	w_1A and w_1B = -16.5 others = 0	13476.5	250
Spar cap (Right)	148.5	w_1A and w_1B = 16.5 others = 0	13476.4	250
Upper Skin	123.8	w_3A and w_3B = -16.5 others = 0	11230.3	145
Lower Skin	123.8	w_3A and w_3B = 16.5 others = 0	11230.3	145

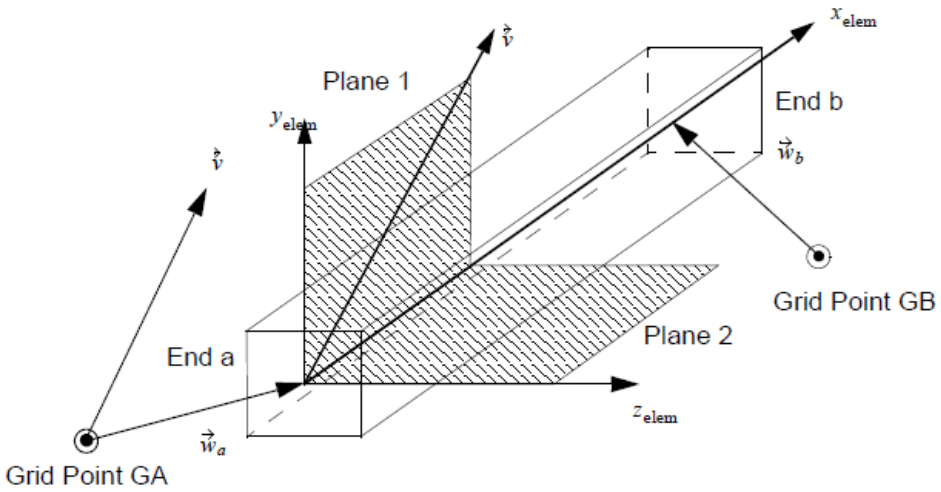

Figure 29 – Bar element (Figure adapted from MSCSoftware (2018))

3.0.3 Model with intermediate level of detail

The model with intermediate level of detail is more complex than model 1, specially in joint regions where the Rutman approach (discussed in 2.1.5) is used.

For this model, all components (spar, skin and ribs), including its reinforcements are going to be modeled considering shell elements with serendipity formulation as it was performed for planar faces in Model 1.

The fasteners are going to be modeled using the methodology described in section 2.1.5. According to the method, two stiffness must be calculated in the region where the fastener touch the plate, translational and rotational stiffness and those values must be assigned to the bush element as presented in Figure 15. The value for translational stiffness is calculated based on equation 2.4 whereas the rotational stiffness is calculated based on equation 2.13.

The values of this stiffness calculated for each region are presented in Table 4. Furthermore, the Figure 31 presents the FEM for intermediate model.

Shell elements with serendipity formulations are going to be used to simulate skins, spars and ribs planar faces. The most of the elements are going to be QUAD4, but in some regions TRIA3 was necessary. The quality of the mesh has followed the pattern described in 3.0.7, in order to avoid bias in the results.

Figure 30 shows the representation of spar, skin and ribs. The average size of the elements is 30mm.

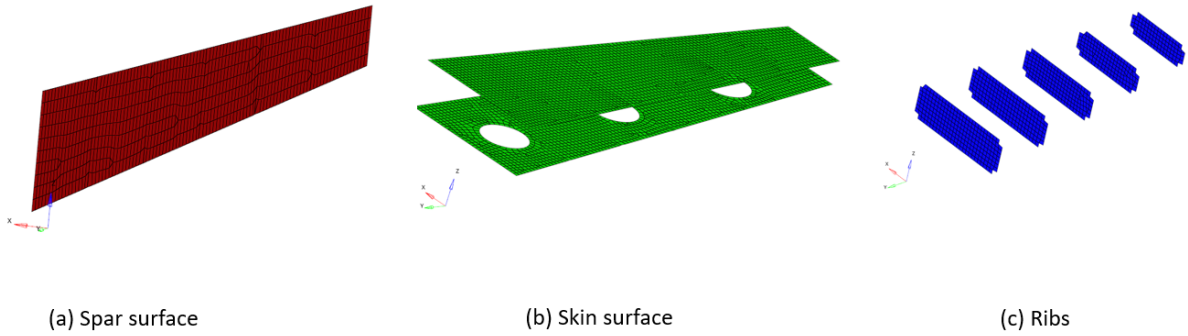

Figure 30 – Shell elements for Model 1

Different from model with low level of detail, there are going to be three different FEM models for the model with intermediate level of detail, one for each type of attachment, Single, double and staggered and the static analysis for each one of this configurations are going to be performed separately. Because of the level of detail of this model, its flow of load are going to be stored and used in more detailed model 3.

Table 4 – Joints properties

Component	Thickness [daN/mm^2]	E_{plate} [daN/mm^2]	$E_{fastener}$ [daN/mm^2]	Translational stiffness [daN/mm]	Rotational stiffness [daN.mm/rad]
Upper skin	3	7100	11400	13125.41	9844.05
Lower skin	3	7100	11400	13125.41	9844.05
Reinforcement upper skin	3.75	7100	11400	16406.76	19226.67
Reinforcement lower skin	3.75	7100	11400	16406.76	19226.67
Ribs	3	7100	11400	13125.41	9844.05
Spar left side	4.5	7100	11400	19688.11	33223.68
Spar right side	4.5	7100	11400	19688.11	33223.68

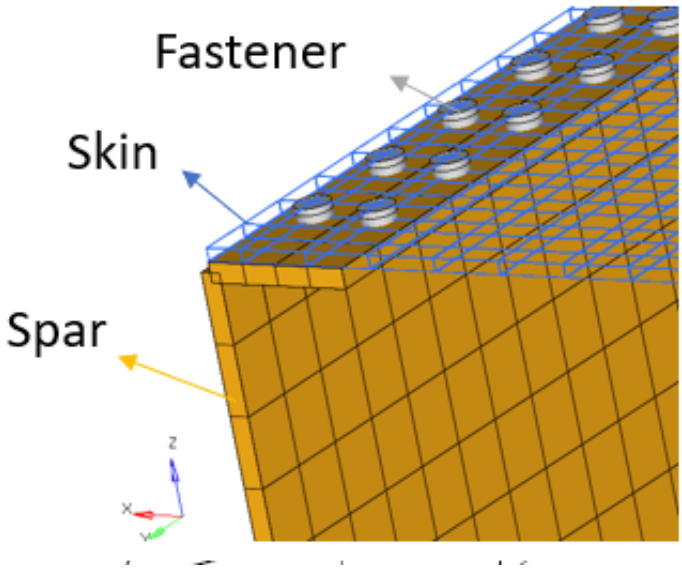

Figure 31 – Intermediate model

3.0.4 Model with high level of detail

The refined model is the most complex of them in numerical point of view, since it is using more complex elements with more complex function of shape besides the nonlinearities which were considered. The most of the elements used are CHEXA with 8 nodes, but when it is not possible CPENTA elements with 6 nodes are also used.

Different from others, this model do not use simplifications to simulate the connections, it uses Finite Element Approach in order to simulate all parts and behaviour of the connection.

Another important difference in this model, when compared with others simplifications, is that it is going to be built only a portion of the whole wing, since it is impracticable to work with the whole model considering this level of detail.

Three models are going to be built in order to comprehend the three types of attachment proposed in this study (single, double and staggered). The region chosen to be portioned will be the one that presents the higher flow of load along the wing span wise. As it can be seen on Figure. 32, the critical region is located near the root of the wing and so close to the first rib. This is an expected behaviour since there is an increase in wing stiffness in rib region and consequently an increase in flow of load.

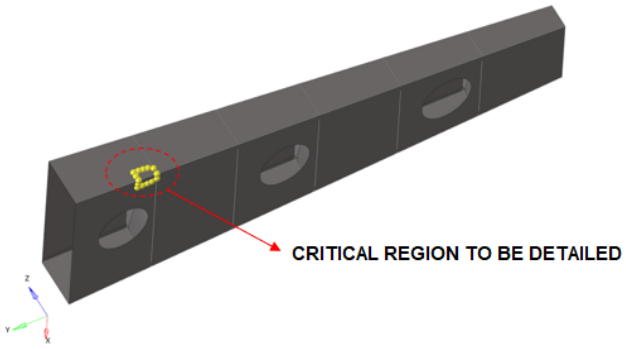

Figure 32 – Region choose to be detailed

The Figure. 60, Figure. 61 and Figure. 62 shows the three models discretized according to the approach proposed. All the models are going to be simulated considering nonlinearities of the material, large displacement and also considering the nonlinearities due to the contact. The models will be considered with no gap between the plates and also with no pre-tension in the fasteners. It is known that the pre-tension load could led to different load distribution in the fasteners, and an parallel study was done in sec. **??**

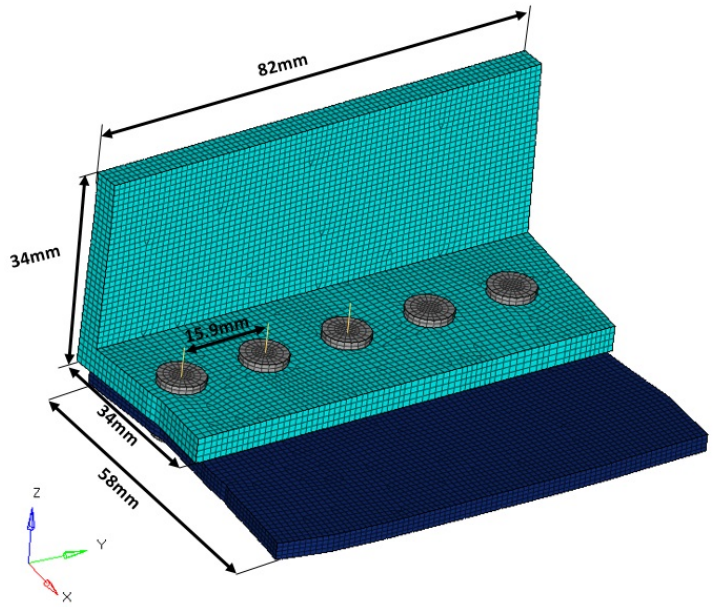

Figure 33 – Region choose to be detailed - Single

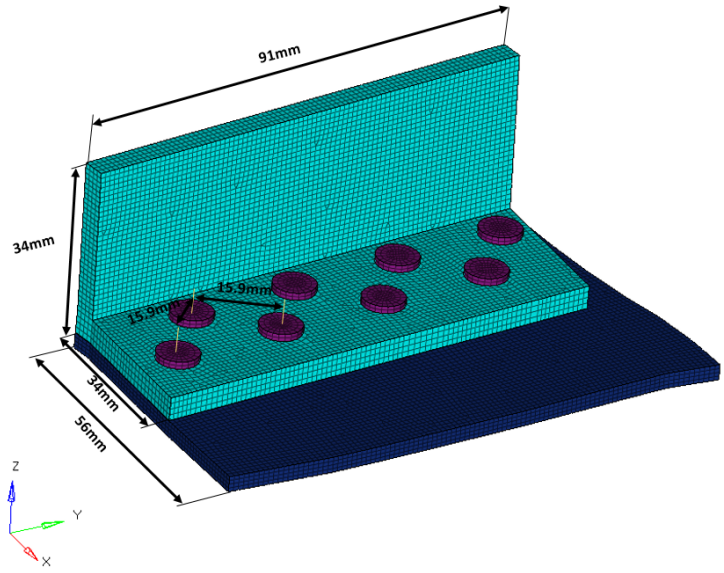

Figure 34 – Region choose to be detailed - Staggered

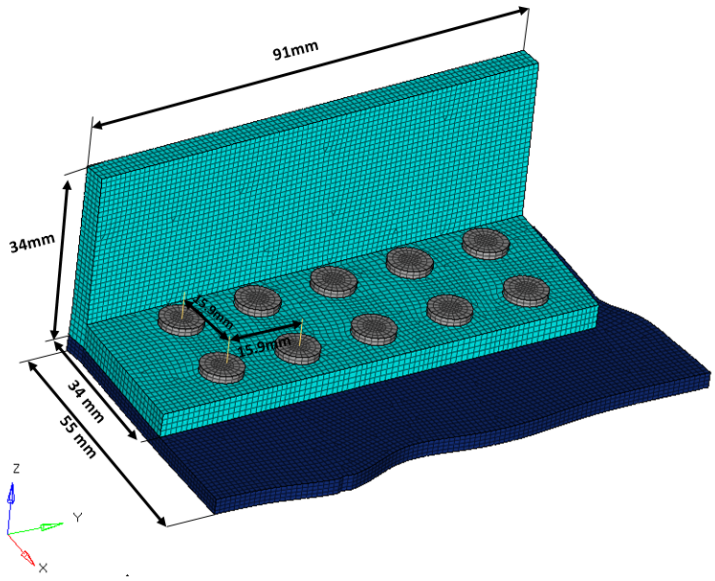

Figure 35 – Region choose to be detailed - Double

Once this model is a dedicated model, specific boundary conditions must be considered, and it will be discussed in section 3.0.5.3

3.0.5 Boundary Conditions

3.0.5.1 Constraints for Global model

During the flight an aircraft is submitted to many loads in different directions and the equilibrium of those loads are responsible to keep the aircraft flying. In a generic point of view, the center of gravity of an aircraft is located in the fuselage while the wings are responsible to carry the flight loads. Figure **??** presents the mainly loads acting in an aircraft, and it is possible to note that the empenage works as a stabilizer for the aircraft loads.

As it can be seen on Figure **??** an aircraft wing can be abstracted as a beam fixed in its root. This is a valid simplification because of the behaviour of the aircraft. In this way, the wing studied in this work is going to be attached in its root by restricting all degrees of freedom of the nodes in such region, as it is presented in Figure 36

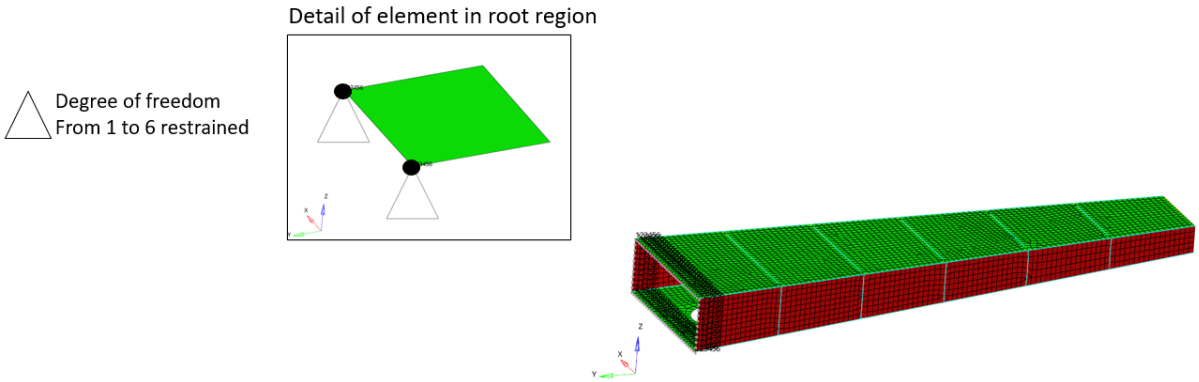

Figure 36 – Constraints in Aircraft wing root

As the skin is simulated using QUAD elements with serendipity formulation, in which each node have 5 degree of freedom, the component of stiffness of those degrees of freedom of the restrict nodes will not be considered in the global stiffness matrix of the model.

This simplification, and specially the stiffness neglected at the root of the wing could result in a unreal values of strain or even in flow of load as it can be noted in the results obtained and presented in section 4.

3.0.5.2 Wing Load Distribution

ISCOLD (2002) in its study has discussed about aircraft loads and several methods are presented. This present work do not aim to go deep in load analysis, since the focus is to investigate the differences between modelling techniques. In order to distribute the load through the wing spanwise using a coherent approach, the Stender method presented by ISCOLD (2002), which is a summary of the elliptical lift distribution discussed deeper by Jr (2010), will be used.

Once the first two modeling approach are going to be a linear analysis, an arbitrary load of 4000daN was supposed to be applied in the didactic semi-wing. As it is considering a linear analysis, this total load applied can be linearized for whatever value needed.

The simple elliptical lift distribution alone is not able to investigate the flow of load in Y direction, specially regarding staggered configuration. In order to solve this problem, the aerodynamic moment was calculated using the approach presented in Abbott e Doenhoff (2012), and according to equation bellow.

$$L = \frac{1}{2}.\rho.V^2.S_w.C_L \tag{3.1}$$

$$M_x = \frac{1}{2}.\rho.V^2.S_w.\bar{c}.C_m \tag{3.2}$$

and then:

$$M_x = \frac{C_m}{C_L}.L.\bar{c}. \tag{3.3}$$

Where: L is the lift

M_x is the moment

ρ is the air density;

V is the reference speed;

S_w is the plain view wing area;

$\bar{c}$ is the mean aerodynamic chord, in this case it is 700mm.

C_m is the moment coefficient.

C_L is the lift coefficient.

By considering the profile NACA 006, from Abbott e Doenhoff (2012), with the angle of attach equal to 0, the C_m value is -0.2 and C_L is 1.2 , the equations above can be combined and the moment can be calculated as it is shown on equation 3.3 . In this way

the forces and moment were distributed considering stender approach and are presented in Table 5 and Figure 37.

Table 5 – Loads distribution through wing span wise

Station [mm]	L [daN]	My [daN.mm]
500	847.22	-98842.16
1000	797.87	-93085.18
1500	734.99	-85749.17
2000	656.18	-76554.18
2500	552.78	-64490.64
3000	246.62	-28772.72

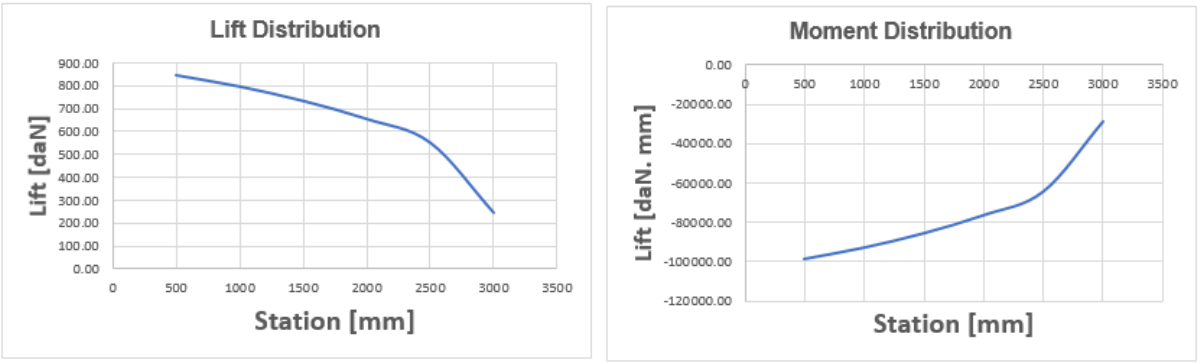

Figure 37 – Forces and moments applied in each station

In the model it was considered each rib as a station and the loads were applied there. In order to apply the forces and moment calculated, a rigid element was used and its independent node was considered being at 1/4 of the chord, as it can be seen on Figure. 38.

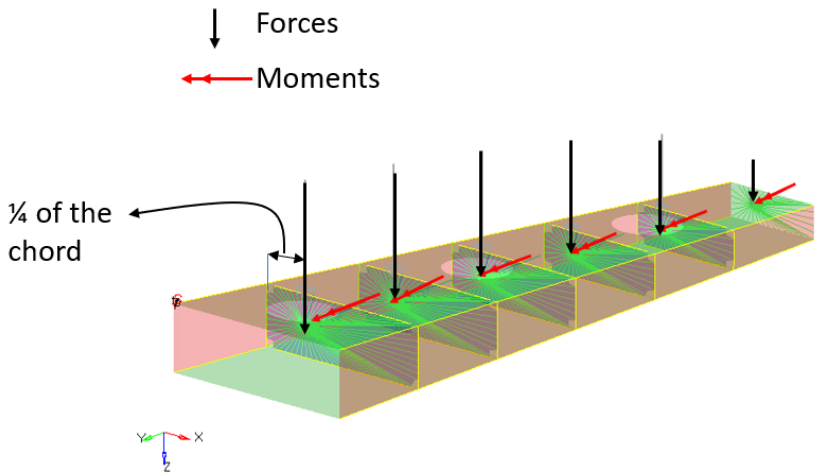

Figure 38 – Equivalent forces and moments applied in each station

3.0.5.3 Boundary condition for dedicated model

The dedicated model aims to simulate the flow of load through the fasteners considering all structural conditions of the actual structure. This technique was adopted since its is practically impossible to simulate all attachment regions of the wing, due to the amount of degrees of freedom requested by a model like that.

The method consist in separate only a portion of the wing and to detail it as much as possible. The region chosen was the one in which have the critical flow of load between model 1 and model 2. The analysis of those two first models were performed and the resultant of the shear load of the fasteners, in spar and skin region were considered as the parameter to point of critical region. Figure. 32 shows this regions.

The boundary condition will consider the displacement of the interface nodes between the portioned region and the rest of the wing, and the enforced displacement will be applied in the model with high level of detail. As the model with such level of detail is more refined than the model with intermediate level of detail, rigid elements will be used to connect the point of enforced displacement and the elements of this model, as it can be seen on Figure. 39

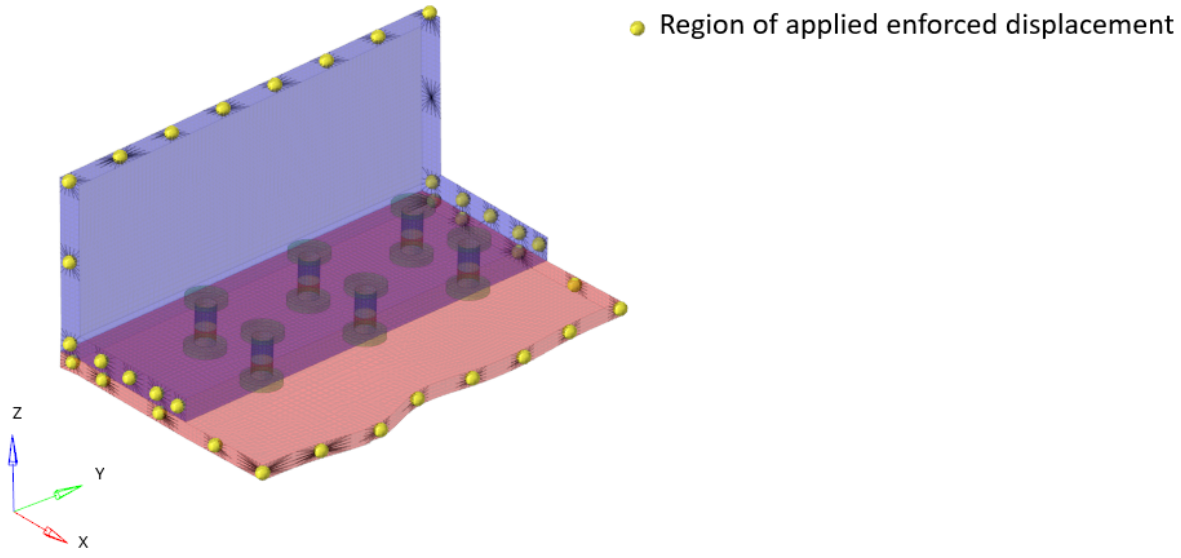

Figure 39 – Enforced displacements for dedicated model

The approach of apply enforced displacement works together with the constraints, thus the stiffness matrix is multiplied by displacement vector in order to obtain the force vector and consequently the stress field can be calculated, therefore no load are applied in this model.

This technique could be validated considering the same portion of the wing but with the original model and the stress field is compared between the models and it is going go be presented in section. 4.4.1

$$[K].[d] = [F] \tag{3.4}$$

Where

K is the stiffness matrix

d is the displacement vector

F is the load vector, and in this case is a vector full of zero

3.0.6 Python packages for results collector

According it was described in section 2.1.7, python code has already implemented in itself several libraries which can help to work with a great amount of data in a fast way as well as using oriented object abstraction.

In order to facilitate the data acquisition and the process of comparison, a oriented object abstraction by using Phyton was performed, and the architecture of the packages created is presented in Figure. 40.

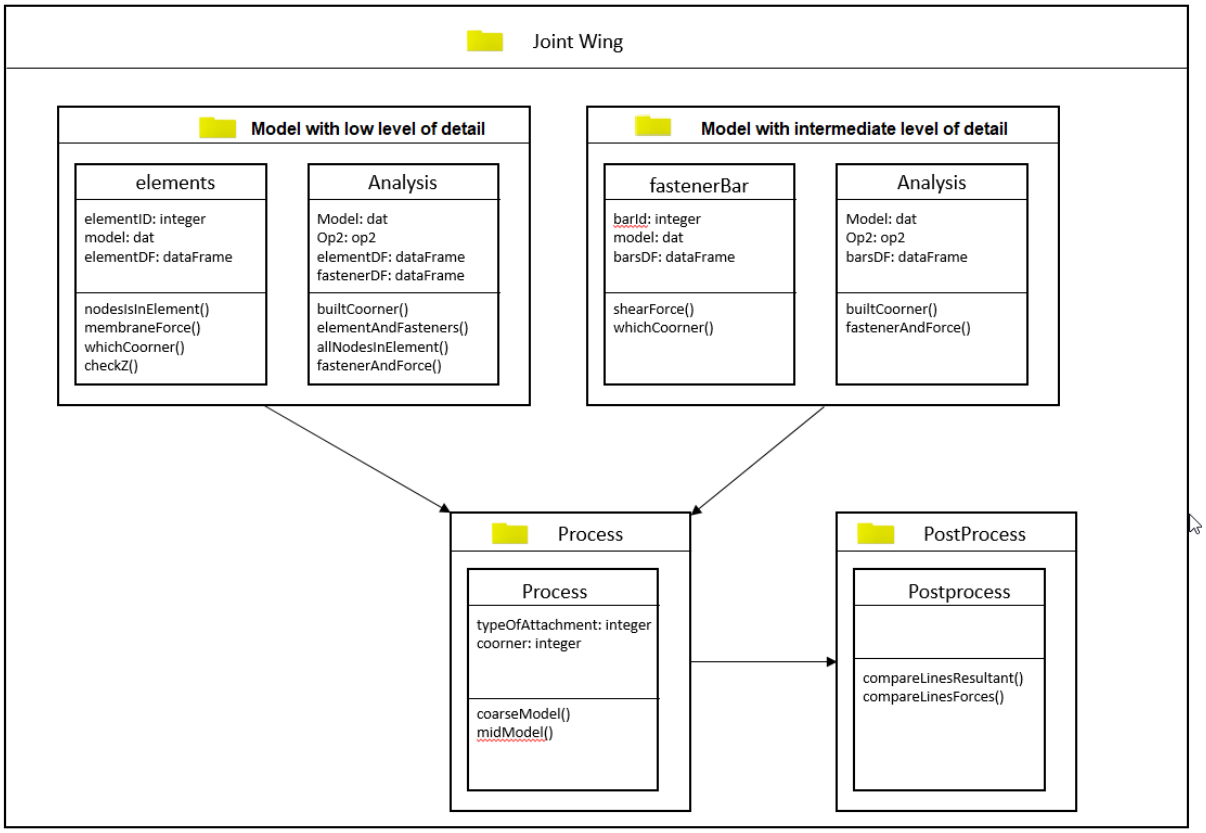

Figure 40 – Packages architecture

As it can be seen, the package "JointWing" contains four others packages and a total of six classes were implemented. The two main packages is related to the models in hierarchical abstraction, the "LessDetailed" and "ILdetail", and those packages have two more packages to support them, the "Process" and "PostProcess" packages.

Two principal classes for the main packages were created, one related to the elements and other to perform the analysis, and they had to be splitted because of the abstraction of the models. The model with low level of detail works with the element flow of load to calculate the fastener load, while the intermediate model represent the fasteners as a combination of springs and bar elements, and the fasteners forces is provided directly from bar element forces.

Basically the classes "elements" (or "fastenerBar") has the role of determine the load acting in each element and organize the data. The main difference between those classes and which is important to point out is the abstraction process for the model with low level of detail.

Related to the model with low level of detail, for each one of the attachment it was took account its coordinate system and it was verified if those fastener is within of the element, and the load that flow through the current element was assigned for the fastener. If there are more than one fastener within the element, the load is divided by the number of fasteners. In order to guarantee the nodes are within the element, a vector product using the node analyzed and the nodes of the element were performed as it can be seen on Figure. 41 , and Figure 42 shows the workflow of the method used to determine those condition.

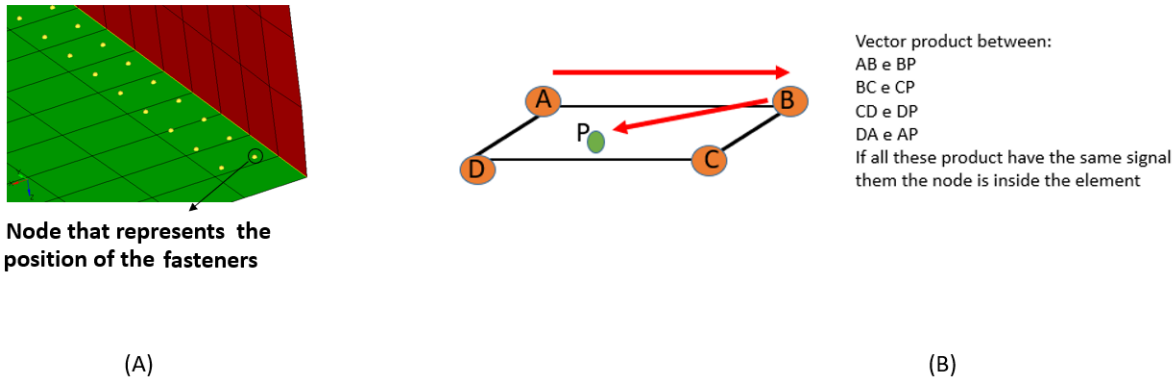

Figure 41 – Fastener Analysis for model with low level of detail

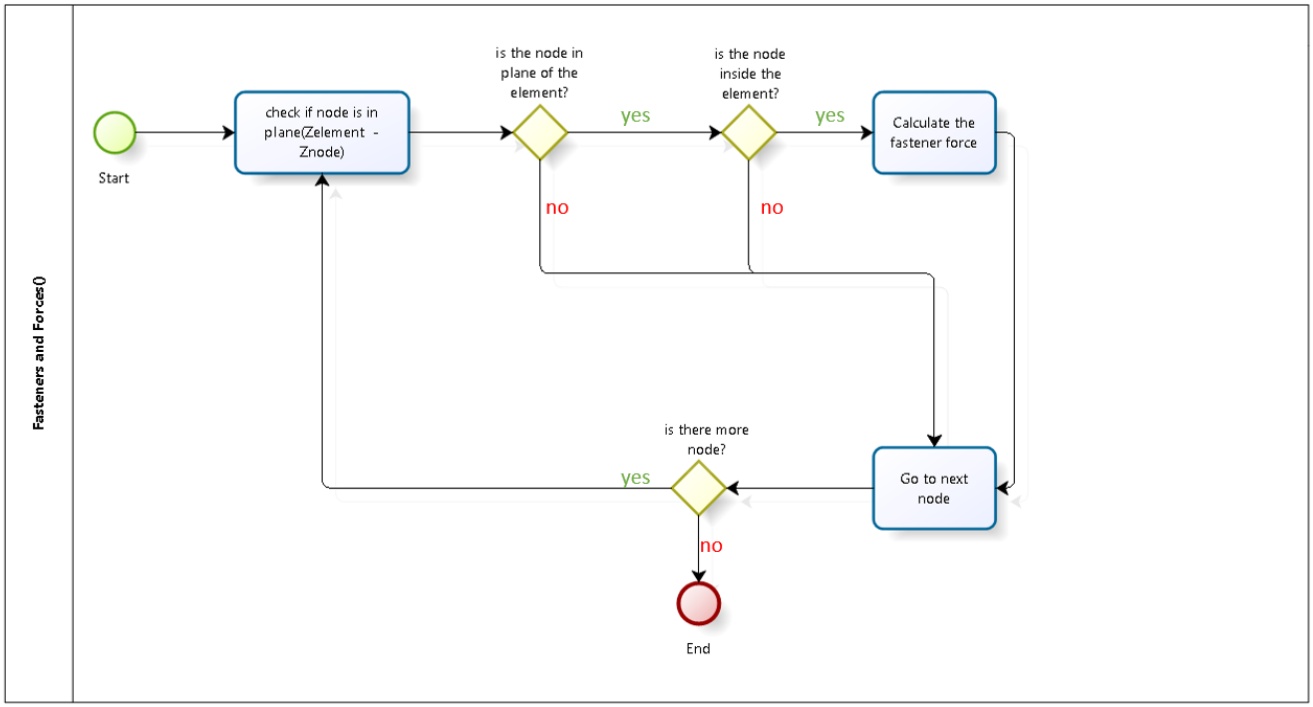

Figure 42 – Workflow to calculate fasteners force for model with low level of detail

The classes "analysis" for both packages have the same functionality, which is to built the corner to be analyzed, using the method "builtcorner", and to built the array with the fasteners analyzed, the forces of those fasteners and its coordinate system along wing spanwise. Those data are going to be very important to generate the graph to compare the results along wing spanwise. Figure. 43 shows each corner analyzed in this study.

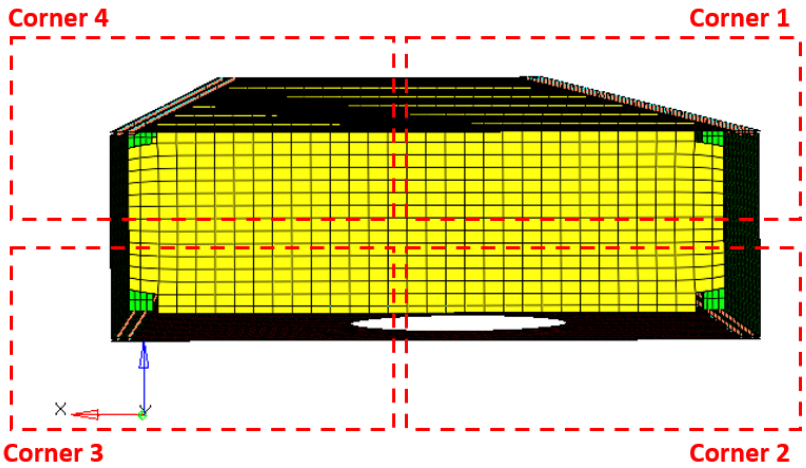

Figure 43 – Detail of each corner analyzed in this study

The package "process" has only one class, called "process" as well, which is responsible to choose which type of model needs to be evaluated being them the model with low level of detail or the model with intermediate level of detail. Besides the type of model, it is also needed to indicate in which corner the results are going to be collected. So, to instantiate the class model, it is mandatory to indicate in which model and which corner the result must be evaluated.

The package "Post Process" is responsible to generate the comparative graphs. The class inside this package is able to compare the results provided from one type of model or compare the data from both models.

Among several examples, it will be listed some kind of comparison which can be accomplished through the class "post process".

- For one type of abstraction (model with low or intermediate level of detail), it is possible to compare the shear load acting in each fastener along wing span wise for the four corners analyzed;
- It is possible to compare the load distribution along wing span wise in each fastener, for a specific corner in both abstraction model.
- It is possible to choose the direction of the load analyzed as well as the resultant of the force vectors.
- it is possible to compare the principal stresses and its directions along wing span wise.

Several others results, which is provided from "*.op2" file, can be extracted and compared using the packages implemented, and the examples aforesaid are only a demonstration of the capability of the packages. It is possible to see in section 4 more results extracted using the packages implemented and presented in this current section.

3.0.7 Mesh Quality

The Nastran solver check some geometric properties of elements before starts to run the analysis. Those pre-check mesh quality is very important in order to guarantee a result more coherent. Five geometry properties of each element are verified as follow:

- Skew angle: must be lower than 30 degree
- minimum internal angle: must be greater than 30 degree
- Maximum internal angle: must be lower than 150 degree
- Warpping factor: must be lower than 0.05
- taper ratio: must be lower than 0.5

Those criteria adopted by the Nastran aims to avoid poor accuracy in the result of the analysis. Bellow it will be described how Nastran calculate those geometrical properties as well as an short explanation of each one of them.

Skew Angle: Two lines that connect the mid point of an edge of the element to another are created and the angle between those lines is measured (see Figure 44). The value of skew is the difference between the ideal angle (90°) and the angle measured. So the value of skew will be the worst value between the four calculated angles.

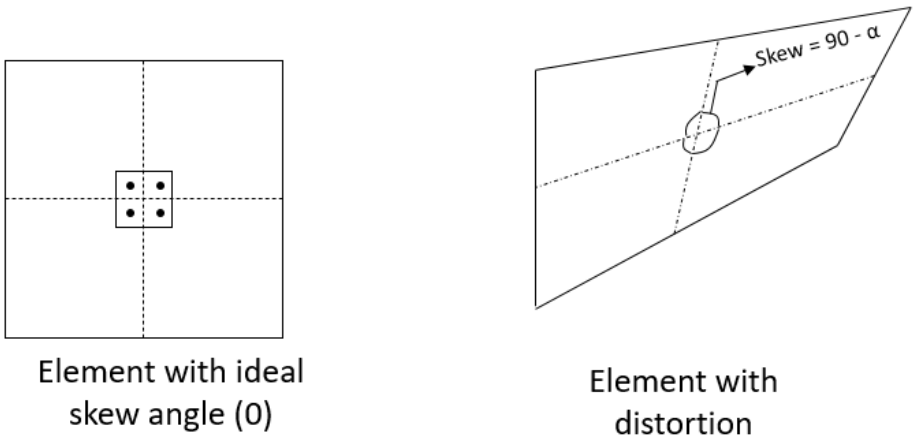

Figure 44 – Skew angle

Minimum and Maximum internal angles: Nastran will calculate internal angle for quad and tria, according it is presented in Figure 45

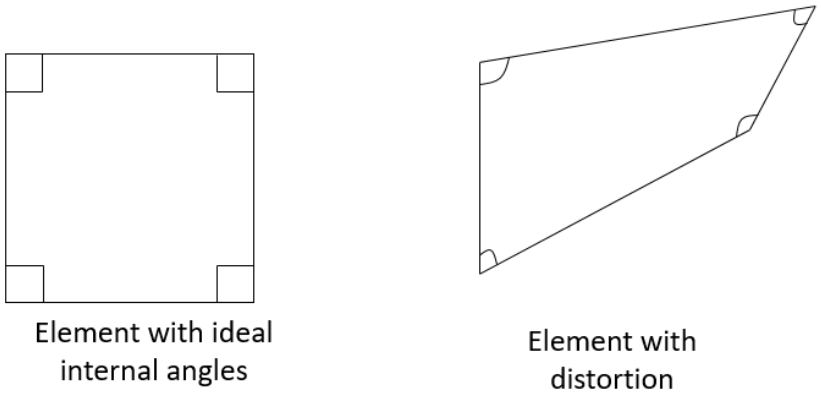

Figure 45 – Internal Angles

Warping factor: This is a measure of how far an element is of being planar. Clearly this factor is not applicable for tria elements since three points define a plane.

For quads, the calculation is done by constructing a plane using the average of four points. This means that the corner points of a warped quad are alternately H units above and bellow the constructed plane. This value is then used along with the length of the elements diagonal in the following equation:

$$WC = \frac{2H}{D1 + D2} \tag{3.5}$$

Where WC is the warping coefficient, H is the height or distance of the nodes to be constructed plane and D1 and D2 are the length of the diagonals. Thus a perfect quad has a WC as zero.

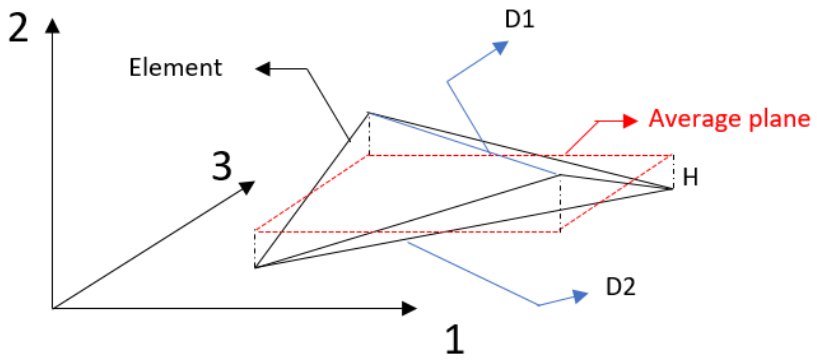

Figure 46 – Warping Factor

Tapper ratio: In order to calculate taper ratio the Nastran "treating" each node as the corner of a triangle (using one of the quads diagonal as the triangle's third leg). The area of each of these four "virtual" triangles are compared to one half of the total area of quadrilateral element to produce a ratio. The largest of these ratio is then compared to the tolerance value.

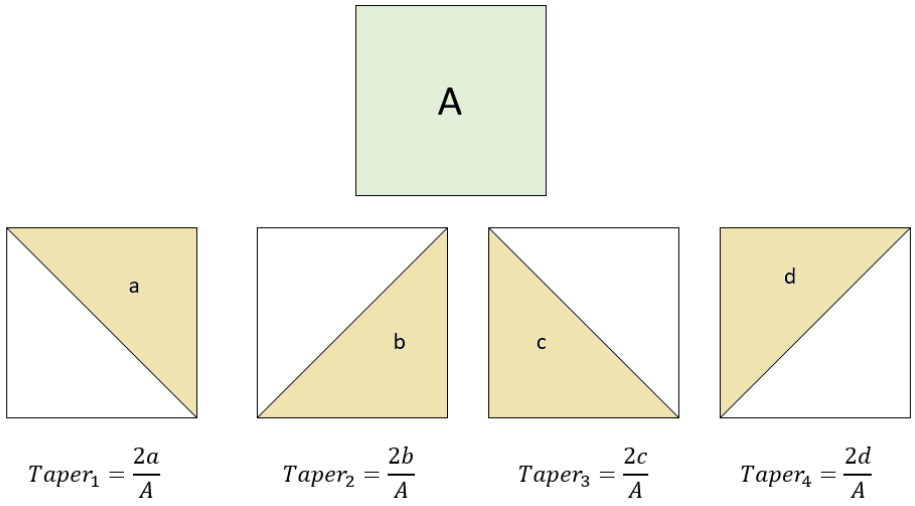

Figure 47 – Taper Factor

A value of 1 is a perfect quadrilateral, and higher number denotes greater taper.

In summary all those geometrical properties evaluated aims to avoid a greater distortion in mesh which can result in a unbalanced stiffness matrix for the element, once this matrix can be obtained as:

$$[k] = \int_V B^T.E.B\, dV \tag{3.6}$$

Where matrix B gives "strains at any point withing the element due to unit values of nodal displacement" (Weaver (2007)) and E is the constitutive matrix which relates stress σ with strain ϵ. The stiffness matrix for a isoparametric shell element can be obtained as:

$$[k] = \int_{-1}^{1}\int_{-1}^{1} B^T(\xi,\eta).E.B(\xi,\eta).|J(\xi,\eta)|.t\, d\xi d\eta \tag{3.7}$$

where ξ and η are the natural coordinates of the element, J is the Jacobian matrix and t the thickness.

As it can be noted, |J| can be ξ and η dependent, which can cause an unbalanced stiffness matrix, making some regions more stiffer than others causing some changes in load

path. For a perfect quadrilateral element, the |J| is 1, so this portion does not influence in stiffness matrix, being this element perfectly balanced.

Those equation above can prove that a distortion in element can cause poor results in which the Nastrar solver tries to avoid. Thus the models proposed in this work have have complied and prevent all critical distortions proposed by the solver.

4 Results

4.1 REFINEMENT

Another important evaluation related to the mesh used in this analysis was the sensibility analysis of the size of mesh, two kinds of refinement were considered, according it is presented in Table 6.

The refinement 1 refers to the current model used for the analysis and comparison presented in this study, and refinement 2 is the same model's dimension but considering the mesh with a half of size of the current model. The comparison of the total displacement was performed and as it can be noted, there is no significant modification in the result.

Those results led to conclude that no matter the element refinement, the behaviour expected will be the same.

The size of mesh used for model with low level of detail is 30mm and for model with intermediate level of detail is 15mm. Besides all models and approaches used were considering the best practices discussed in Schwer (2009).

Table 6 – Mesh sensibility analysis

	Total Displacement [mm]	
Model	Refinement 1	Refinement 2
Low level of detail	18.81	19.14
Intermediate level of detail	21.48	21.66

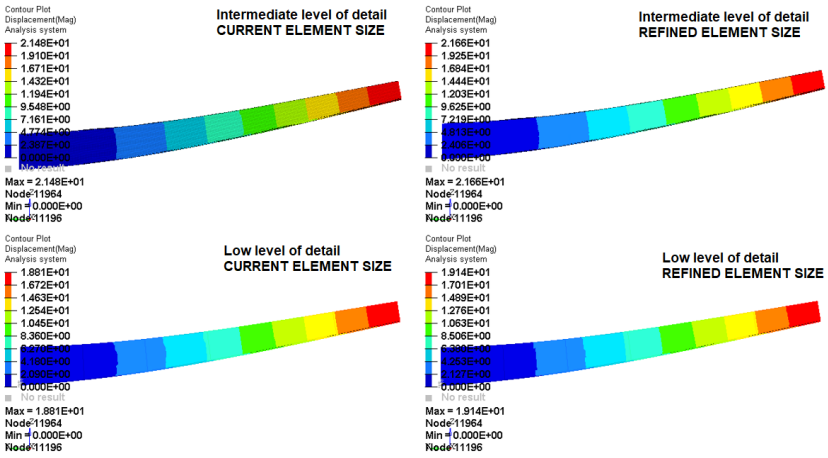

Figure 48 – Displacement Comparison

4.2 MODEL WITH LOW LEVEL OF DETAIL

The results for model with low level of detail are going to be presented in this section and as it was discussed previously, this model consist in a simple representation of a wing lower and upper skin attached to two spars and divided by another five ribs along spanwise. This mathematical simplification do not represent faithfully the stiffness in the attachment region, instead the attachment region is represented as a coincident node of spars, skin and ribs.

The first plot performed and presented in Figure 49 is related to the von-Mises stress field along wing span wise. The von-Mises stress is a scalar value calculated using the relation between principal stresses of each element and it is a good criteria to identify if the material will yield or fracture at some point of the structure. Basically the von-Mises stress is obtained by normalizing the stress tensor of the element and the spectral results of this normalization, which represent the principal stresses are manipulated so as to obtain the scalar von-Mises value .

$$\sigma_{von} = \frac{\sqrt{2}}{2}.[(\sigma_x - \sigma_y)^2 + (\sigma_y - \sigma_z)^2 + (\sigma_z - \sigma_x)^2 + 6(\tau_{yz})^2 + 6(\tau_{zx})^2 + 6(\tau_{xy})^2]^{1/2} \quad (4.1)$$

The results provided from Finite Element model give a discrete stress tensor for each element and it can change depend on the level of detail and refinement of the model, being necessary a good correlation between the actual structure and the mathematical model used to represent it.

As it can be noted, the maximum von-Mises stress happen at the root of the wing where the load is driven for, furthermore there are stress concentration at the inspection holes where it is created a section discontinuity in the wing chordwise. Moreover, while observing corners results, it is possible to conclude that the corner 2 is the most critical among other corners and this results will be also observed for other comparison performed, and also it is important to highlighted that the von-Mises stress field for the model with low level of detail will not change depend on the type of attachment configuration choose (single, double or staggered), since the analysis for considering the load in each fastener will be performed by hand calculation as it was described in section 3.0.2

Another important result to be evaluated in order to have an overall point of view of the model analyzed are the maximum principal stresses an its orientation. In a cantilever beam with a normal load or moment applied in its end, for instance, the load distribution can be calculated according to linear elastic theory and no shear load is expected along beam chordwise.

Conversely, for the aircraft wing proposed in this study and in which it was calculated according it was described in section 3.0.5, in addition to bending moment,

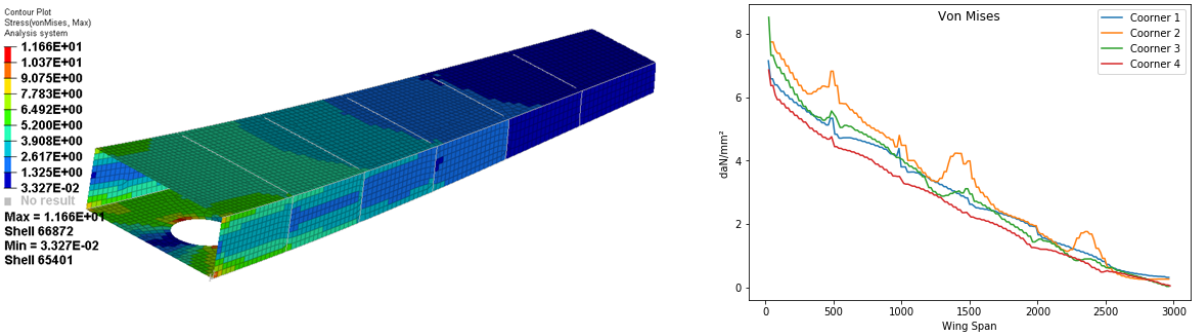

Figure 49 – Von-Mises Stress for model with low level of detail

some torsional moment is expected, and it can cause variation in maximum principal stress direction and consequently appear a shear load along chordwhilse.

The figure 50 presents an example of the stress tensor of two elements located at the root and tip of the wing and, as it can be observed, the maximum principal direction is almost oriented in wing spanwise, but this behavior is not observed at the tip of wing.

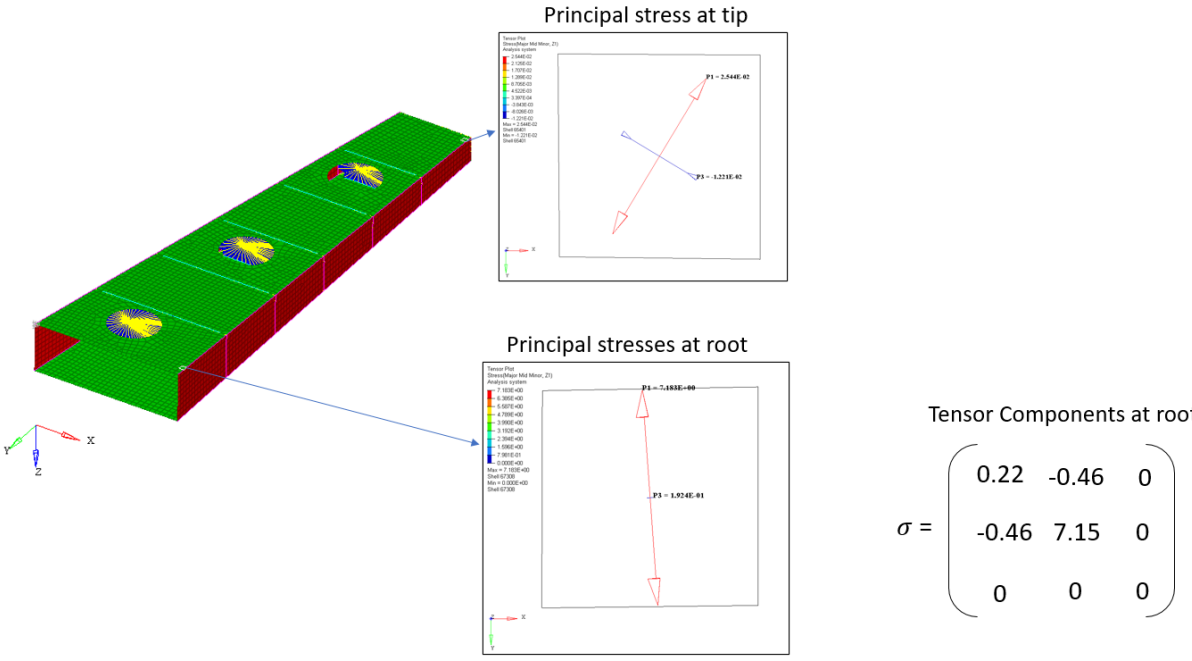

Figure 50 – Tensor Stress components

The result for maximum principal stress and its orientation, it means the positive eigenvalue and the eigenvector for this eigenvalue after normalization of stress tensor of each element, is presented in the following figures.

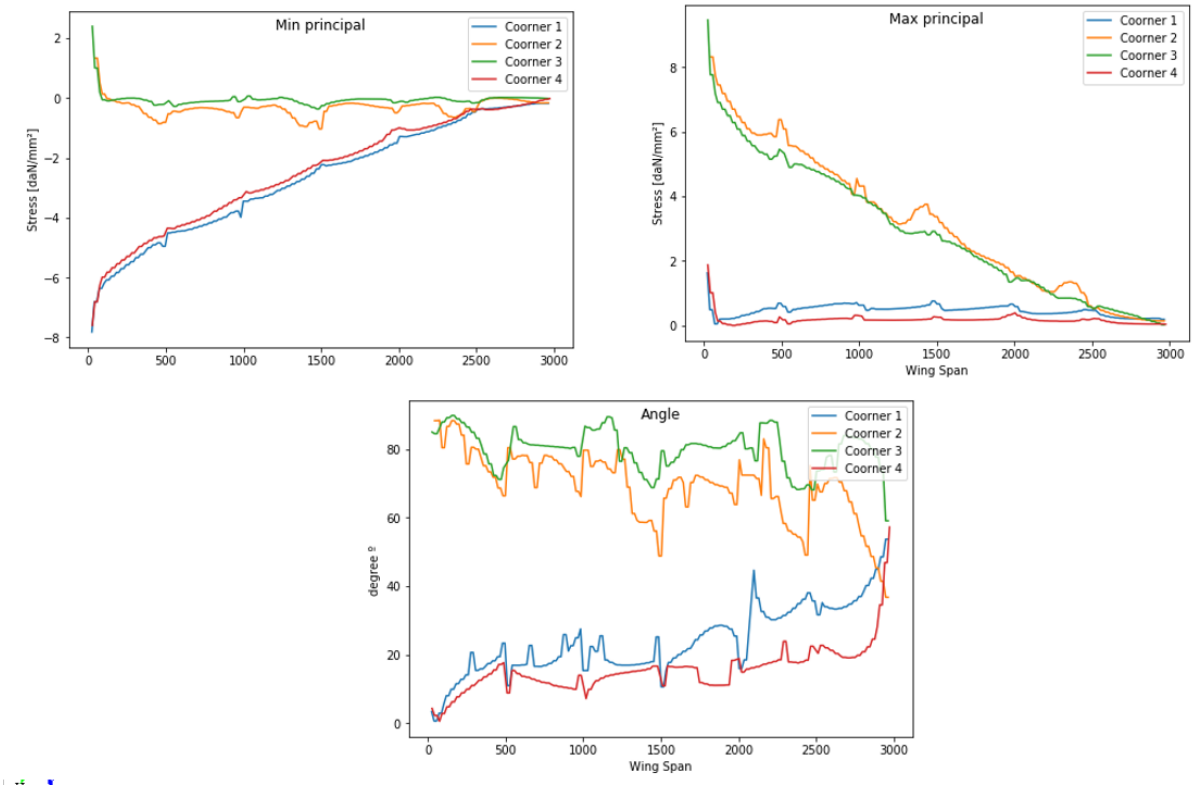

Figure 51 – Principal Stress and its eigenvectors

Once the stress field have presented a good behavior for the model proposed, the focus of this work is to compare the load that flows through the attachment regions (from skin to spars) and the impact in simplify the model to perform such type of analysis during the process of sizing an aircraft wing.

The Figure 52 presents the shear load in X direction along wing spanwise for each one of the corner(already described in section 3.0.1). As it can be noted, the corner 2 is the most critical among others and it was already observed while comparing von mises stress.The Figure 53 shows the shear load for Y direction and, as same as it was observed in X direction load, the corner 2 is the most critical for Y direction. Besides, Y direction is the most critical shear load, since the main load path happen in Y direction, being X direction only responsible to react to torsional load.

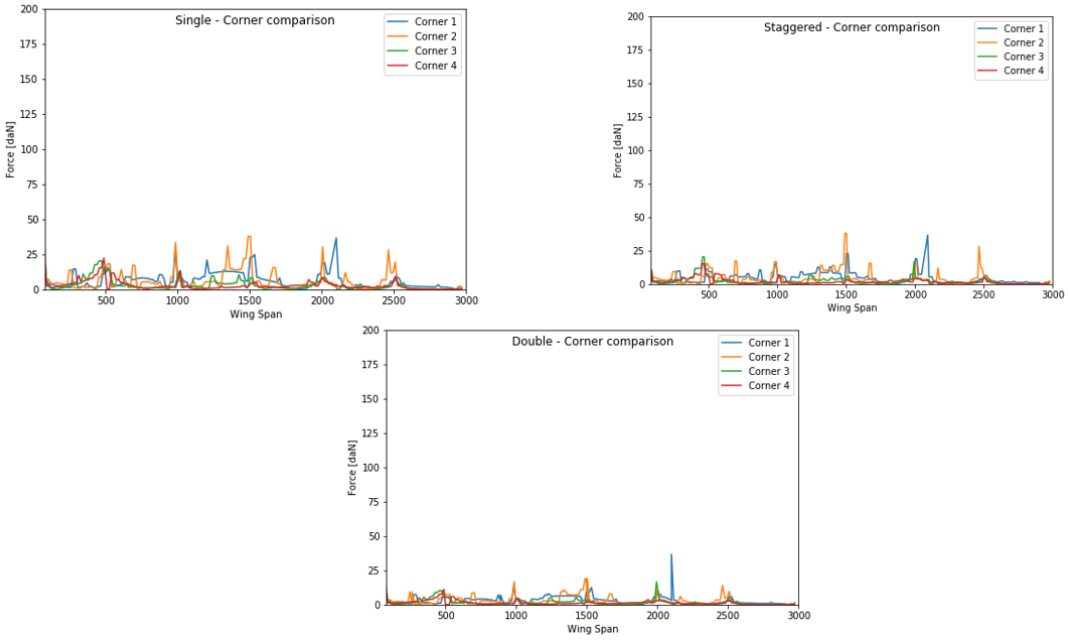

Figure 52 – Model with low level of detail - Shear Load in X direction

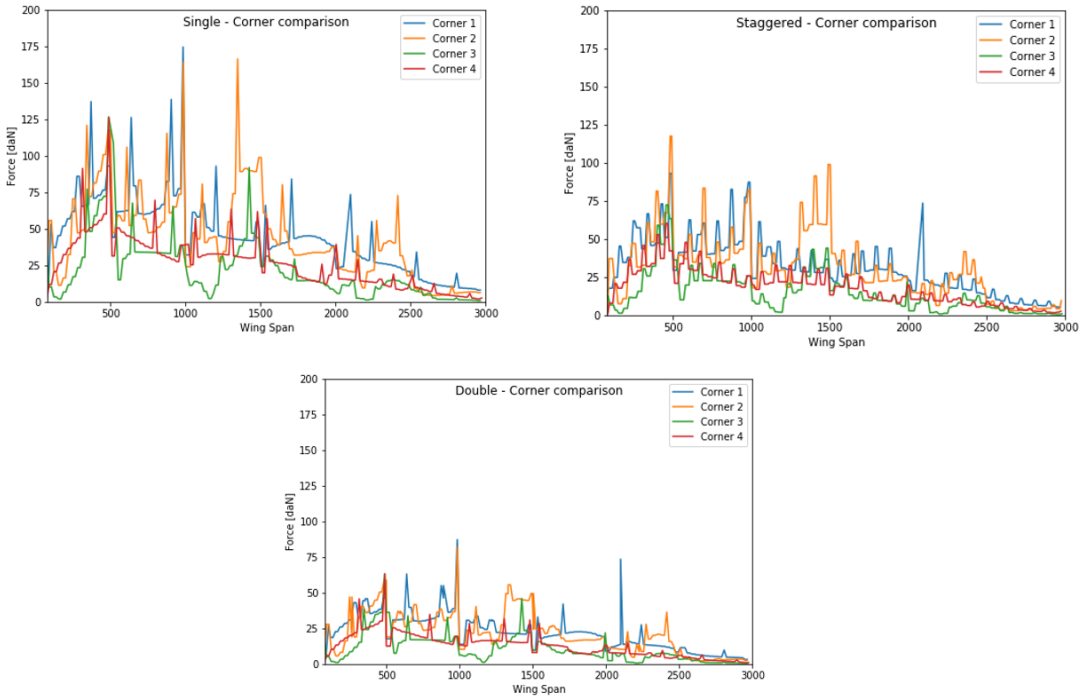

Figure 53 – Model with low level of detail - Shear Load in Y direction

Similarly, Figure 54 present the resultant load for the attachment in the corners. This load represent the resultant shear loads considering a vector summation of Y and X direction . It is not expected great values for normal load for the fasteners due to the nature of the load and those load will not be considered in the comparison. Furthermore the resultant shear load graphs have the same behaviour and almost the same value of shear load in Y direction.

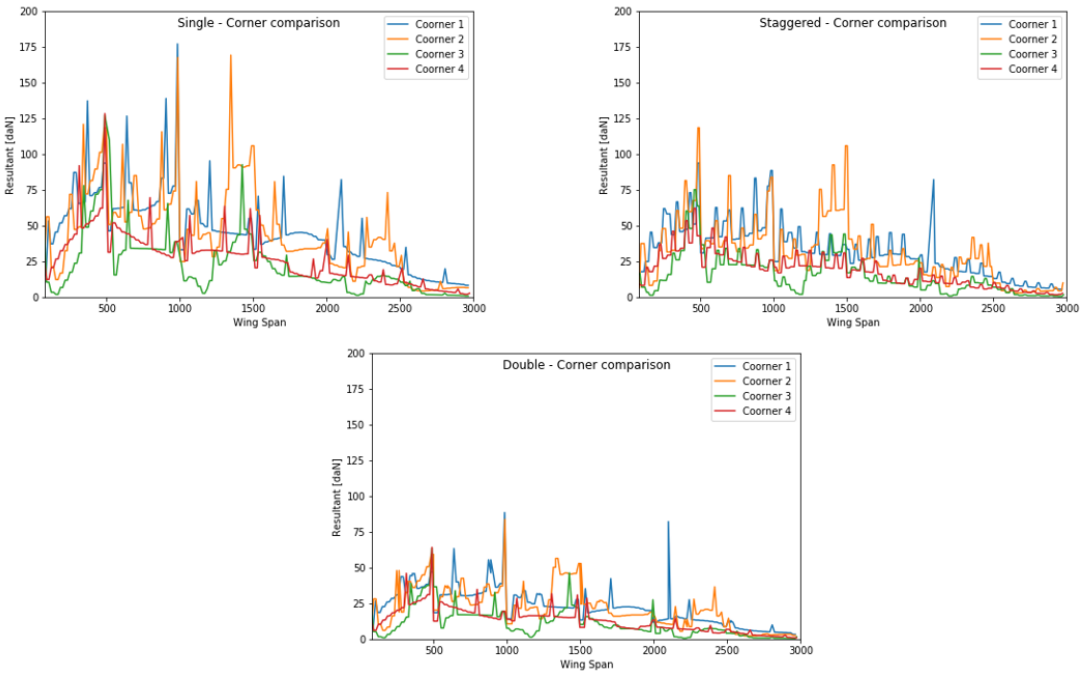

Figure 54 – Model with low level of detail - Resultant Shear Load (X and Y direction)

Figure. 55 presents the resultant shear load along wing span wise in each corner and also for each configuration analyzed. Based on the project premises for the pitch of the fasteners, the single configuration have the lower number of attachment along wing span wise following by staggered and finally the double configuration. The quantities of fasteners influences directly in the maximum load, and as it can be seen the single configuration is the most critical among the others analyzed.

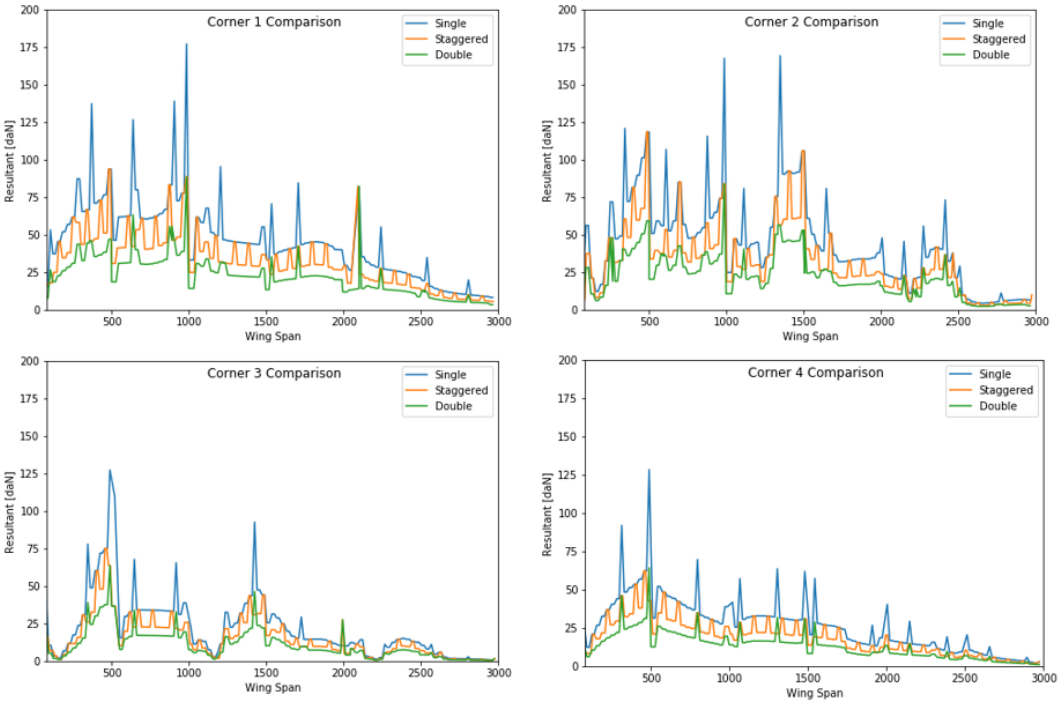

Figure 55 – Model with low level of detail - Corner Comparison (Resultant X and Y load)

4.3 MODEL WITH INTERMEDIATE LEVEL OF DETAIL

The model with intermediate level of detail was built considering the premises described in section 3.0.3, where each fastener is represented considering the Rutman approach and the load distribution for the fasteners along wing span wise is collected in each bar element. In order to collect and organize the data, the packages described in section 3.0.6 were used considering the abstraction for the model with intermediate level of detail.

It is going to present herein the same comparison performed for model with low level of detail. As it can be seen on Figure 56, which presents the shear X load for each corner and each type of attachment, the load in X direction has presented low level of load no matter the corner or configuration, being their values bellow of 25daN and those same behaviour was observed for the model with low level of detail. For the Y direction, the Figure. 57 has presented the load distribution along wing span wise, and also the behaviour is the same as it was observed in the model with low level of detail including the level of load observed

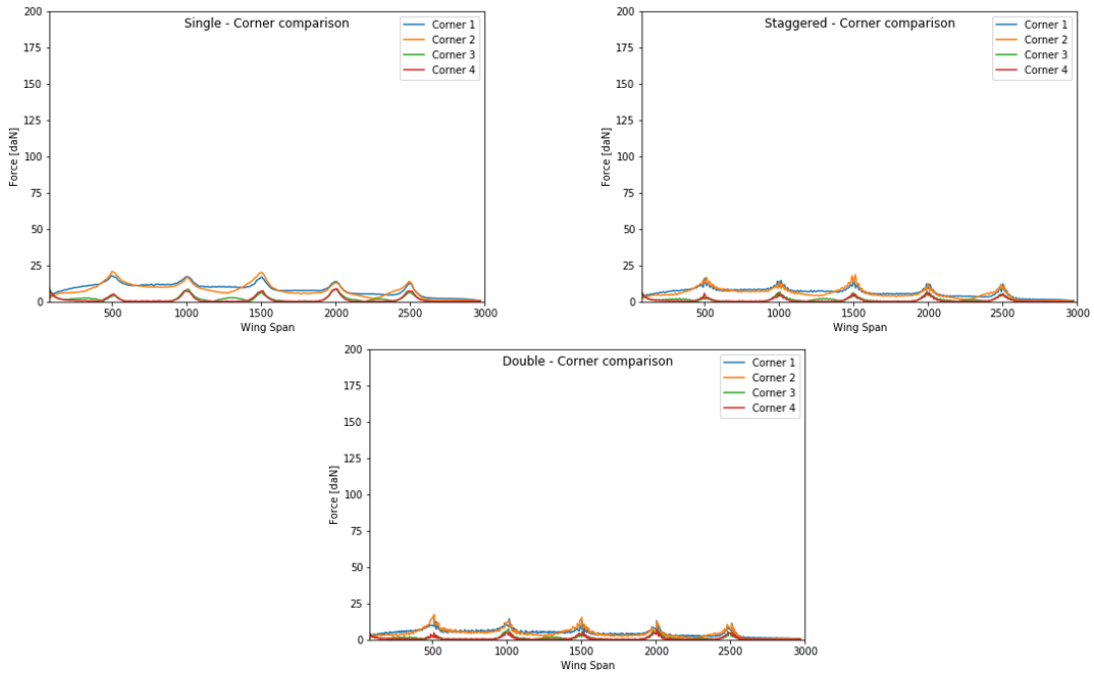

Figure 56 – Model with intermediate level of detail - Shear Load in X direction

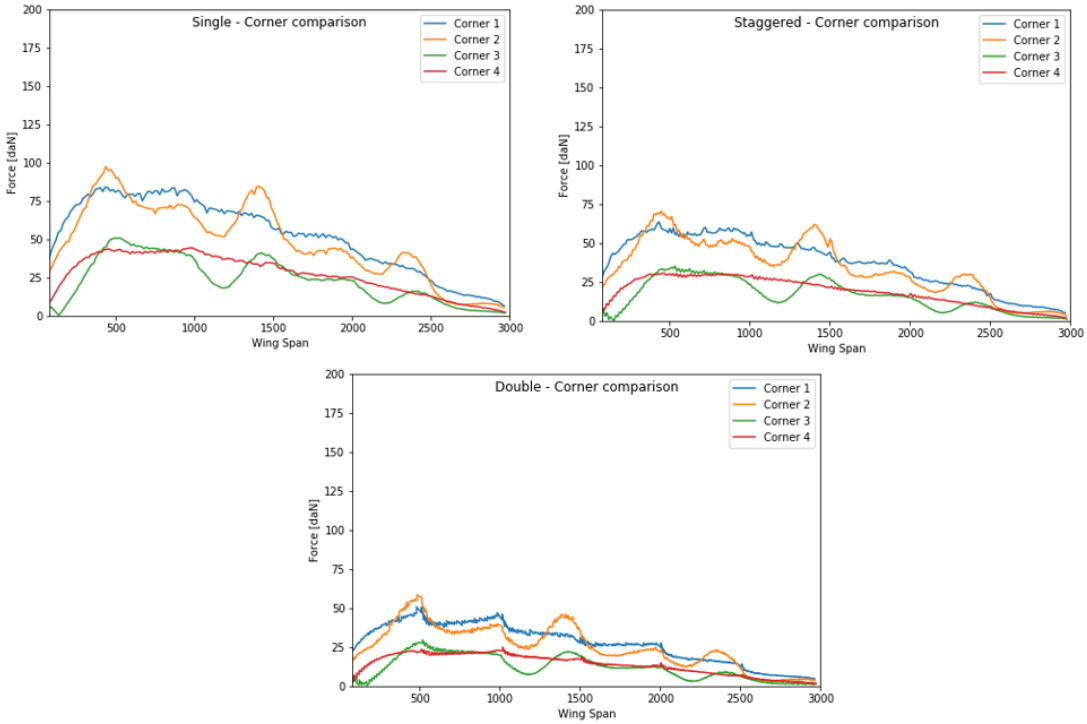

Figure 57 – Model with intermediate level of detail - Shear Load in Y direction

Figure 58 presents the shear resultant load along wing span wise for each corner and each type of attachment and as it was observed previously, the load distribution has the same behaviour and the comparable magnitude it was presented for the load in Y direction, which is the main load path.

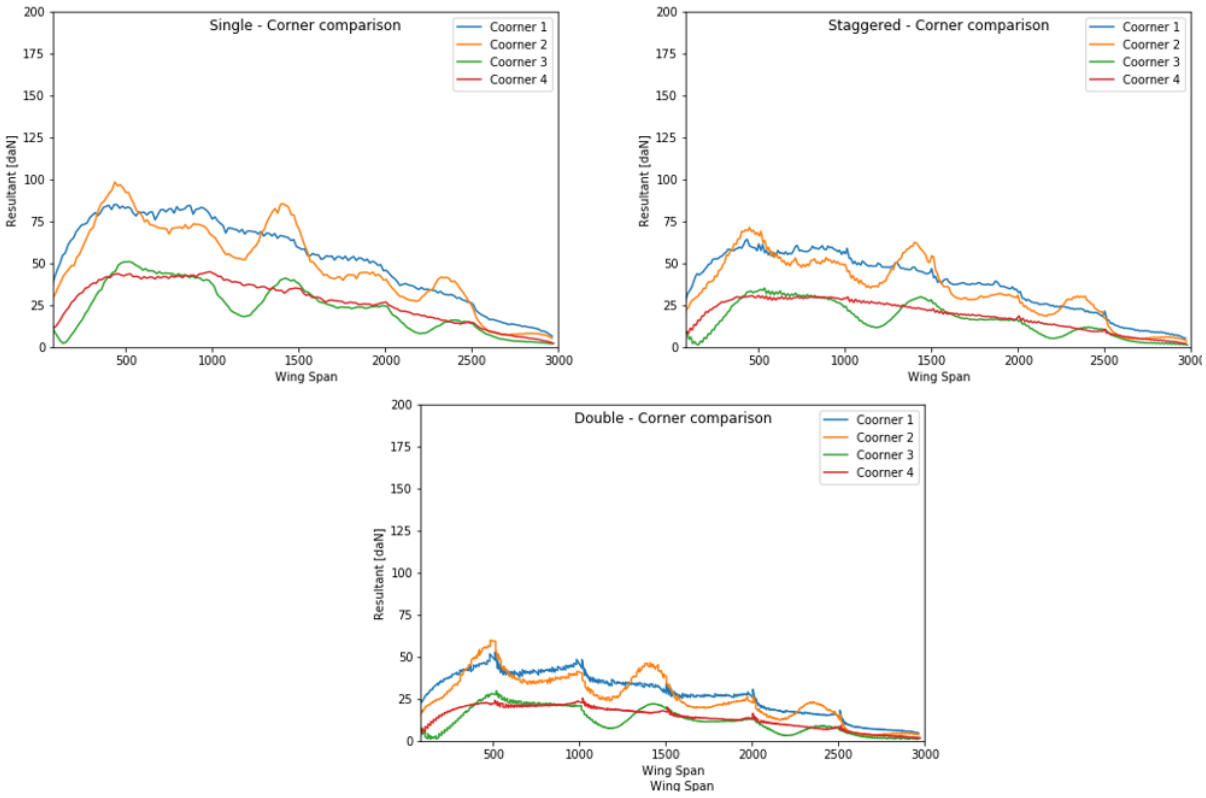

Figure 58 – Model with intermediate level of detail - Resultant Shear Load (X and Y direction)

The load distribution considering the corner separately as well as the type of attachment is presented in Figure. 59, and as it can be noted, the load distribution along corner 2 is the most severe among other and for that corner the single configuration is the most severe, behaviour also observed in load distribution for the model with low level of detail. Furthermore it can be observed a high level of load acting at the root of the wing, specifically close to the first rib and this behaviour occurs no matter the corner analyzed, this condition is easy explained while observing the load distribution at the span wise and the path for where the load is driven for, which is from the tip to the root. It is also observed a high level of load acting near of each rib, and this fact can be explained because each rib section is stiffer than the adjacent regions.

Finally the load distribution for the intermediate detailed model has presented more behaved when compared with model with low level of detail, and this can be explained

because of the way the load was extracted. While for the intermediate detailed model the load is extracted for each fastener separately, for the low detailed model the load is extracted by means of membrane shell element force and extrapolated for the fastener position.

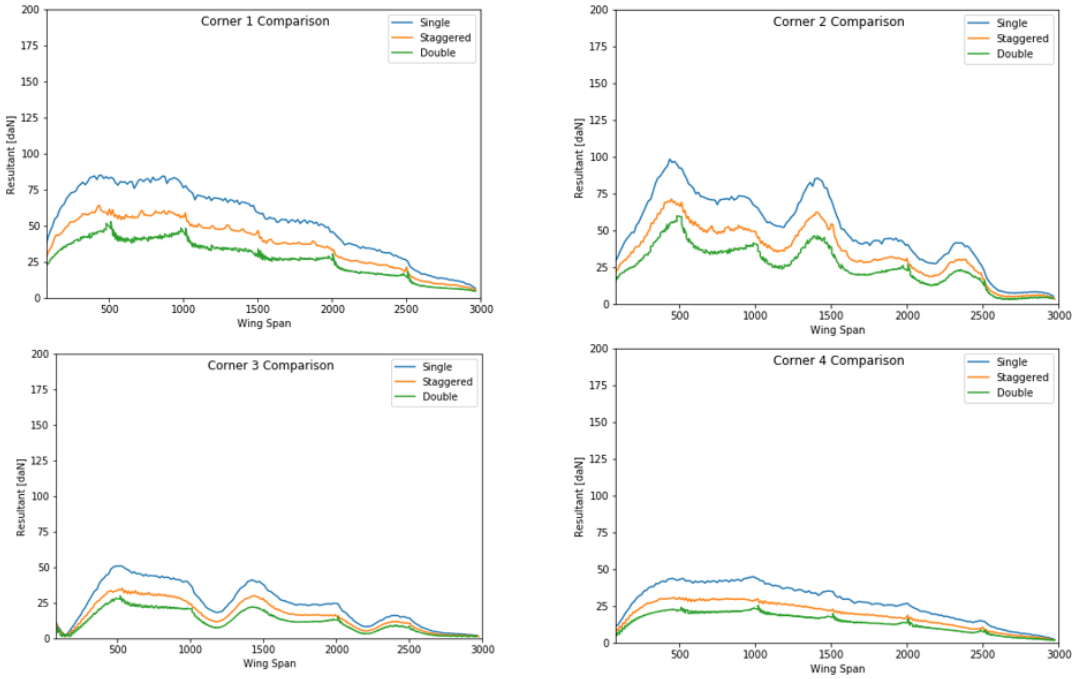

Figure 59 – Model with intermediate level of detail - Corner Comparison (Resultant X and Y load)

4.4 MODEL WITH HIGH LEVEL OF DETAIL

4.4.1 Critical Region to be detailed

The analysis for the model with high level of detail involves several nonlinearities such as considering material plasticity, geometrical and contact between the parts and a detailed model considering the entire wing and all those nonlinearities is not viable. Firstly due to the great amount of time necessary to built a finite element model with such level of detail and, at second, due to the number of degrees of freedom present in such model demands a unthinkable computational capability.

Because of these inconvenient, the model with high level of detail will be only a portion of the wing, which was already described in section 3.0.4. The shear load along wing span wise will be the parameter to be used in order to find the critical region to be portioned.

In figure 60, Figure. 61 and Figure. 62 it is possible to see the convergence of critical region among the models. At the corner two in wing root near rib 1 is the region more loaded. In this way this region was chosen to be portioned.

Note that it was used the same dimensions for the three models analyzed (single, staggered and double), but the number of fastener of each model changes. It is because of the minimum pitch considered to built the models. Thus single model have less quantities of fasteners than staggered configuration and, consequently, this last has less fasteners than the double configurations.

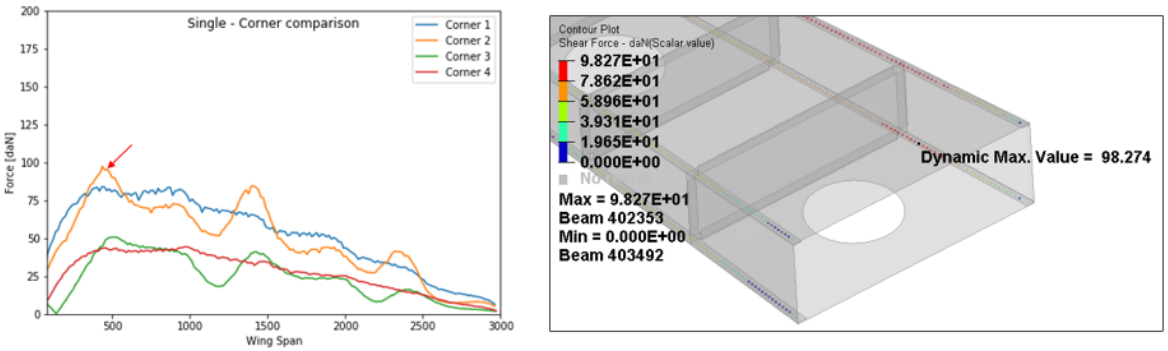

Figure 60 – Chosen Region - Single (the corners were numbered according to Figure. 43)

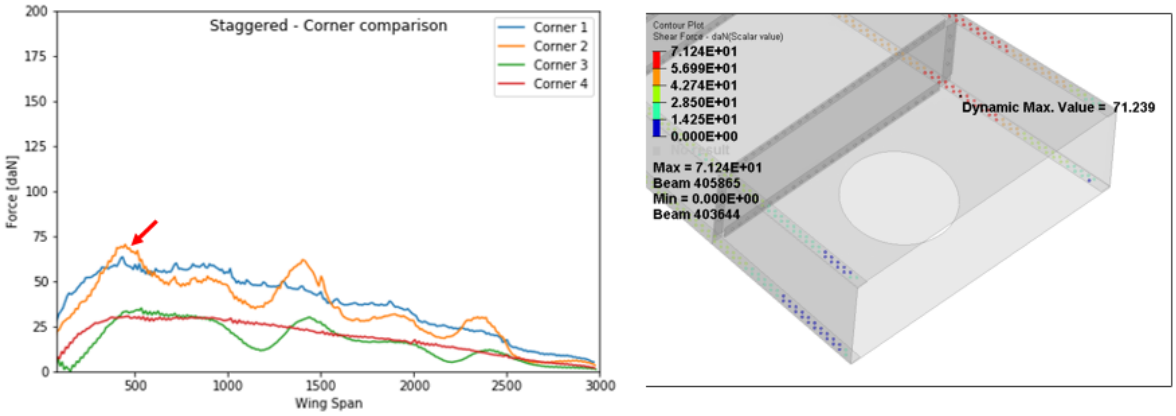

Figure 61 – Chosen Region - Staggered (the corners were numbered according to Figure. 43

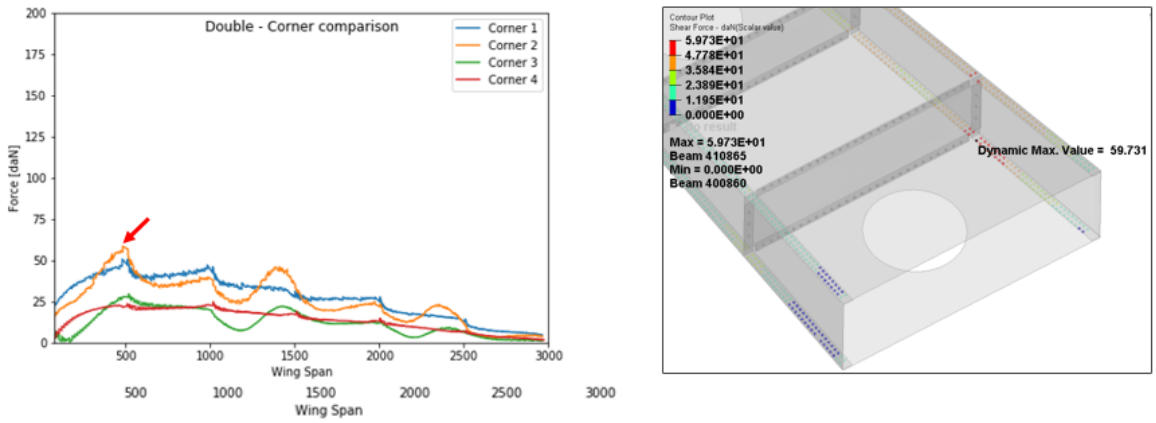

Figure 62 – Chosen Region - Double (the corners were numbered according to Figure. 43)

4.4.2 Detailed Model Validation

In order to validate the approach used, in which it focus only in a small part of the entire model, the model with intermediate level of detail was portioned and some results obtained in that part were compared with the results obtained for the whole model.

At first it was applied enforced displacement and rotations at each node in the extremity of the detailed model, as it was already detailed in section 3.0.4. This approach seeks in provide the same relative displacement between the parts connected parts, in this

case the lower skin and spar, in order to evaluate the load transferred between those parts throughout the fasteners.

After separate the models and run the analysis for each configuration, the total displacement of the models were compared, and as it can be noted in Figure. 63, Figure. 64 and Figure. 65., in which the figure at the left represent the whole model and the ones at the right represents the detailed mode. It is also can be depicted that no matter the model observed, they have the same behaviour in a displacement point of view.

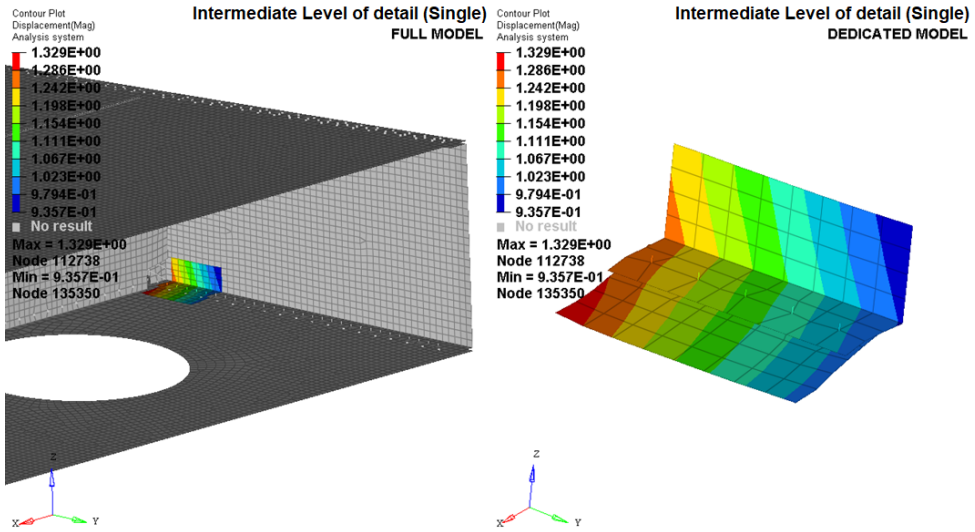

Figure 63 – Displacement comparison - Single

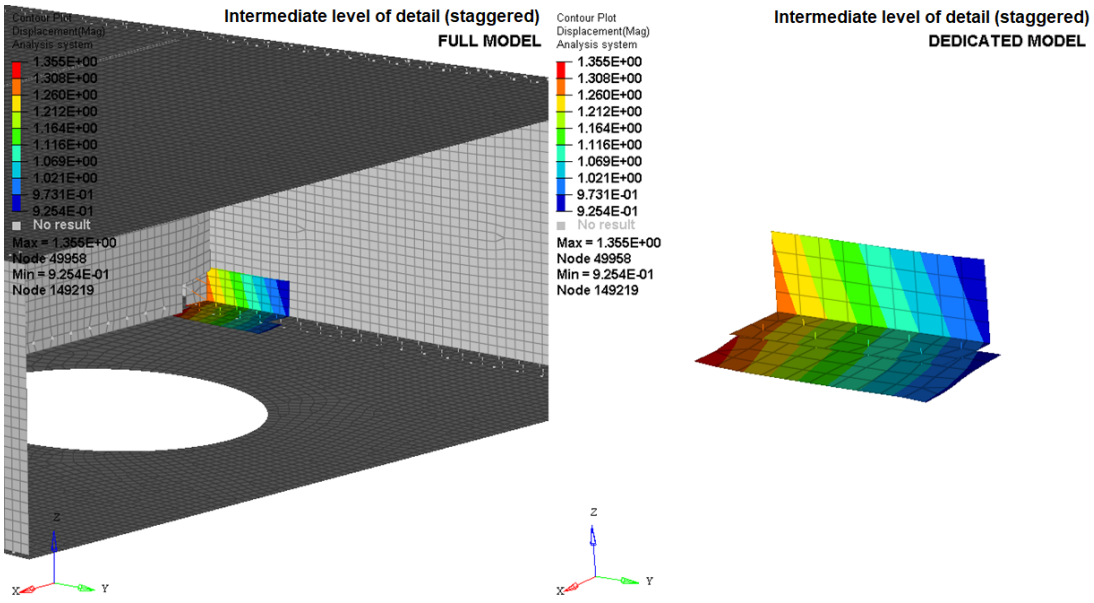

Figure 64 – Displacement comparison - Staggered

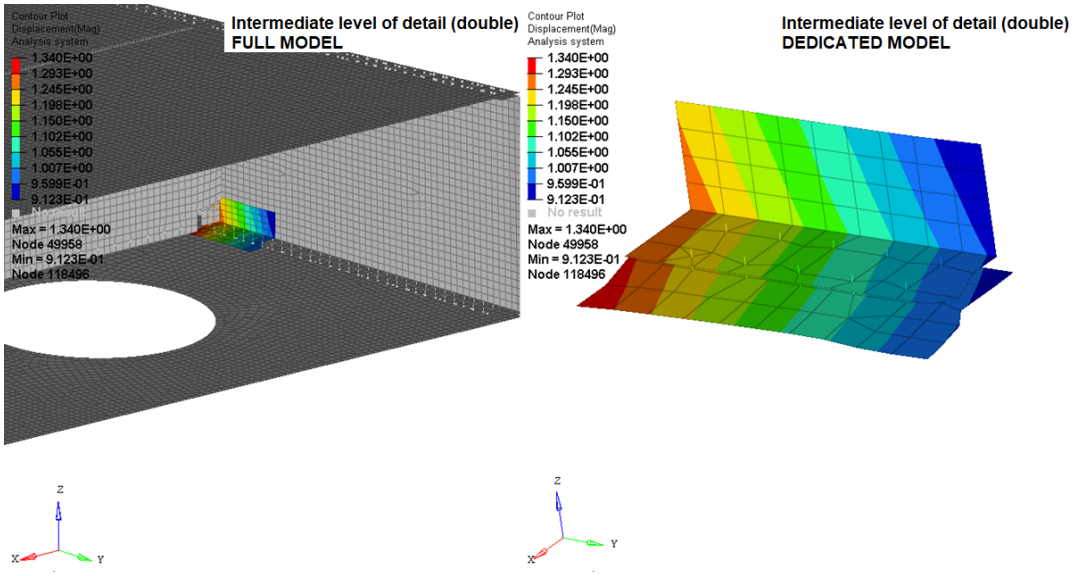

Figure 65 – Displacement comparison - Double

So, the scalar Von Mises stress field was mapped for the detailed region and Figure 66, Figure. 67 and Figure. 68 shows the comparison among the models. As well as the displacement comparison, there is no differences between the models compared regarding Von Mises stress.

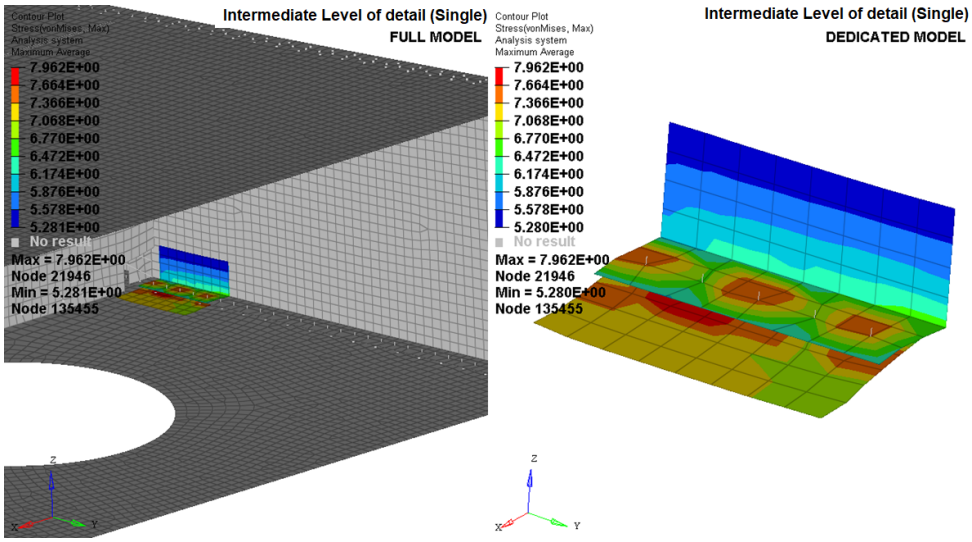

Figure 66 – VonMises comparison - Single

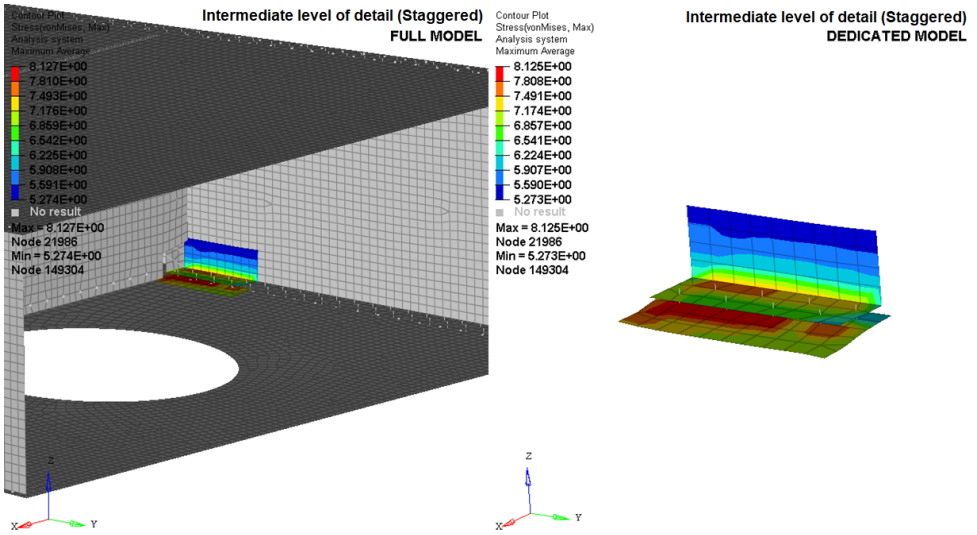

Figure 67 – VonMises comparison - Staggered

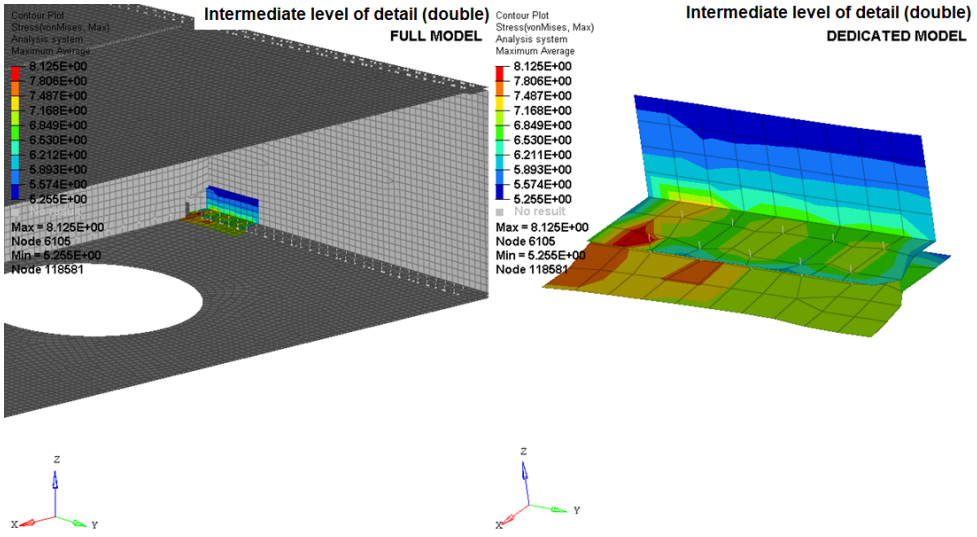

Figure 68 – VonMises comparison - Double

Furthermore, the shear force for the fasteners in focused region were compared and presented in Figure. 69, Figure. 70 and Figure. 71. It were no observed significant differences between the models.

It is important to observe that the relative displacement between lower skin and spar, which is generated by the enforced displacements, produce the equal fasteners force, an this happen because of the stiffness of the joint which was calculated in section 3.0.3 and do not change from the complete to the portioned model. This parameters will be interesting to be monitored while analyzing only the model with high level of detail,

because the stiffness of the joint could change because of the approach adopted and this modification in the behaviour can be noted and will be discussed in next sections.

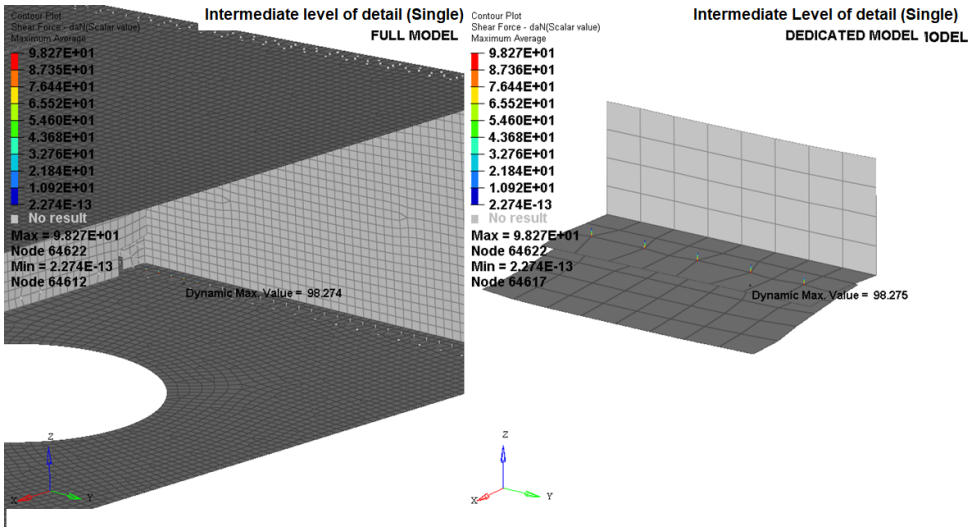

Figure 69 – Shear force comparison - Single

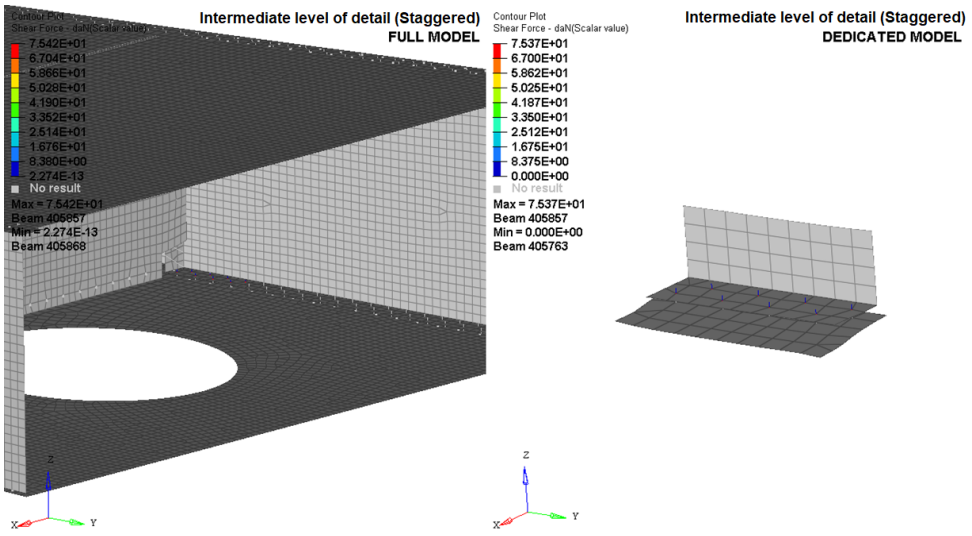

Figure 70 – Shear force comparison - Staggered

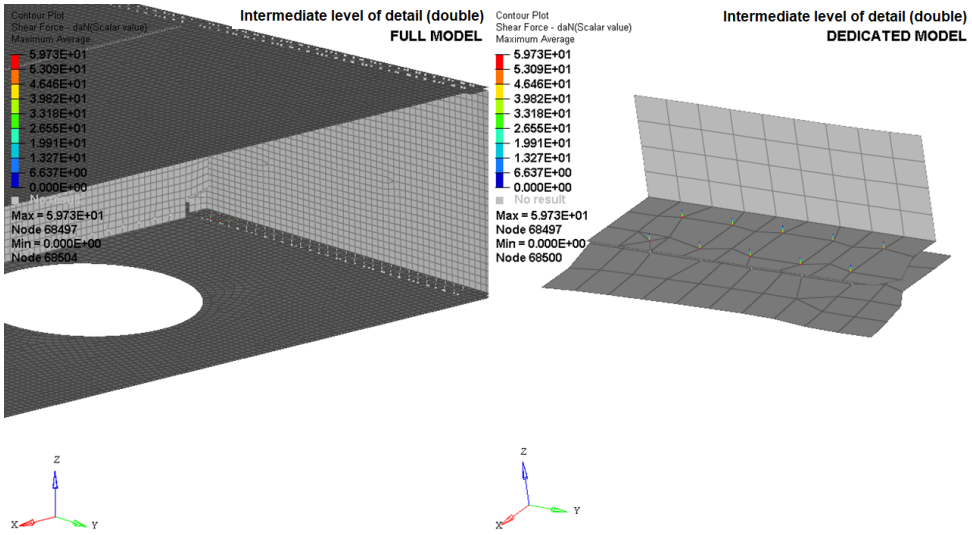

Figure 71 – Shear force comparison - Double

Finally, the total displacement for the models were compared and presented in Figure. 72, Figure. 73 and Figure. 74.

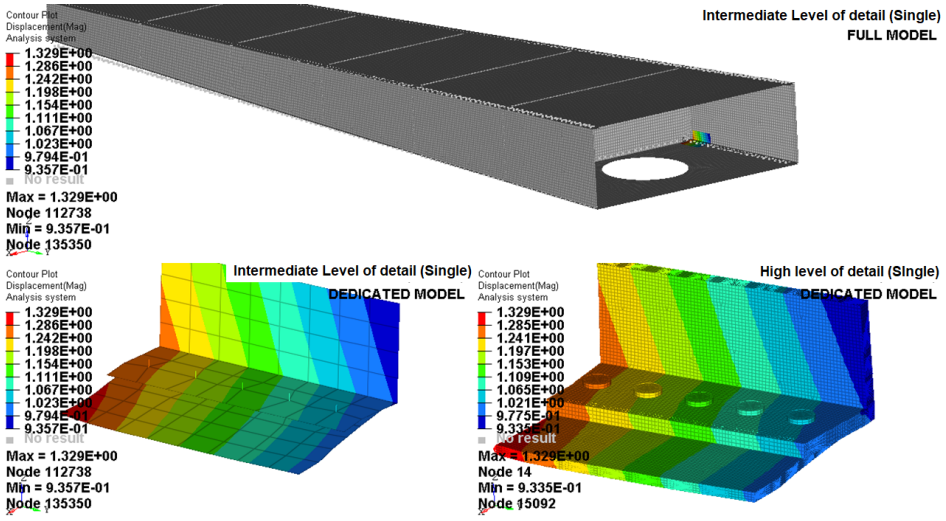

Figure 72 – Displacement comparison (model with high level of detail) - Single

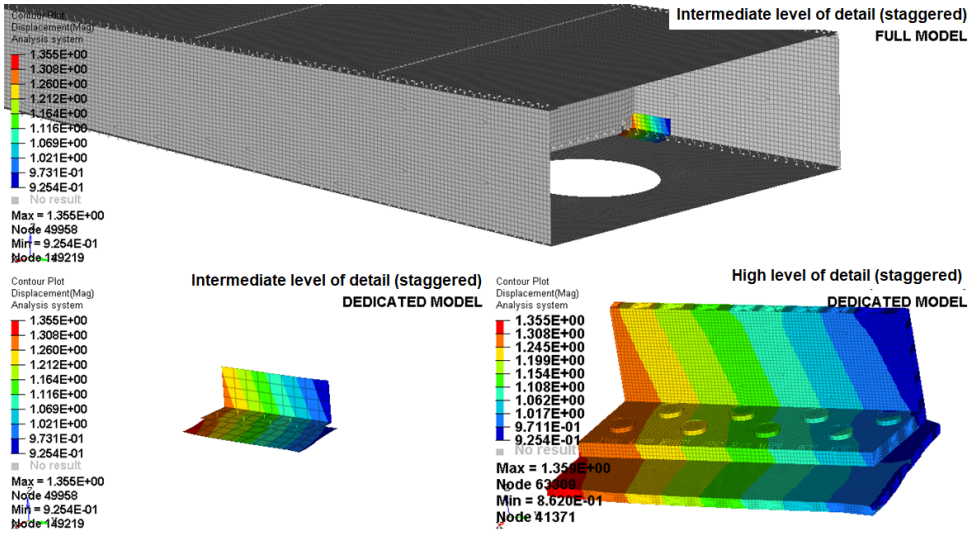

Figure 73 – Displacement comparison (model with high level of detail) - Staggered

As it was observed in the results depicted, by using enforced displacement at the extremity of the analyzed region shows a strong approach in order to evaluate small parts of the model, but it is also important to be carefully while using it. Enforced displacement for models with different level of simplifications could provide parts with different stiffness and it can result in a inaccurate results.

Dedicated models must be used considering all the difficulties inherent in the process, and it have to be validated as much as possible including validation with experimental

data in order to obtain better accuracy. The difficulties to simulate the connection between the parts include material properties, the way the parts were connected and also how those parts were connected, whether using a machine or the human force.

The next sections will detail more results for the model with high level of detail, the load acting in each fasteners due to relative displacement between parts and also the impact of using squeeze force in the analysis and in stiffness of the joint.

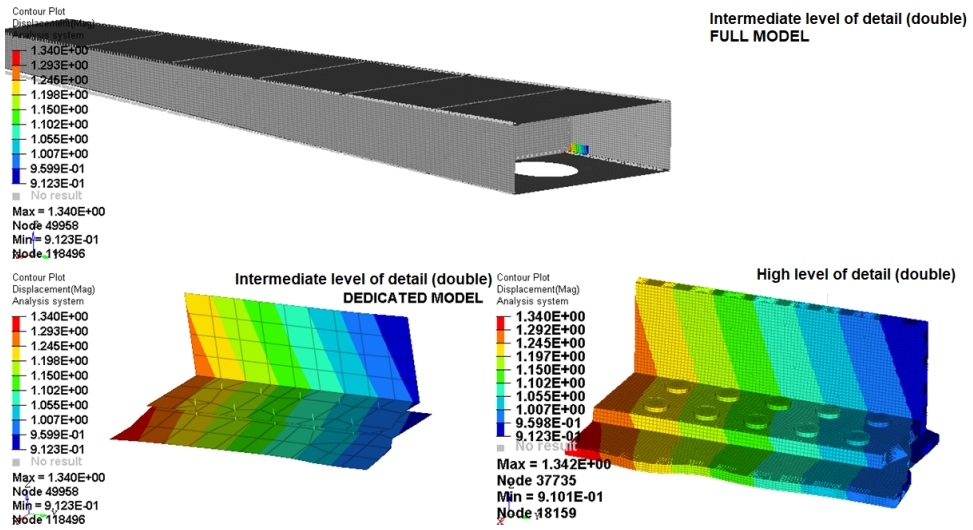

Figure 74 – Displacement comparison (model with high level of detail) - Double

4.4.3 Results for model with high level of detail

The model with high level of detail were built considering solid elements with a good accuracy and it was also considered a good level of refinement which has increase the number of degrees of freedom of the models. The models were also separated in three different properties in order to facilitate the manipulation in post processor solver.

The boundary condition for the model with high level of detail was discussed in section 3.0.5.3 and Table. 7, Table 8 and Table. 9 gives a statement of the models in which it was built considering the best practice of Finite element model considered in section 3.0.7. Note that the number of elements, number of nodes and the numbers of points in which the enforced displacement is applied changes from one model to another. Those little changes are because of the differences in the number of fastener in each model and the level of refinement of each fasteners, as it can be seen on Figure.75.

Table 7 – Statement for model with high level of detail - Single

Type	quantities
Nodes	51571
Hexa elements	39075
Penta Elements	656
Rigid Elements	56
SPC	56
Enforced Displacement	56

Table 8 – Statement for model with high level of detail - Staggered

Type	quantities
Nodes	68832
Hexa elements	52148
Penta Elements	996
Rigid Elements	62
SPC	62
Enforced Displacement	62

Table 9 – Statement for model with high level of detail - Double

Type	quantities
Nodes	65816
Hexa elements	49586
Penta Elements	760
Rigid Elements	42
SPC	42
Enforced Displacement	42

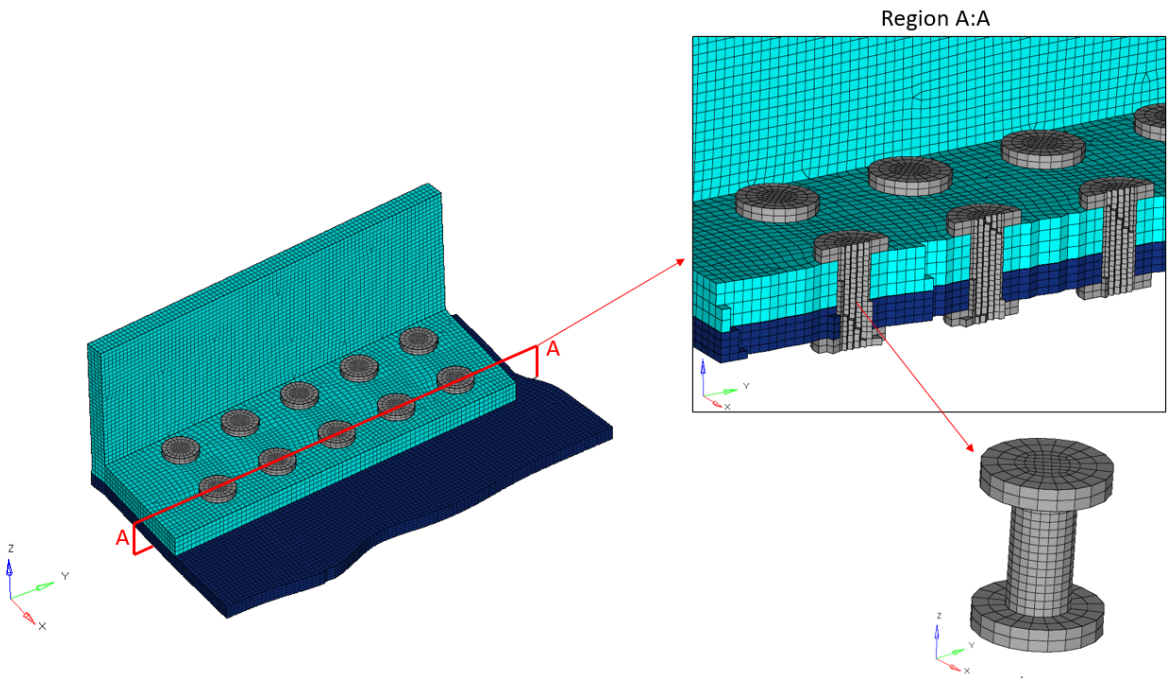

Figure 75 – Detail for model with high level of detail

The process time for each model analyzed changes significantly from the models with lower level of detail, specially because of the nonlinearities in the model. But this is not only because of this, the number of degrees of freedom of the models is also very different. The Figure. 76 presents the ".sts" file, provided from Nastran solver in which it is possible to follow the interaction process of the solver, and the convergence. The Figure shows the file only for Staggered model, but this behaviour can be observed for all models analyzed.

```
information summary of job:  ./Model_Staggered_High_fidelity
version: MSC Nastran 2021.1.0, Built on Mar 10, 2021
date:     Mar 19, 2022; Day Time: 19:29:26
```

subcase /step #	inc #	cycl #	sepa #	cut #	cycl #	split #	separ #	cut #	rmesh #	time step of the inc	total time of the job	wall time	cpu time	max resp. type
1000		--of the inc--			----------of the analysis----------									
1	0	0	0	0	0	0	0	0	0	0.0000E+00	0.0000E+00	8.00	8.33	0.0000E+00 disp
1	1	72	70	0	73	0	70	0	0	1.0000E-02	1.0000E-02	693.00	1679.21	1.2919E-02 disp
1	2	11	9	0	84	0	79	0	0	1.2000E-02	2.2000E-02	791.00	1921.36	2.8421E-02 disp
1	3	8	6	0	92	0	85	0	0	1.4400E-02	3.6400E-02	861.00	2094.23	4.7024E-02 disp
1	4	7	5	0	99	0	90	0	0	1.7280E-02	5.3680E-02	929.00	2260.89	6.9348E-02 disp
1	5	7	5	0	106	0	95	0	0	2.0736E-02	7.4416E-02	1001.00	2435.08	9.6136E-02 disp
1	6	6	4	0	112	0	99	0	0	2.4883E-02	9.9299E-02	1055.00	2567.09	1.2828E-01 disp
1	7	6	4	0	118	0	103	0	0	2.9860E-02	1.2916E-01	1110.00	2703.50	1.6686E-01 disp
1	8	5	3	0	123	0	106	0	0	3.5832E-02	1.6499E-01	1154.00	2812.53	2.1315E-01 disp
1	9	5	3	0	128	0	109	0	0	4.2998E-02	2.0799E-01	1202.00	2928.12	2.6870E-01 disp
1	10	5	3	0	133	0	112	0	0	5.1598E-02	2.5959E-01	1253.00	3052.54	3.3535E-01 disp
1	11	4	2	0	137	0	114	0	0	6.1917E-02	3.2150E-01	1293.00	3150.63	4.1534E-01 disp
1	12	4	2	0	141	0	116	0	0	7.4301E-02	3.9581E-01	1334.00	3251.57	5.1133E-01 disp
1	13	4	2	0	145	0	118	0	0	8.9161E-02	4.8497E-01	1375.00	3349.60	6.2651E-01 disp
1	14	4	2	0	149	0	120	0	0	1.0699E-01	5.9196E-01	1415.00	3447.89	7.6474E-01 disp
1	15	4	2	0	153	0	122	0	0	1.2839E-01	7.2035E-01	1454.00	3543.32	9.3060E-01 disp
1	16	5	3	0	158	0	125	0	0	1.5407E-01	8.7442E-01	1499.00	3652.62	1.1296E+00 disp
1	17	8	6	0	166	0	131	0	0	1.2558E-01	1.0000E+00	1572.00	3829.26	1.2919E+00 disp

```
Job ends with exit number :       0
          total wall time:       1588.00
          total cpu  time:       3846.73
```

Figure 76 – ".sts" Nastran file

The main focus of this work is to study the way the load flows between the connected plates through its fasteners. As it was discussed previously, the fastener force provided from the model with low level of detail is calculated considering membrane force of each skin elements at the interface skin/spar. For the models with intermediate level of detail, the load flowing is obtained directly from the beam elements, where the shear and tension load of the bars represents the fasteners load.

The model with high level of detail represents each part as it is actually is without out simplifications, and it is not possible to obtain the fasteners load directly. The finite element solver provides results for each element separately and some tools able only in the post processor solver must be used in order to obtain the fastener force.

In order to obtain the fastener load, two approach were considered. The first one is to consider a free body diagram at a specific section of the fastener (section immediately between the two plates). The free body diagram tool is a specific capability of the post processor solver and it is not able as a natural result of FEM model. The Figure. 77 shows the section in which the load will be extracted.

The second one focus in obtain the actual load which is "going" from the fastener to the plate. In this way a freebody diagram was performed considering the "washer" region of the plate where the fastener is connected. Figure. 78 shows the plate region from where the freebody diagram was obtained.

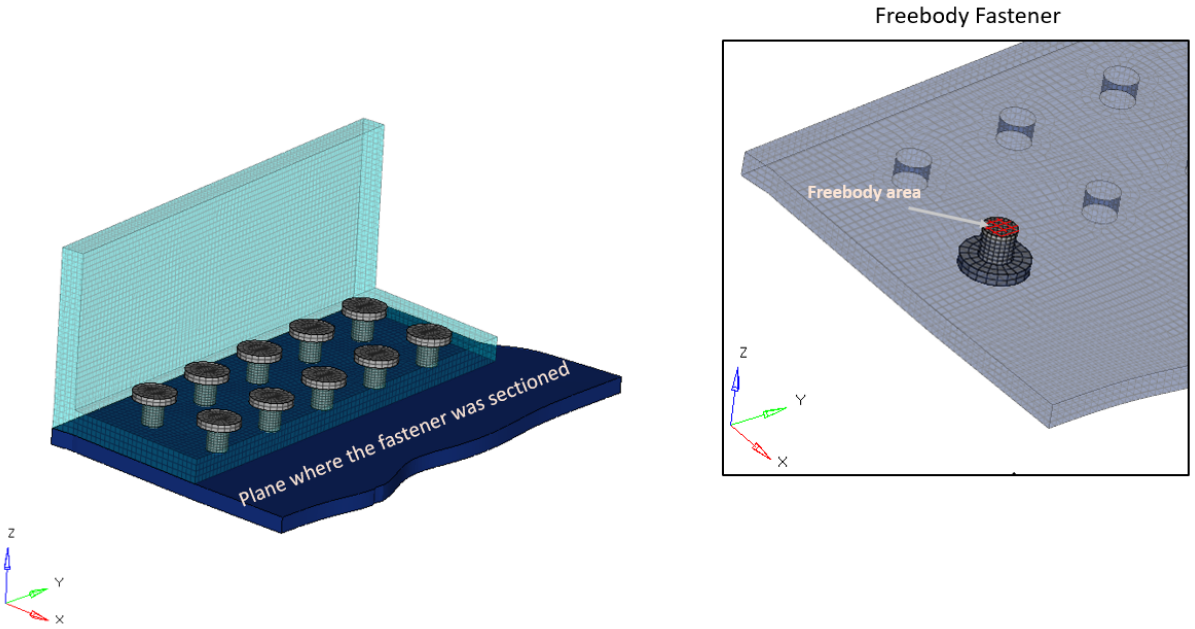

Figure 77 – Free body at Fastener Section

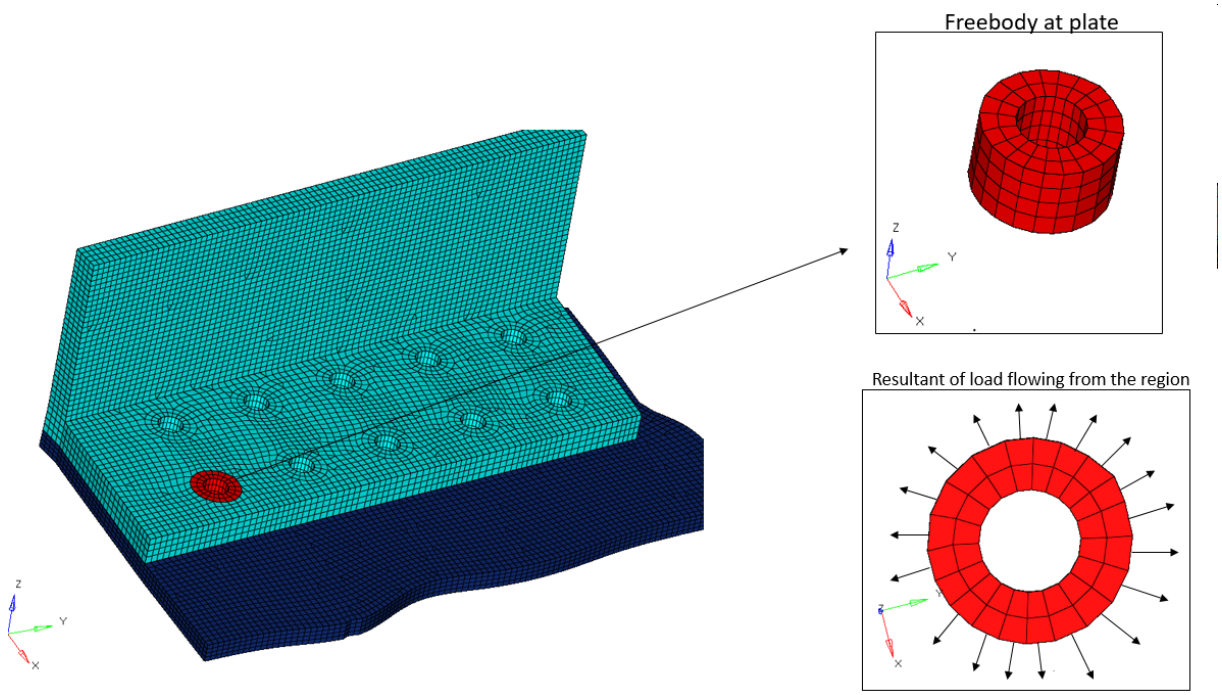

Figure 78 – Free body at Plate region

Those results were considered for each fastener region and for each configuration

proposed and it will be presented hereafter.

Single: The Figure. 79, Figure. 78 and Figure. 69 presents the result for model considering only one row of fastener

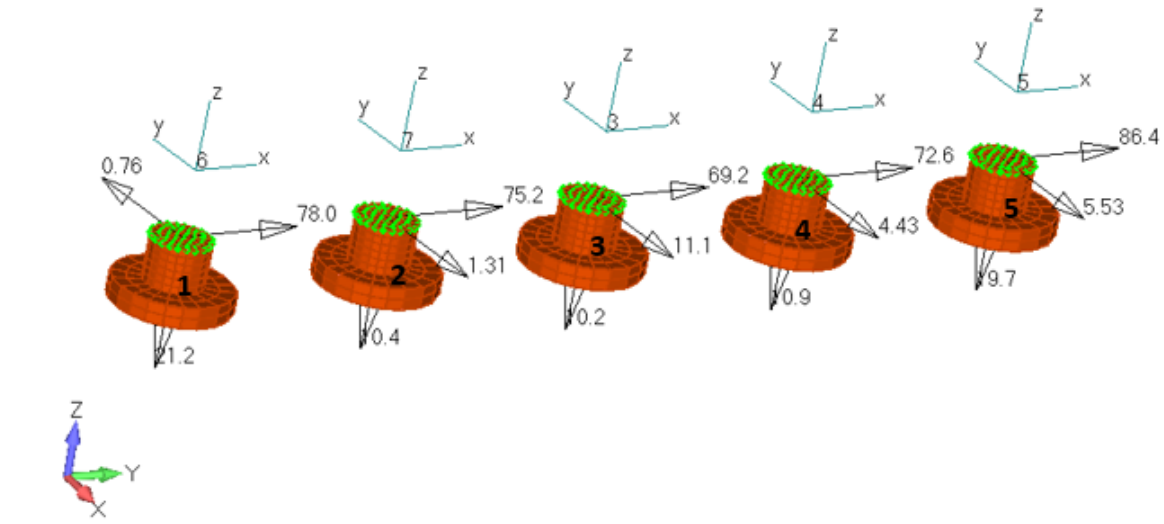

Output Set: Case 1 Time 1.
Freebodies: Fastener 1, Fastener 2, Fastener3, Fastener 4, Fastener 5

Figure 79 – Freebody at fastener - single

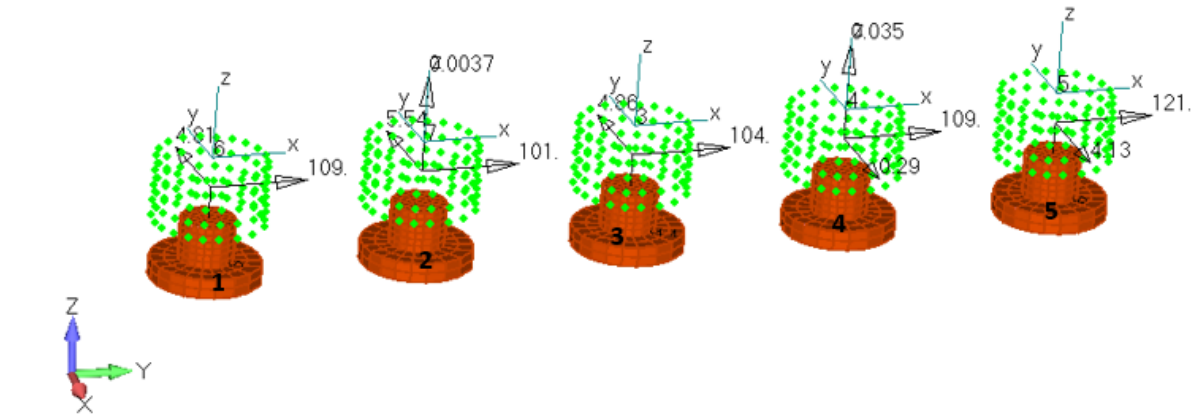

Output Set: Case 1 Time 1.
Freebodies: Fastener 1, Fastener 2, Fastener3, Fastener 4, Fastener 5

Figure 80 – Freebody at plate - single

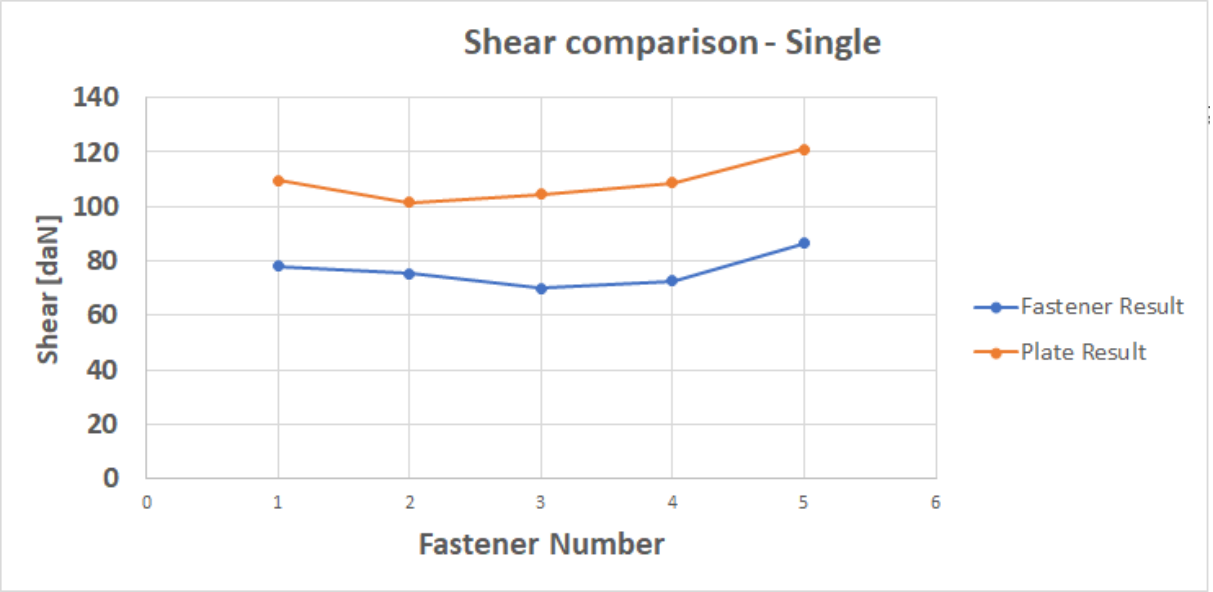

Figure 81 – Shear load comparison - single

- Staggered: The Figure. 79, Figure. 78 and Figure. 69 presents the result for model considering Staggered configuration

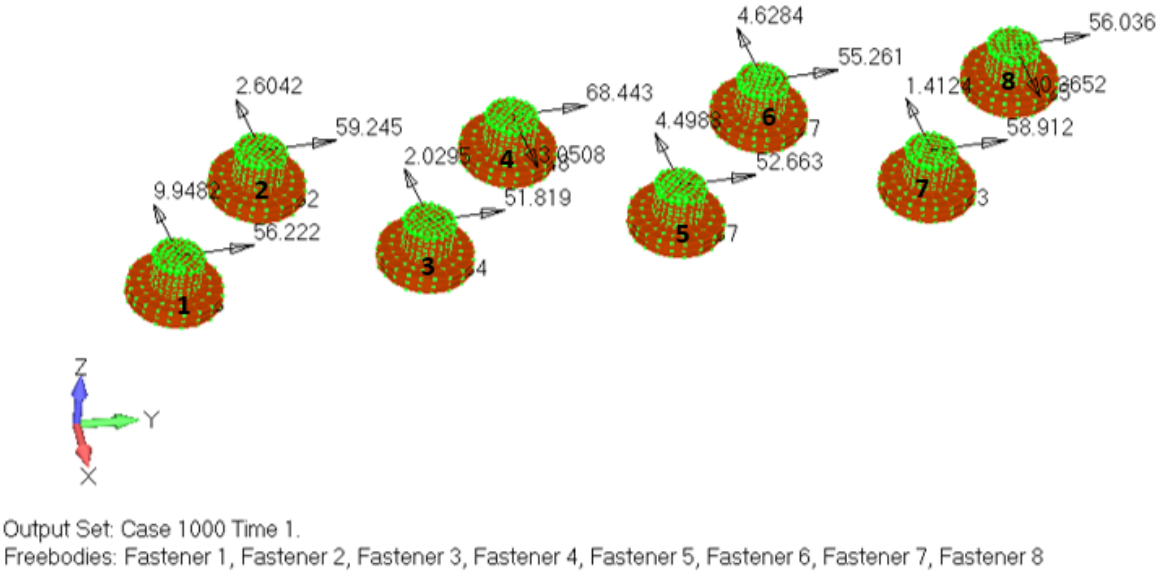

Figure 82 – Freebody at fastener - Staggered

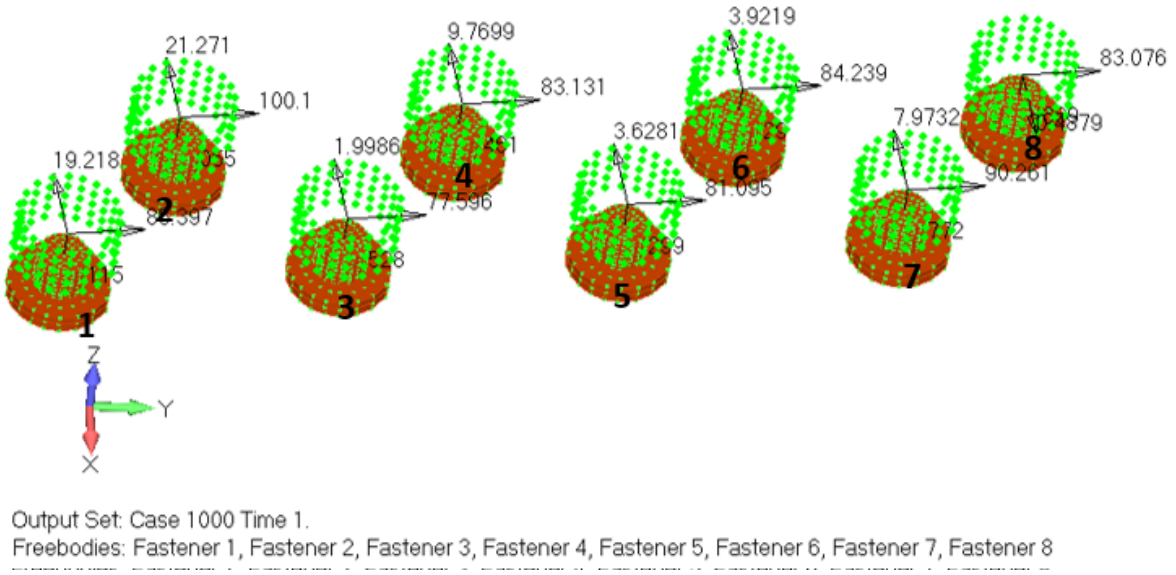

Figure 83 – Freebody at plate - Staggered

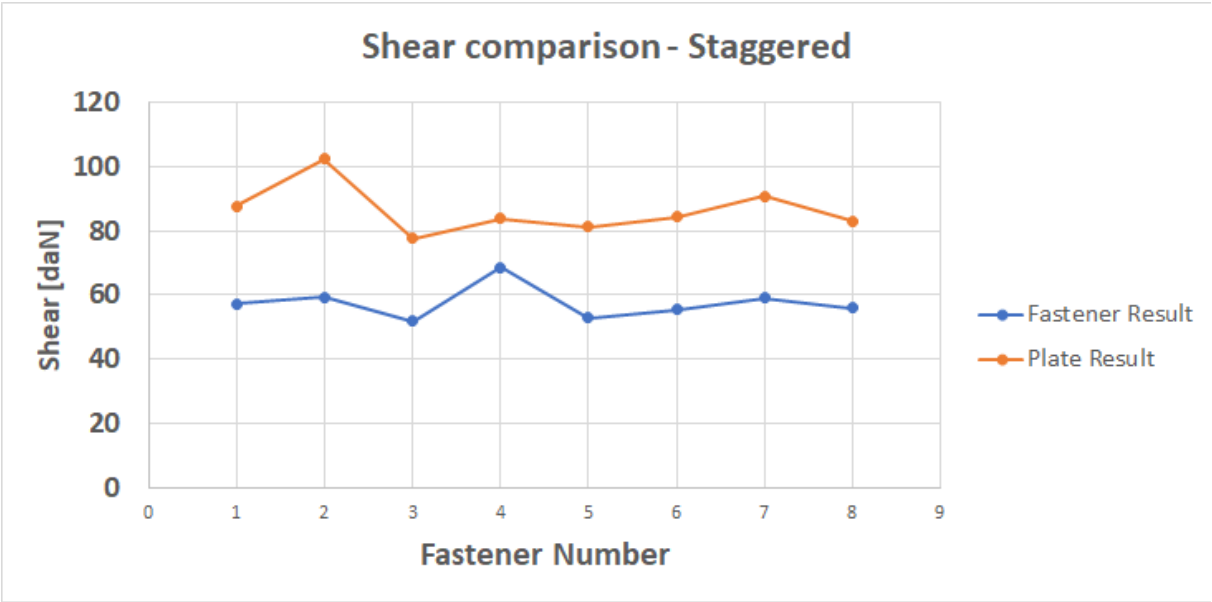

Figure 84 – Shear load comparison - Staggered

- Double: The Figure. 79, Figure. 78 and Figure. 69 presents the result for model considering double fastener configuration

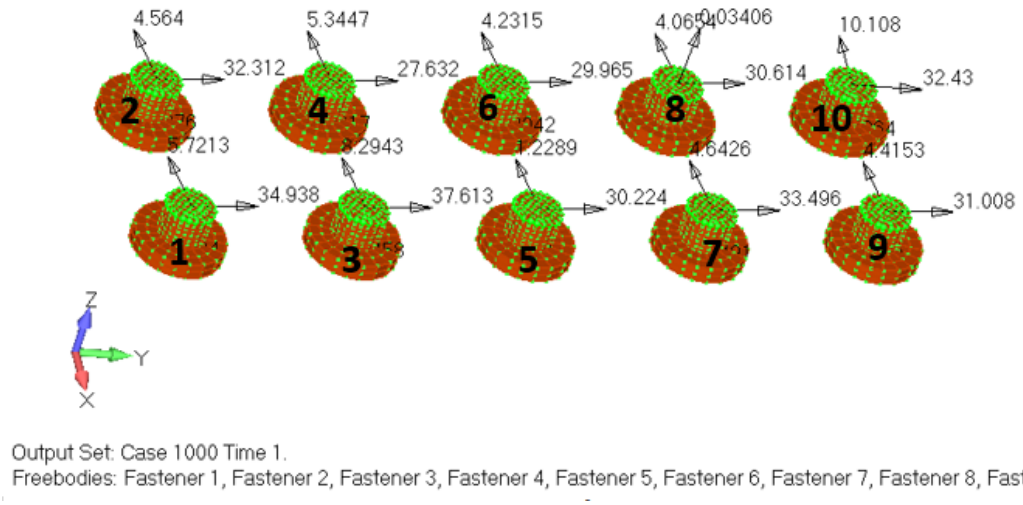

Output Set: Case 1000 Time 1.
Freebodies: Fastener 1, Fastener 2, Fastener 3, Fastener 4, Fastener 5, Fastener 6, Fastener 7, Fastener 8, Fastener 9, Fastener 10

Figure 85 – Freebody at fastener - Double

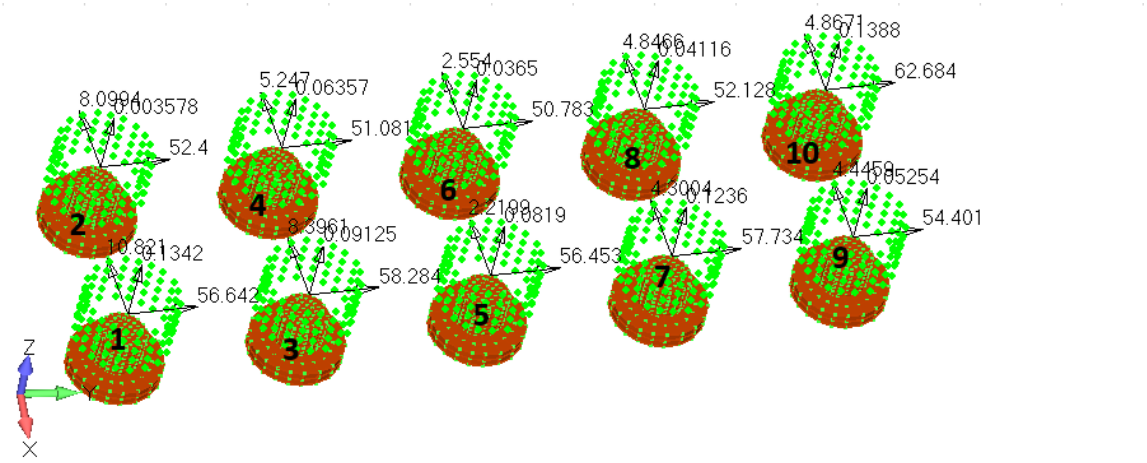

Output Set: Case 1000 Time 1.
Freebodies: Fastener 1, Fastener 2, Fastener 3, Fastener 4, Fastener 5, Fastener 6, Fastener 7, Fastener 8, Fastener 9, Fastener 10

Figure 86 – Freebody at plate - Double

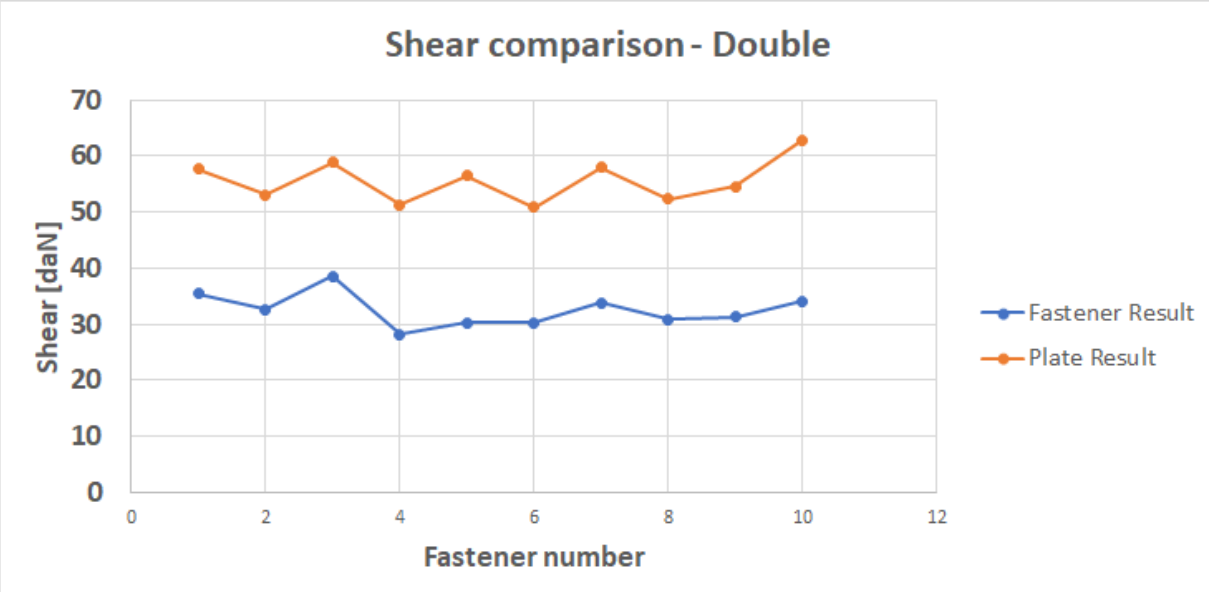

Figure 87 – Shear load comparison - Double

As it can be noted in the figures, no matter the approach used, the single configuration is the more loaded among others analyzed. This is very simple to explain specially because of the number of fastener in each. Single model have less fastener to connect spar with the skin.

So as to understand the stress level that the relative displacement between the plates generates, the scalar von-mises stress field was also plotted and it is presented in Figure. 88

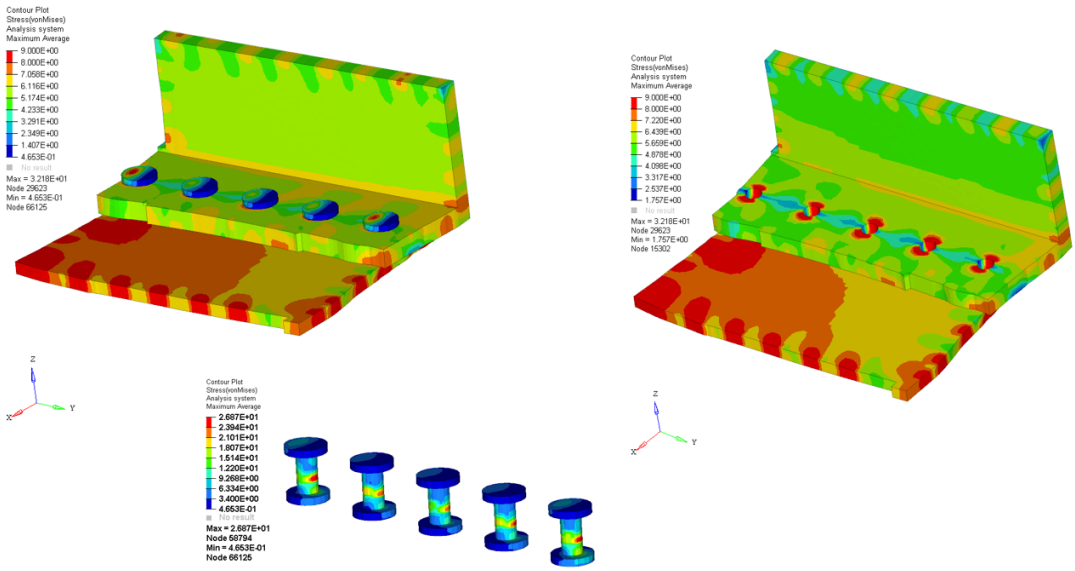

Figure 88 – Von Mises Stress - single

4.5 COMPARISON

After all the analysis performed, and several data obtained and compiled from the results, this section aims to show the results collected for the three levels of detail studied.

First of all, it is going to be shown the shear force for each fasteners along the wing spanwise for the models with low and intermediate level of detail. As it was discussed previously, the corner two (presented in Figure. 43) is the most loaded among others and it will be used in order to plot the data of the models.

Figure 89, Figure. 90 and Figure. 91 presents the shear load distribution considering the two level of detail analyzed. As can be noted both of the models analyzed, no matter the configuration analyzed, present peaks of loads near the ribs regions (stations for each 500mm) being the low detailed model the most loaded in this regions.

Furthermore the model with low level of detail presents irregularities in load distribution with peaks with high values and this fact can be explained due to the methodology used to extract the load for each fastener, while for the low detailed model it was used a membrane force extrapolation, for the intermediate detailed model it was used a discrete force for each fastener separately. Thus, eventually it can be observed a conservatism in using the model with low level of detail to perform the sizing in wing connections.

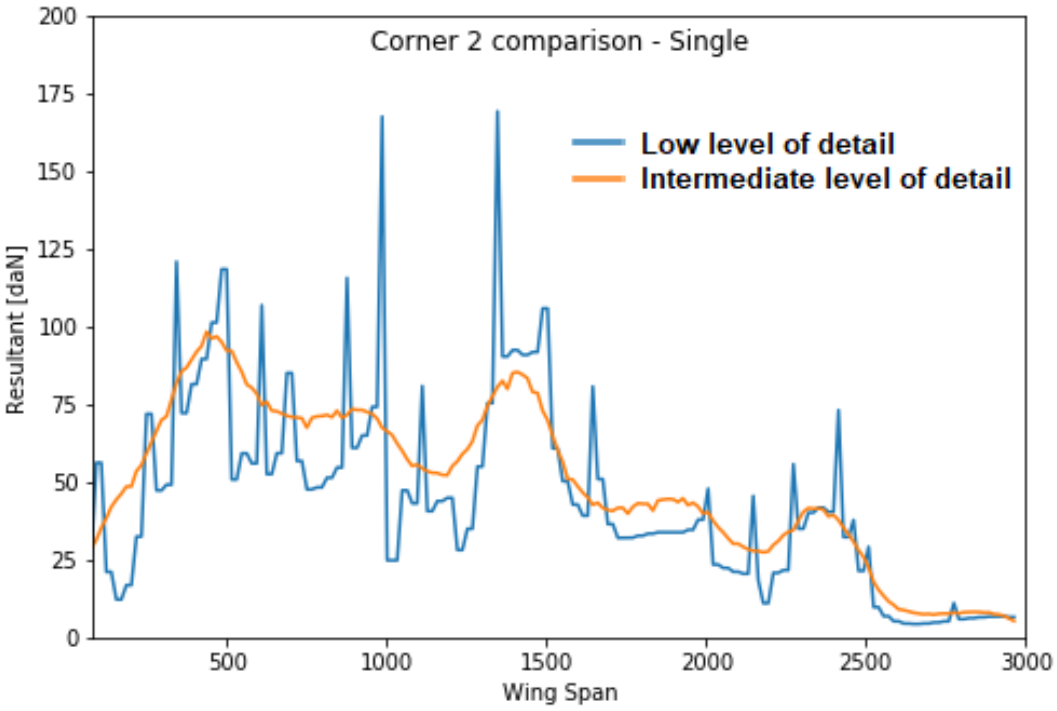

Figure 89 – Shear load comparison - Single

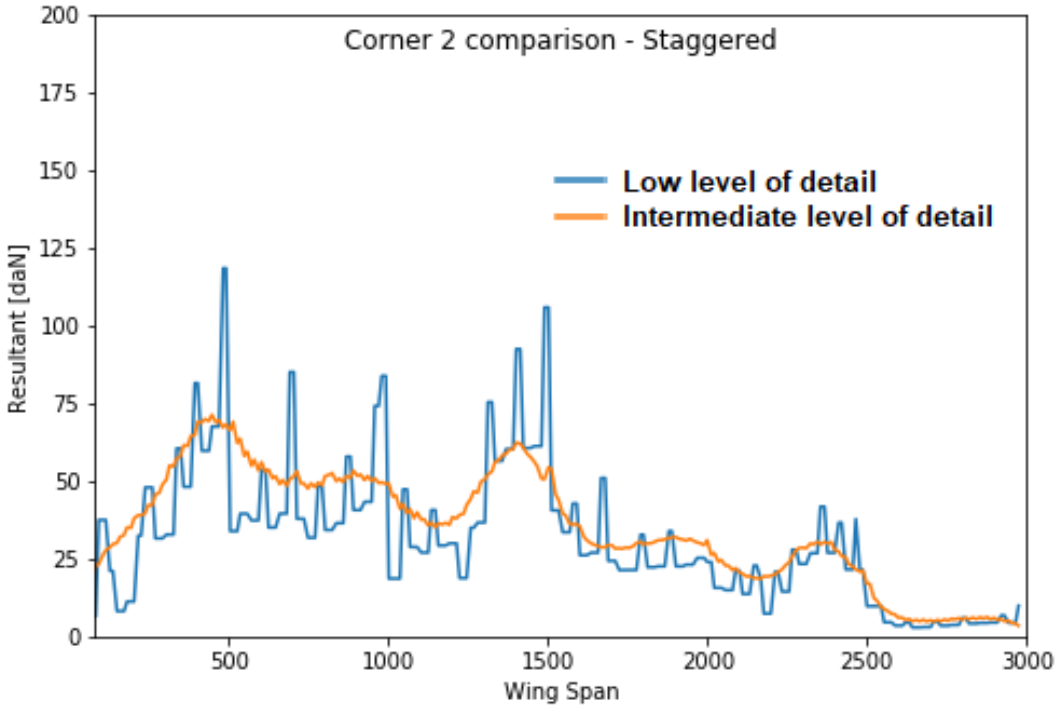

Figure 90 – Shear load comparison - staggered

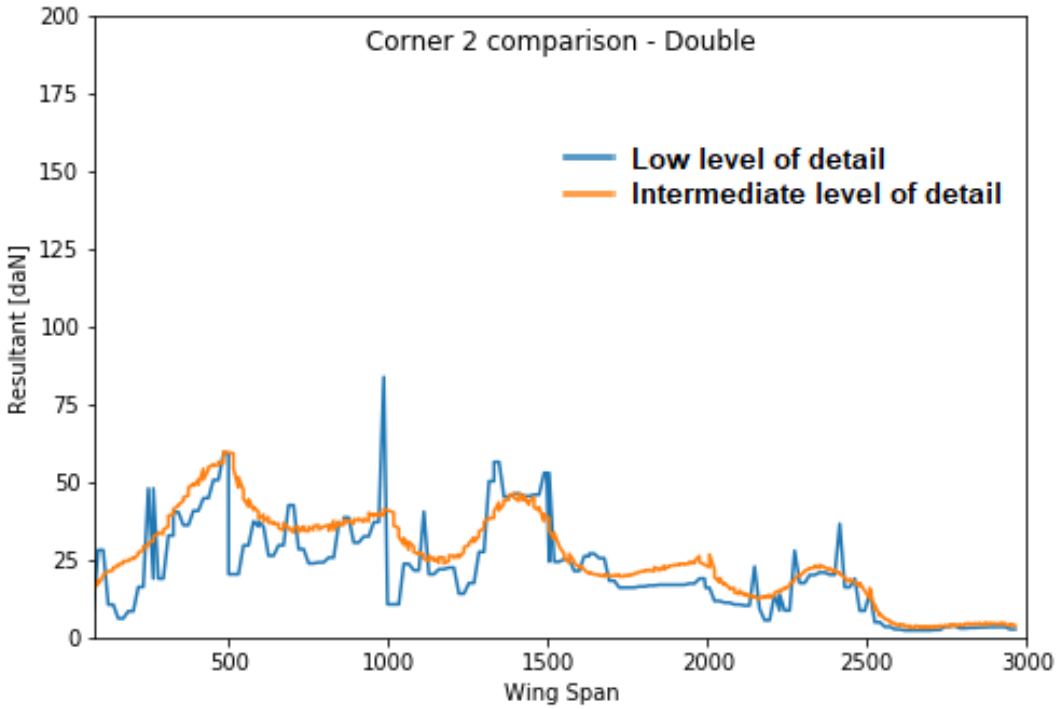

Figure 91 – Shear load comparison - double

Finally it is going to be shown the shear load for the fasteners in the detailed region. The results presented hereafter is similar to get the graphs of Figure 89, Figure. 90 and Figure. 91 and make a zoom ate the region near the position y=500 for the last fasteners before reach the rib 1.

Thus the Figure. 92, Figure. 93 and Figure.94 shows the comparison for the three types of configuration analyzed at the detailed region (region specified in Figure. 32). As can be observed the envelope of the load distribution, considering all the models evaluated, shows that the model with low level of detail is more loaded among single and staggered model and have almost the same value for the double configuration (see Table.10) , corroborating with the thesis that uses the this model is a conservative approach to perform attachment analysis between the wing and the spar.

It is also important to highlight the meaning of the load distribution for the high detailed model. The methodology adopted to perform the analysis for the most detailed model, give us the ability to understand the stiffness of the connection and not the actual load distribution even knowing the stiffness have a direct relation with the load distribution. Thus, it means that a calculation of the actual stiffness of the joint, which can be provided from the high detailed model, and updating the model with intermediate level of detail (by updating the rotational and translational stiffness for the rutman approach) will give a load distribution lower than it was observed for the low detailed model.

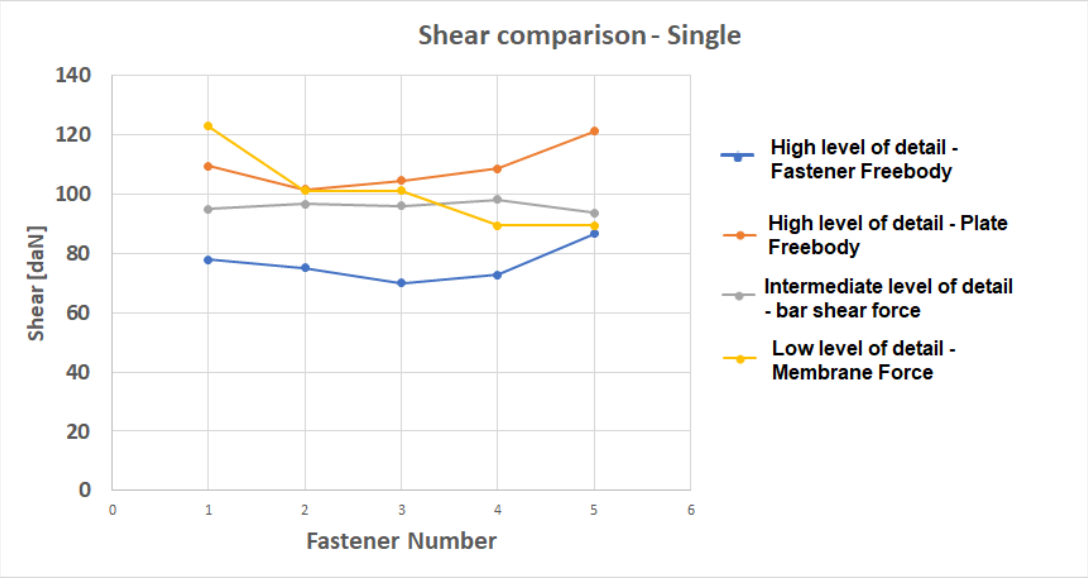

Figure 92 – Shear load comparison for all models - Single

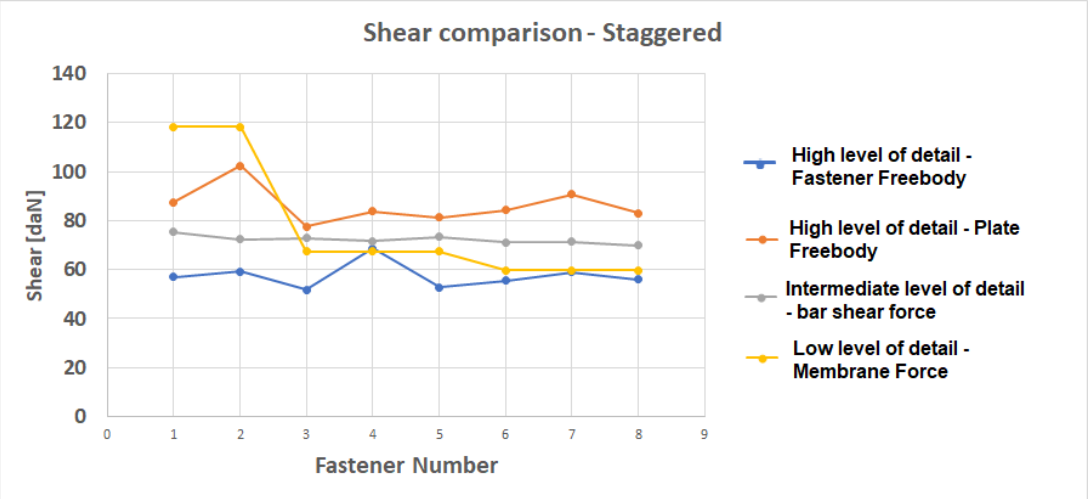

Figure 93 – Shear load comparison for all models - Staggered

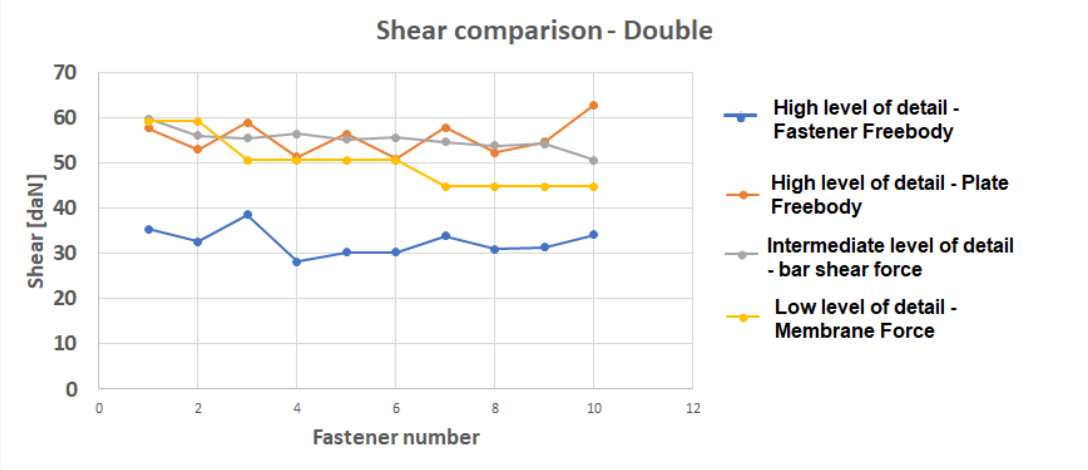

Figure 94 – Shear load comparison for all models - Double

Table 10 – Relative error in respect to model with high level of detail

Model	Low level of detail	Intermediate level of detail
Single	-1.5%	18.9%
Staggered	-15.6%	26.3%
Double	5.9%	5.0%

5 Conclusion

By concluding this work, it were observed few impacts in changing from one type of detail to another, by focusing in joint region, and at the first observation is that the overall stiffness have little change from the model with low level of detail to the model with intermediate level of detail, as it were observed in table Table 6.

Furthermore it were also observed a discontinue load distribution for the model with low level of detail and this behaviour could be observed because of the approach adopted to extract the load, which depends on the fastener position and the elements' membrane force. If there is only one fastener within the element, the total shear load flowing from one element to another will be distributed only for one fastener. Besides it can be note that the load distribution between the fasteners is not equal.

For the model with intermediate level of detail it were observed the similar load distribution but a more behaved flow of load. For those level of detail the joint stiffness representation using Rutman approach and the load in each fastener were obtained from the shear load at the bar element presented in rutmam methodology. Note that the critical load occurs at the corner two near the rib 1.

The model with high level of detail uses the more complex numerical methods regarding element formulation, large displacement behaviour and contact equations enable and which will better represent the analyzed region. It was observed a dubious method to obtain the fastener load, whether a freebody at the fastener section or at the plate section. It was observed differences in flow of load depending the way it was obtained, but it was clear that a conservative approach is to obtain the load from the freebody in a plate.

Furthermore, the enforced displacement methodology has shown a powerful approach to transport the boundary condition from a full scale model with intermediate level of detail to a portion of a more detailed model. Although the advantages of this approach, it must to be careful to interpret the results obtained, since the representation of the model with high level of detail must to keep with similar stiffness, otherwise the load distribution and the strain tensor field presents different results.

It can be concluded that by using the model with low level of detail has shown a safety method since the fasteners' load distribution are higher than the other models. Those method is specific good in the beginning of the cycle of the product development, where the data related to the load distribution and the characteristics of the product are in low maturity and changes in the product are expected all the time.

In this way a model with such level of detail is faster to be modified and also faster

to be reanalyzed than a model with high level of detail. The model can be built with parameterization and the specified parameter could be altered and the analysis can be performed very fast.

The knowledge of the level of detail must be used for each component is very important and must be studied more and more. Some authors have already proposed those study for specific parts, but a deeper investigation could be done and will be very useful for structural analysis departments in the industry and specially in aeronautical sector.

6 Future Works

This present work has shown the potential of using a mathematical model with low level of detail in order to evaluate the load distribution thought the skin of a wing to the spars. Although this work has presented a good results where it also enable to achieve important conclusion, this is only a begin for something bigger.

One important analysis that can enrich more this work, is the expansion of the hierarchical tree for a model with less level of detail. For this model it can be used only analytical equations in order to obtain the load distribution at the fasteners that connect the skin with the spars along the wing span wise. Those approach probably will shown the most conservative among others but it needs to be confirmed by means of calculation.

Another important task that compensate to be done and in which it will increase the understandable of the theme is to re-evaluate the model with intermediate level of detail by calculating the actual stiffness using the model with high level of detail. Thus, it will be possible to improve the Rutman approach for the specific region analyzed.

Furthemore it is also possible to improve the Rutman formulation by using models with high level of detail to obtain the stiffness. Thus, by simulating different configurations and also different source and type of load it is possible to obtain the actual translational and rotational stiffness to be assign for spring element in Rutman approach.

Aircraft attachment analysis are also a complex theme which involves several analysis and sometimes inconclusive results and is always needed to improve this type of analysis and perform deep studies in order to improve the aeronautical industry regarding its analysis.

Bibliography

ABBOTT, I. H.; DOENHOFF, A. E. V. *Theory of wing sections: including a summary of airfoil data*. [S.l.]: Courier Corporation, 2012.

Altair Hyperworks. *Hyperworks*. 2014. Disponível em: <https://Altairhyperworks.com>.

ASKRI, R.; BOIS, C.; DANOUN, A. Numerical approach to study the effect of shape defect in multi-fastened joints during the assembly process. *CIRP Journal of Manufacturing Science and Technology*, Elsevier, v. 33, p. 506–519, 2021.

ASKRI, R.; BOIS, C.; WARGNIER, H. Effect of hole-location error on the strength of fastened multi-material joints. *Procedia Cirp*, Elsevier, v. 43, p. 292–296, 2016.

ASKRI, R. et al. Reduced bolted joint model using multi-connected rigid surfaces and continuum shell elements. In: *20-th International Conference On Composite Materials (ICCM20), Copenhagen*. [S.l.: s.n.], 2015. p. 19–24.

BLACK, A. P. Object-oriented programming: Some History, and challenges for the next fifty years. *Information and Computation*, n. August, p. 3–20, 2013.

BORESI, A. P.; CHONG, K.; LEE, J. D. *Elasticity in engineering mechanics*. [S.l.]: John Wiley & Sons, 2010.

BRUHN, E. Airplane structures. vol. i. alfred s. niles and joseph s. newell. wiley, new york, and chapman & hall, london, ed. 4, 1954. xv+ 607 pp. illus. 7.75. *Science*, *American Association for the Advancement of Science*, *v.* 120, *n.* 3117, *p.*488−−488, 1954.

BUCALEM, M. L.; BATHE, K.-J. *The mechanics of solids and structures-hierarchical modeling and the finite element solution*. [S.l.]: Springer Science & Business Media, 2011.

CHAVES, C. E.; FERNANDEZ, F. F. A review on aircraft joints design. *Aircraft Engineering and Aerospace Technology: An International Journal*, Emerald Group Publishing Limited, 2016.

CHOLLET, F. *Keras 2.4.3*. 2020. Disponível em: <https://pypi.org/project/Keras/>.

DEVELPOERS, S. *Scipy 1.6.1*. 2021. Disponível em: <https://pypi.org/project/scipy/>.

DOYLE, S. *pyNastran 1.3.3*. 2020. Disponível em: <https://pypi.org/project/pyNastran/>.

FAA. *Aviation Maintenance Technical Handbook - Airframe Volume 1*. [S.l.: s.n.], 2018.

FALSONE, G.; SETTINERI, D. An euler–bernoulli-like finite element method for timoshenko beams. *Mechanics Research Communications*, Elsevier, v. 38, n. 1, p. 12–16, 2011.

GOOGLE. *Tensor Flow*. 2021. Disponível em: <https://pypi.org/project/tensorflow/>.

GRAY, P.; MCCARTHY, C. A highly efficient user-defined finite element for load distribution analysis of large-scale bolted composite structures. *Composites Science and Technology*, Elsevier, v. 71, n. 12, p. 1517–1527, 2011.

HUAN, H.; LIU, M. Effects of squeeze force on static behavior of riveted lap joints. *Advances in Mechanical Engineering*, SAGE Publications Sage UK: London, England, v. 9, n. 5, p. 1687814016686891, 2017.

HUGHES, T. J. *The finite element method: linear static and dynamic finite element analysis*. [S.l.]: Courier Corporation, 2012.

HUSKAMURI, M.; LAGDIVE, H. Stress analysis of riveted lap joint using finite element method. *STRESS*, v. 3, n. 3, 2017.

ISCOLD, P. H. Introdução às cargas nas aeronaves. *Belo Horizonte*, 2002.

JACOB, F.; TED, B. *A first course in finite elements*. [S.l.]: Wiley, 2007.

JR, J. D. A. *Fundamentals of aerodynamics*. [S.l.]: Tata McGraw-Hill Education, 2010.

KJ, B. *Finite element procedures in engineering analysis*. [S.l.]: Prentice-Hall Inc. Englewood Cliffs, NJ, 1982.

LABORATORY, L. *Theano 1.0.5*. 2020. Disponível em: <https://pypi.org/project/theano/>.

LIU, F. et al. An improved 2d finite element model for bolt load distribution analysis of composite multi-bolt single-lap joints. *Composite Structures*, Elsevier, v. 253, p. 112770, 2020.

LIU, F. et al. An analytical joint stiffness model for load transfer analysis in highly torqued multi-bolt composite joints with clearances. *Composite Structures*, Elsevier, v. 131, p. 625–636, 2015.

MAL, A. K.; SINGH, S. J. *Deformation of Elastic Solids*. [S.l.]: Prentice Hall., 1991.

MARTINS, R.; ERNANI, S.; SANTOS, M. Fastening analysis using low fidelity finite element models. In: *31st Congress of the International Council of the Aeronautical Sciences*. [S.l.: s.n.], 2018.

MIRZAZADEH, M. M.; GREEN, M. F. Non-linear finite element analysis of reinforced concrete beams with temperature differentials. *Engineering Structures*, Elsevier, v. 152, p. 920–933, 2017.

MSC Nastran. *Nastran*. 2021. Disponível em: <https://www.mscsoftware.com/product/msc-nastran>.

MSCSOFTWARE. *Quick Reference Guide*. [s.n.], 2018. Disponível em: <http://www.mscsoftware.com>.

NIU, C. *Airframe stress analysis and sizing*. [S.l.]: AD Adaso/Adastra Engineering LLC, 1997.

PANDASTREAM. *Panda 0.3.1*. 2015. Disponível em: <https://pypi.org/project/electricpy/>.

PYTEENS. *Phisics 2.0.0*. 2018. Disponível em: <https://pypi.org/project/phisics/>.

RICE, R. C. et al. Metallic materials properties development and standardization. *MMPDS). National Technical Information Service, cap*, p. 1–4, 2003.

ROSSUM, G. V.; JR, F. L. D. *Python reference manual*. [S.l.]: Centrum voor Wiskunde en Informatica Amsterdam, 1995.

RUTMAN, A. et al. Fastener modeling for joining parts modeled by shell and solid elements. In: *Americas Virtual Product Development Conference*. [S.l.: s.n.], 2007. p. 1–26.

RUTMAN, A. et al. Fastener modeling for joining composite parts. In: *Americas Virtual Product Development Conference*. [S.l.: s.n.], 2009. p. 1–28.

RUTMAN, A.; VIISOREANU, A.; PARAD, J. Fasteners modeling for msc. nastran finite element analysis. In: *2000 World Aviation Conference*. [S.l.: s.n.], 2000. p. 5585.

SADOWSKI, T. et al. Modern hybrid joints in arospace: modelling and testing. *Archives of Metallurgy and Materials*, v. 58, p. 163–169, 2013.

SADOWSKI, T.; GOLEWSKI, P.; ZARZEKA-RACZKOWSKA, E. Damage and failure processes of hybrid joints: adhesive bonded aluminium plates reinforced by rivets. *Computational Materials Science*, Elsevier, v. 50, n. 4, p. 1256–1262, 2011.

SCHWER, L. E. Guide for verification and validation in computational solid mechanics. IASMiRT, 2009.

Simcenter FEMAP. *FEMAP*. 2019. Disponível em: <https://www.plm.automation.siemens.com/global/pt/products/simcenter/femap.html>.

SKORUPA, M.; KORBEL, A. Modelling the secondary bending in riveted joints with eccentricities. *Archive of Mechanical Engineering*, Polish Academy of Sciences, Committee on Machine Building, p. 369–387, 2008.

SKORUPA, M. et al. Rivet flexibility and load transmission for a riveted lap joint. *Archive of Mechanical Engineering*, v. 57, n. 3, p. 235–245, 2010.

STANLEY ose. *Eletricpy 0.2.0*. 2021. Disponível em: <https://pypi.org/project/eletricpy/>.

SWIFT, T. Development of the fail-safe design features of the dc-10. In: *Damage tolerance in aircraft structures*. [S.l.]: ASTM International, 1971.

TEK.COM/ https://jet. *Jet-Tek*. 2018. Disponível em: <https://jet-tek.com/>.

THOTABOOT, P. *Engineering Tools 0.0.2*. 2018. Disponível em: <https://pypi.org/project/engineering-tool/>.

VERWAERDE, R.; GUIDAULT, P.-A.; BOUCARD, P.-A. A non-linear finite element connector model with friction and plasticity for the simulation of bolted assemblies. *Finite Elements in Analysis and Design*, Elsevier, v. 195, p. 103586, 2021.

WEAVER, J. W. *Finite Elements for Structural analysis*. [S.l.: s.n.], 2007. ISBN 0-13-317099-3.

ZHAO, H. et al. A review on solid riveting techniques in aircraft assembling. *Manufacturing Review*, EDP Sciences, v. 7, p. 40, 2020.

ZIENCKIEWIC, O.; TAYLOR, R. L.; ZHU, J. *The Finite Element Method: Its Basis and Fundamentals*. [S.l.: s.n.], 2013. ISBN 978-1856176330.

ZIENCKIEWICS, O.; MORGAN k. *Finite elements approximations*. [S.l.: s.n.], 2006. ISBN 978-0486453019.

Appendix

APPENDIX A – Fasteners load considering Squeeze force

As it was described previously, the stiffness of complex structures attached each other by fasteners is very difficult to be obtained and can be incur in mistakes while performing the analysis. In order to better understand the load distribution, this annex focus in analyze the load in the fasteners by considering the squeeze force in the fasteners before the load application.

The analysis considered at this point will be performed in two steps, in which the first one will consider only the squeeze force at the fasteners and the second one will consider the enforced displacement provided from the model with high level of detail with single configuration as described in section. 3.0.1. The strain field will be keep from one step to another and the tightening force will be keep as well. The squeeze force applied was provided from Liu et al. (2015), which is the greater force studied by the author.

In order to apply the force exactly at the axial direction of each fastener, a coordinate system was created at the center of each fastener and the z direction will be at the axial and the the other directions will be at the shear plane of the fastener. Figure. 3.0.5 presents the overall of the model used to perform the analysis.

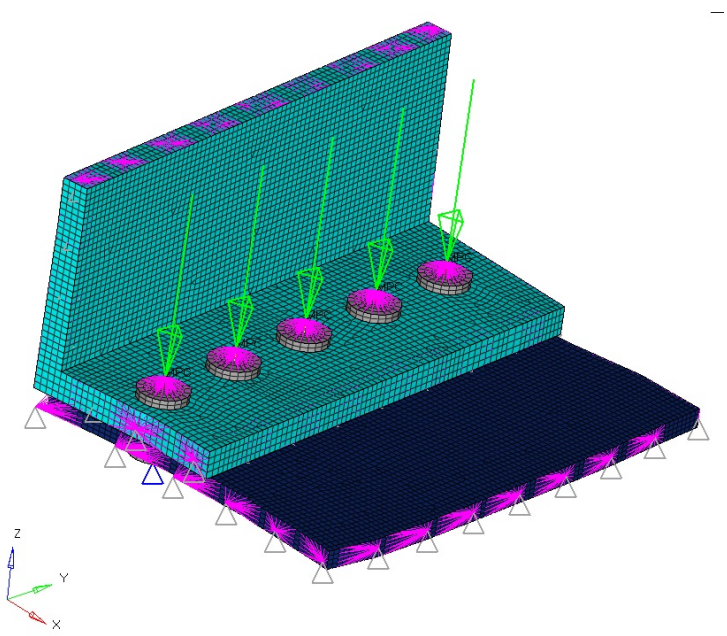

Figure 95 – Boundary condition

In Figure. 96 it is possible to see the boundary condition applied for each fastener. As it can be seen the force is applied at the axial direction of the fastener and a boundary condition is applied in the other extremity of the fastener and the value used to apply the force was 31kN (or 3100 daN).

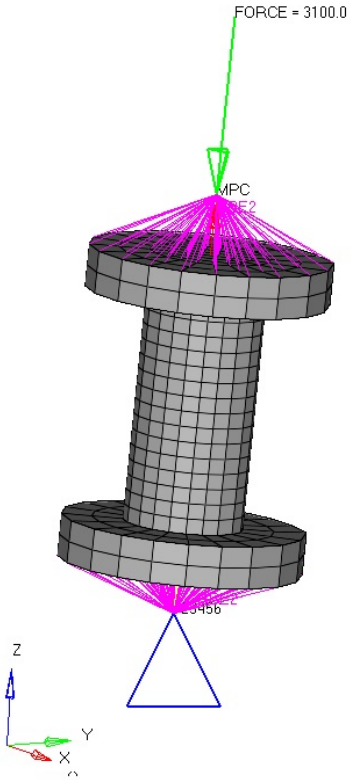

Figure 96 – Boundary condition at fastener

After proceed with the two steps of analysis it is possible to see the contact status at the fastener region as it can be seen on figure 97. The Figure presents only two value, zero or one, in which the value one means it was detected some contact between the parts and zero represents no contact between the parts. As it is observed the contact happens only in the region of the fasteners and for the other regions no contact happen between the two parts.

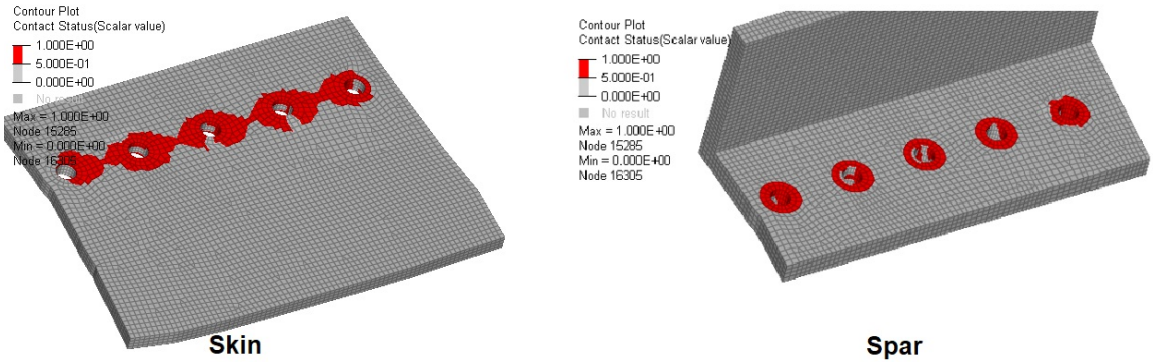

Figure 97 – Contact status

In the Figure. 98 it was performed a section near the first fastener in order to shows the contact force in the region. As it can be highlighted there is a complete contact between the parts and those forces generated is responsible to keep the region stiffer.

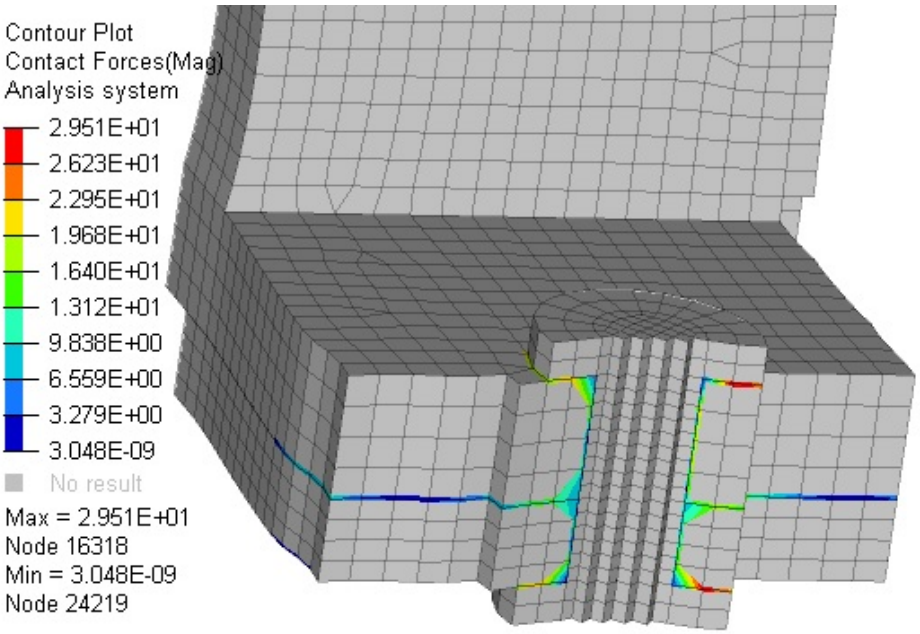

Figure 98 – Contact Force - Values in daN

Figure 99 shows the comparative in load distribution between the fasteners when compared with the analysis presented in the current work. Clearly the squeeze force keep the joint more stiffer since the load distribution in the fasteners is higher than the other compared models. This is more evident when compared the load distribution from

a freebody at the plate, in which the load distribution is much higher than the other obtained from the model without squeeze force.

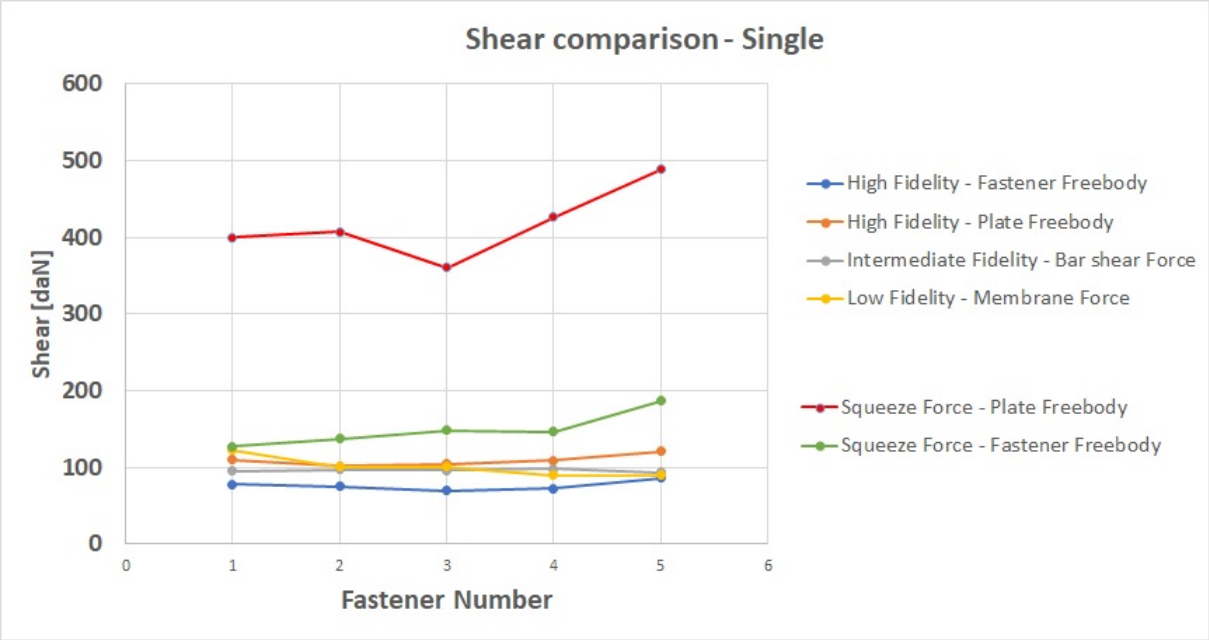

Figure 99 – Shear comparative for fasteners

Another important observation is the load distribution during the iteration process, as it was depicted in figure 100. The fasteners at the extremity became more loaded in the begining of the iteration process and due to the deformation of those fasteners the fasteners at the center start to divide the load and at the end the load are almost the same for each fastener.

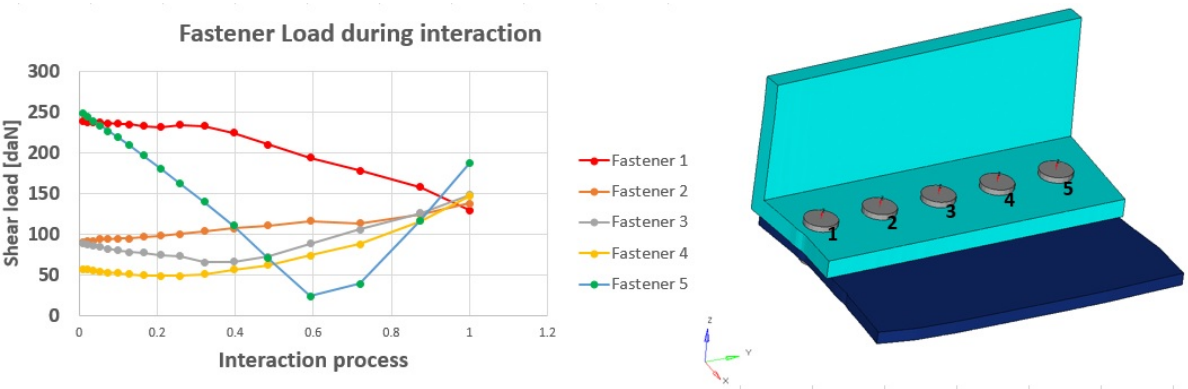

Figure 100 – Fastener load during interaction

With those short study, it was possible to understand the difference in evaluation the load distribution in the fasteners during a process of sizing a component. The stiffness of the joints can changes depend on the approach adopted and it is very important to use experimental data to keep the methodology more strong and reliable.